WestVirginiaUniversity
THE RESEARCH REPOSITORY @ WVU

Graduate Theses, Dissertations, and Problem Reports

2017

Novel Treatment Strategies for Brain metastases of Breast Cancer

Afroz Shareef Mohammad

Follow this and additional works at: https://researchrepository.wvu.edu/etd

Novel Treatment Strategies for Brain metastases of Breast Cancer

Afroz Shareef Mohammad

Dissertation submitted
to School of Pharmacy
at West Virginia University

in partial fulfillment of the requirements for the degree of

Doctor of Philosophy in
Pharmaceutical and Pharmacological Sciences

Paul R. Lockman, Ph.D., Chair
Erik A. Bey, Ph.D.,
Yon Rojanasakul, Ph.D,
Michael D. Schaller, Ph.D.
James W. Simpkins, Ph.D.

Department of Pharmaceutical and Pharmacological Sciences
Robert C. Byrd Health Sciences Center

Morgantown, West Virginia
2017

ABSTRACT

Novel Treatment Strategies for Brain metastases of breast cancer

Afroz Shareef Mohammad

About 20-40% of advanced breast cancer patients will develop symptomatic brain metastases. Once the patients diagnosed with metastatic brain tumors, there is 80% mortality rate within one year. The presence of blood-brain barrier makes it difficult for drugs to reach site of action in brain related ailments. To overcome we came up with two strategies: First, we encapsulated the chemotherapy in a liposome and thereby significantly improving the plasma pharmacokinetics of chemotherapy. We also observed that tumor drug exposure significantly improved by liposomal formulation. This improvement in plasma drug pharmacokinetics and tumor drug accumulation after administration of liposomal formulation, decreased the tumor burden and significantly increased the median survival by 40% when compared to vehicle group in an experimental model of brain metastases. In another strategy, we want to modulate blood-brain barrier in brain metastases to increase permeation. Notch-4 signaling pathway plays an important role in angiogenesis and inhibition of Notch-4 by DAPT will increase the expression of vascular endothelial growth factor receptor-2 ultimately leading to leaky vasculature in metastatic brain tumor. In our studies, we found that inhibition of Notch-4 by DAPT increased the permeation ^{14}C- Aminoisobutyric acid specifically in the brain metastases. We also observed that the progression of tumor burden was decreased when animals were administered both Notch-4 inhibitor and chemotherapy. We also found that median survival is increased by 20% in animals treated with chemotherapy with concurrent Notch-4 inhibition by DAPT. Finally, we evaluated the effect of chemotherapy on normal brain region adjacent to brain metastases. We found that the permeation of fluorescent tracers and ^{14}C-Palcitaxel increased in brain adjacent to tumor. We also found that the expression of activated astrocytes increased in brain adjacent to tumors after chronic chemotherapy treatment in our brain metastases model. Together these results suggest that novel strategies improved survival in brain metastases of breast cancer. Future studies should aim at combining these individual strategies to further increase survival in preclinical model. At the same time care should be taken not increase chemotherapy permeation into the normal brain as it may lead to unwanted effects like chemo-fog.

ACKOWLEDGEMENTS

The work presented here could not have been possible without the support of many individuals throughout my years in graduate school.

I would like to start by thanking my mentor and advisor Dr. Paul Lockman for giving me this opportunity to be a part of Lockman Lab Family. Dr. Lockman, you made the process of learning so much fun and I love the way you motivate students towards research and carry out experiments. I feel very fortunate to learn brain uptake experiments and pharmacokinetics from you. Thanks a lot for your input on manuscript preparation and writing, it was by far the best advice given. I have learned so many life lessons to be a better person from you. I have countless memories to cherish from our lab and your impact on my life and scientific career will be indelible.

I would like to thank each member of my committee for contributing throughout my graduate school. Thanks a lot, Dr. Eric Bey, Dr. Yon Rojanasakul, Dr. Michael Schaller and Dr. James Simpkins, for all the discussions regarding my research and providing me with valuable suggestions and guidance that has reinforced the projects herein as well as my progression as a graduate student. Your questions during my qualifying exams and during committee meetings really helped my projects to shape well and meaningful. I could not have asked for any better committee. It was really an honor to be associated with you all.

I would like to thank all my lab mates for being very nice to me and also teaching me all the techniques patiently. Dr. Chris Adkins, it was really my pleasure to spend time with you and

Finally, I would like to thank my family, my mom, dad, sisters, brother-in-law, and my niece without their support and motivation it is tough to imagine my achievements. I really thank them for understanding my absence during many occasions back home. I would also like to thanks my friends back home and here, sorry for not meeting more frequently.

Table of Contents

LIST OF TABLES

LIST OF FIGURES

ABBREVIATIONS

AUC	Area under the curve
BBB	Blood-brain barrier
BTB	Blood-tumor barrier
CL	Clearance
CNS	Central nervous system
DAPI	4',6-diamidino-2-phenylindole
Dil5	Carbocyanine tracer DiIC18 (5)-DS
EPR	Enhanced permeation and retention
ER	Estrogen receptor
HER2	Human epidermal growth factor receptor 2
IRN-50	Non-liposomal Irinotecan (50 mg/kg)
MRT	Mean residence time
nal-IRI-10	Nano-liposomal Irinotecan (10 mg/kg, Irinotecan equivalent)
nal-IRI-50	Nano-liposomal (50 mg/kg, Irinotecan equivalent)
P-gp	P-glycoprotein (ABCB1)
PK	Pharmacokinetics
PR	Progesterone receptor
SRS	Stereotaxic radiosurgery
TNBC	Triple negative breast cancer
V_d	Apparent volume of distribution
WBRT	Whole brain radiotherapy

CHAPTER 1

INTRODUCTION

1.1 Introduction

Over 500,000 people die every year of cancer in US and over 8 million people die of cancer worldwide every year. The incidence of cancer is rising with the rise in life expectancy, by 2030 it was estimated that over 20 million people worldwide would be effected by cancer every year with about 14 million estimated cancer deaths worldwide. Metastasis refers to spreading of cancer to distant organ from the primary site of origin and most of the cancer deaths are due to metastases.

With improved therapies for metastases, patients are surviving longer but brain metastases remains a singular obstacle. The incidence of brain metastases is increasing and many predict that this increase is due to improved survival of patients with primary cancer. About 10-40% of advanced breast cancer patients develop brain metastases. Once diagnosed with brain metastases of breast cancer, the survival rate at one year is around 20%. Brain metastases from breast cancer cause seizures, headache, and neurologic deficits beyond mortality. Primary therapeutic options involves surgery, followed by radiation therapy. Unfortunately, the bioavailability of most of the chemotherapy is limited due to the presence of blood-brain barrier (BBB).

The blood vessels in brain are different when compared to rest of the body; the blood vessels in brain are formed by compact endothelial cells with tight junctions surrounded by astrocytic foot processes and pericytes. These cells also express various efflux transporters and

are enzymatically active forming a unique barrier called BBB to maintain brain homeostasis. BBB regulates the movement of many solutes into the brain and unfortunately, most of the anticancer agents does not qualify to be the candidates to cross BBB and treat metastatic brain tumors.

In this dissertation, we investigate treatment strategies to overcome BBB at the tumor, blood-tumor barrier (BTB) for efficacious chemotherapy concentration in the tumor. First, we administer liposomal irinotecan in an experimental model of brain metastases of breast cancer and will evaluate the efficacy to the drug in reduction of tumors burden and improvement of median survival when compared with vehicle and conventional non-liposomal formulation. These nano-liposomes owing to its size take the advantage of enhanced permeation and retention (EPR) effect and accumulate in the metastatic lesions. Liposomes will also mask the drug related disadvantages in crossing the BTB like efflux from BTB and cancer cells. We evaluate novel methodologies to modulate BTB specifically such that the BTB permeability is increased which will lead to increased chemotherapy concentration in the metastatic lesion and ultimately, will improve the survival in an experimental model of metastatic brain tumors from breast cancer. Additionally, we also explored the effect of anticancer agents in normal brain adjacent to tumors.

Chapter 2 discusses a review of current treatment strategies of metastatic brain tumors. Here we discuss all the current treatment strategies including surgical resection, radiation therapy and chemotherapy and their shortcomings in the management of metastatic brain tumors. Other CNS drug delivery strategies were reviewed for the treatment of metastatic brain tumors.

Chapter 3 discusses the Pharmacokinetics of a Nano-liposomal formulation in experimental brain tumor model of triple negative breast cancer. Nano-liposomal formulation of irinotecan is hypothesized to have improved distribution to brain tumors because the formulation avoids

efflux transporters at BTB and takes advantage of the enhanced permeability and retention (EPR) effect of brain metastases. We investigate the concentration of irinotecan and its active metabolite SN-38 from both liposomal formulation and non-liposomal irinotecan in plasma and brain tumors. We evaluate the half-lives of drugs from non-liposomal irinotecan and liposomal irinotecan and finally, we investigate drug exposure to brain tumors by studying area under the curve for both non-liposomal irinotecan and liposomal irinotecan.

After studying the pharmacokinetics of liposomal irinotecan, we evaluate pharmacodynamics of liposomal irinotecan in chapter 4. Here, we study the accumulation of fluorescently tagged liposomes in brain tumors and then we study the progression of tumor burden in different treatment groups. Finally, we investigate pharmacodynamics effect by studying median survival after treatment with vehicle, non-liposomal irinotecan and liposomal irinotecan.

In Chapter 5, we examine a new strategy to increase the permeation of the BTB. Notch-4 signaling pathway plays an important role in maintaining endothelial quiescence and thereby maintaining the integrity of blood vessels in brain by down regulation of vascular endothelial growth factor receptor-2 (VEGFR-2). We hypothesize, inhibiting the Notch-4 signaling pathway will lead to formation of leaky vasculature in the tumor thereby increasing the permeation of BTB. We administer chemotherapy with concurrent inhibition of Notch-4. We expect this strategy will improve the chemotherapy concentration reaching the brain tumors ultimately leading to increased median survival. We study mRNA and protein levels of VEGFR-2 on human brain endothelial cells (HBEC) upon inhibition of Notch-4 signaling pathway. We investigate permeation changes in tumors after Noth-4 inhibition by [14]C- 2-Aminoisobutyric

acid. Finally, we study the survival in an experimental model after chemotherapy administration with concurrent Notch-4 inhibition.

With many new strategies to treat metastatic brain tumors involves overcoming BBB, in Chapter 6 we study the permeation changes and effect of chemotherapy on normal brain surrounding the tumor. We study transfer rate constant of fluorescent tracers in brain adjacent to tumors (BAT) and then we investigate the concentrations of ^{14}C-paclitaxel using quantitative autoradiography. Finally, we study the effect of chemotherapeutic agents on astrocytes in BAT regions.

In summary, this dissertation evaluates current treatment strategies for metastatic brain tumor as well as new strategies to overcome the BTB and treat metastatic brain tumors. This dissertation provides novel strategies where, chemotherapy is administered in Nano-liposomal formulation and a proangiogenic strategy, where we hypothesize increase in permeation at the BTB by increasing inefficient angiogenesis. This dissertation also documents the cytotoxic effects of chemotherapy on normal brain region around the tumors. As a whole, the data emphasizes the need of novel strategies to improve drug concentrations specifically in the brain tumors without affecting BBB in normal brain region.

CHAPTER 2

CURRENT TREATMENT STRTEGIES FOR TREATMENT OF METASTATIC BRAIN TUMORS

2.1 Blood-Brain Barrier

Blood vessels deliver blood from the heart to different organs and the blood vessels especially the microvasculature has different properties to meet the requirements of the particular organ or tissue they vascularize (Palade 1961). Neurons of brain communicate and function by chemical and electrical signals. For these signals to be reliable and reproducible, the ionic concentration of the tissue has to be constant maintaining homeostasis (Abbott, Patabendige et al. 2010). The microvasculature of the brain plays an important role in regulating the entry of any solute into the brain parenchyma and helps in maintaining homoeostasis for proper neuronal function (Abbott, Patabendige et al. 2010). This unique property of brain microvasculature was described as Blood-brain barrier (BBB). The BBB is formed by continuous non-fenestrated capillaries, where endothelial cells are attached together by tight junction protein complexes (TJs), including claudins, occludins and intercellular adhesion molecules, which restricts the paracellular diffusion of solutes (**Fig 2.1**) (Reese and Karnovsky 1967, Ballabh, Braun et al. 2004). The brain endothelial cells also restricts vesicle mediated transcellular movement compared to peripheral endothelium(Coomber and Stewart 1985). The endothelial cells are surrounded by pericytes on the abluminal side which, have contractile proteins and they can regulate the diameter of the capillary (Peppiatt, Howarth et al. 2006). Astrocytic foot processes also ensheeth the capillaries providing link between neurons and blood vessels (**Fig 2.1**). Through this cellular link, astrocytes mediate blood flow in accordance with neuronal activity

5

(Attwell, Buchan et al. 2010, Gordon, Howarth et al. 2011). Astrocytes play an important role in

formation of BBB and astrocyte secreted factors play an important role in BBB function (Janzer

and Raff 1987). In addition to physical barrier properties of brain capillaries, there are efflux

transporters including p-glycoprotein, breast cancer resistance protein and the family of multi-

drug resistance proteins expressed on brain endothelium, which will limit lipophilic solutes form

entering the brain (Cordon-Cardo, O'Brien et al. 1989, Thiebaut, Tsuruo et al. 1989). Enzymes

secreted by BBB (e.g., phosphatases) will inactivate some molecules like peptides and

neuropeptides, preventing them to cross BBB (Minn, Ghersi-Egea et al. 1991, Witt, Gillespie et

al. 2001).

2.1.1 Functions of BBB

BBB provides stable environment for the neuronal activity by ion regulation. The ion

concentration is kept constant despite the changes in plasma ion concentration due to

exercise/meal/some disease condition (Bradbury, Stubbs et al. 1963, Hansen 1985, Somjen

2002). The BBB also separates the pool of central neurotransmitters from that of peripheral

neurotransmitters, though both the neurotransmitters are same, the peripheral neuroexcitatory

amino acid glutamate which is present in high concentrations in blood may cause permanent

neurotoxic damage if unregulated by BBB (Abbott, Patabendige et al. 2010). Macromolecules

like albumin, pro-thrombin and plasminogen may initiate apoptosis and are detrimental to central

nervous system. BBB restricts these macromolecules from entering into the brain tissue (Nadal,

Fuentes et al. 1995, Gingrich and Traynelis 2000). BBB prevents the entry of many neurotoxic

substance into the CNS by various active efflux mechanisms present. The neurotoxic substance

may be endogenous metabolites or xenobiotics ingested (Abbott, Patabendige et al. 2010). BBB

also plays an important role in delivery of nutrients to brain. It has specific transport systems to

transport various essential water-soluble nutrients (Abbott, Patabendige et al. 2010). Angiogenesis and vasculogenesis is regulated by many pathways including vascular endothelial growth factor (VEGF) and its receptors (VEGFR) and Notch signaling plays an important role in regulating the endothelial cell functions (Hofer and Schweighofer 2007, Kume 2009).

While the BBB helps in maintaining the homeostasis for proper functioning of the brain, it restricts delivery of many central nervous system (CNS) drugs including chemotherapies (Toth, Veszelka et al. 2011). Some of the chemotherapeutics like paclitaxel and doxorubicin are most significantly subjected to efflux transport mechanisms present at the BBB (Löscher and Potschka 2005, Thomas, Taskar et al. 2009).

2.2 Brain Metastases

Joseph Recamier in 1829 coined the term metastases to describe spread of cancer in treatise *"Recherches sur le traitement du cancer"(Fisher 2008).* In Greek metastases means, migration; removal or change. In 1858 Rudolf Virchow described the process of metastasis was determined by mechanical factors like the arrest of tumor-cell emboli in the vasculature (Fisher 2008). Stephen Paget, the father of metastases in 1889 published a paper "The distribution of secondary growth in cancer of the breast", where he analyzed 735 breast cancer patients and argued that metastatic distribution is not due to chance. Paget came up with "seed and soil" hypothesis, where cancer cells are referred to as "seeds" and the distribution of these cancer cells in the body should be understood by the "properties of soil" which refers to the secondary organs. The quote from the paper is "When a plant goes to seed, its seeds are carried in all directions, but they can only live and grow if they fall on congenial soil" suggesting that the metastatic distribution pattern doesn't not follow blood flow distribution as proposed by Virchow (Paget 1889). In 1928, James Ewing, questioned "seed and soil" hypothesis and proposed that

7

the pattern of metastases was determined by the anatomy of vascular and lymphatic drainage from the primary tumor (Pienta, Robertson et al. 2013). Isaiah Fidler from MD Anderson in 1970 published series of studies, where he demonstrated that metastasis occurred in sequential steps where cancer cells interact with microenvironment and selecting for successful cancer cells in stochastic manner. The process proposed by him took into account Virchow, Paget and Ewing's models (Talmadge and Fidler 2010).

The incidence of metastatic brain tumors was estimated between 200,000 and 300,000 according to American Brain Tumor Association. About 20-40 % of all cancers eventually metastasize to brain(Ostrom, Gittleman et al. 2016). More than 80% of metastatic brain tumors develop multiple metastatic lesions in the brain. The site of origin for brain metastases is mostly from lung, followed by breast and melanoma (Ostrom, Gittleman et al. 2016). Brain metastases from breast cancer is second most common type of metastatic brain tumors after lung cancer. In about 30% breast cancer patients, metastatic lesions in brain were found via autopsy (Mueller and Jeffries 1975, Tsukada, Fouad et al. 1983, Sant, Capocaccia et al. 1998, Lin, Bellon et al. 2004). Once the patient diagnosed with metastatic brain tumors from breast cancer, one-year survival is only 20%. The main reason for this grim prognosis is the inability of chemotherapeutic agents to cross BBB (Lockman, Mittapalli et al. 2010).

2.3 Blood-Tumor Barrier

Once the metastatic lesions start developing in the brain, the integrity of the BBB is lost in the tumor and microvasculature in the tumor is often referred to as blood-tumor-barrier (BTB) **(Fig 2.2)** (Lockman, Mittapalli et al. 2010). As the tumors grow, they promote the growth of new blood vessels, a process called angiogenesis. These new blood vessels in brain tumors lack tight

junctions and also proper astrocytic contact, as result the blood vessels in the tumors (BTB) have increased permeability and reduced blood flow (Front, Israel et al. 1984, Bertossi, Virgintino et al. 1997, Liu, Xue et al. 2008). In addition, the angiogenic vessels also have fenestrations, which increase the permeability through paracellular pathways (Blasberg, Gazendam et al. 1980, Groothuis, Fischer et al. 1983).

The BTB permeability is not homogenous from tumor to tumor and within the metastatic lesion (Lockman, Mittapalli et al. 2010). BTB permeability between different tumor preclinical tumor models were heterogeneous. Brain metastases become hypoxic as they grow beyond their blood supply, to meet their oxygen and nutrition requirements, tumor cells secrete vascular endothelial growth factor (VEGF) to initiate the process of new blood vessel formation (Folkman 1971). VEGF secretion is associated with increased turnover of endothelial cells leading to increased permeability (Folkman 1971). Angiogenesis is a dynamic process and the heterogeneity of BTB permeability between the tumors and within the tumors can be attributed to this dynamic nature (LeBlanc, Krishnan et al. 2012, Betz, Lenard et al. 2016).

2.4 Current Treatment modalities for brain metastases of breast cancer.

Current treatment for metastatic brain tumors include surgery, stereotactic radiosurgery (SRS), whole brain radiation therapy (WBRT), and chemotherapy. Usually, more than one type of treatment is suggested and treatment has become increasingly individualized. Treatment for patients with karnofsky performance score (KPS) 70 or higher, age < 65 years and with single metastatic brain tumor includes surgical resection followed by WBRT or SRS. There was no difference in overall survival with WBRT or SRS but with SRS cognitive deterioration free survival was observed. Treatment for patients with multiple metastatic lesions who are not candidates for surgical resection includes either WBRT or SRS (Aoyama, Shirato et al. 2006,

Chang, Wefel et al. 2009, Kocher, Soffietti et al. 2011). Treatment for patients with poor prognosis (KPS <70) WBRT is the preferred treatment modality. With SRS the median brain recurrence-free survival was 6 months (range, 4 to 11 months) and median overall survival was 10 months (range, 4 to 18 months)(Kelly, Lin et al. 2012). Chemotherapy for treatment of metastatic brain tumors from breast cancer include commonly used cytotoxic agents for breast cancer like cyclophosphamide, fluorouracil, methotrexate, and doxorubicin (Boogerd, Dalesio et al. 1992, Lin, Bellon et al. 2004). However, the penetration of chemotherapy is limited due to the presence of blood-tumor barrier. An objective response rate of 50 percent and a median duration of response of 7 months was observed with a variety of chemotherapy regimens (Rosner, Nemoto et al. 1986). For treatment of brain metastases from HER2-positive breast cancer, targeted agents like lapatinib, transtuzumab have proven to be effective. The combination therapy of lapatinib and capecitabine was evaluated in many trials, in Lapatinib Expanded Access Program (LEAP), the objective response rate was 18 percent (Boccardo, Kaufman et al. 2008). In another Italian trial, 32 percent partial response rate was observed with a combination therapy of capecitabine and lapatinib (Metro, Foglietta et al. 2011).

2.5 Current strategies to bypass BBB or BTB

Drugs used in the treatment of CNS disorders like Psychosis, Parkinson's disease, Alzheimer's disease, Affective mood disorders, Pain and Brain tumors experience a peculiar hurdle of passing into the brain because of a selective barrier between brain and blood (Oldendorf 1974). There is a need for development of successful techniques to deliver effective concentrations of the drug across the BBB. Currently, there are two general strategies employed for drug delivery across the BBB, invasive and non-invasive techniques. Invasive strategies that are employed for drug delivery in CNS include intracranial drug delivery though intra-

10

cerebroventricular (ICV) injection and intra-cerebral implants (Pathan, Iqbal et al. 2009). Non-invasive approaches include osmotic disruption of BBB/BTB, disruption of BBB/BTB through focused ultrasound and carrier mediated drug delivery system (Pathan, Iqbal et al. 2009, Kuo, Lin et al. 2011).

2.5.1 Convection-enhanced delivery (CED): Bobo et al., in 1994 first described CED, where catheters are surgically implanted to administer chemotherapeutic agents directly into the tumor using positive pressure micro-perfusion (Bobo, Laske et al. 1994). Many chemotherapeutic agents are under investigation using CED (Kunwar 2003, Kioi, Husain et al. 2006, Sampson, Akabani et al. 2006). The major limitation with CED is poor drug distribution due to backflow and it is highly invasive (Rapoport 2001, Tanner, Holtmannspotter et al. 2007, Sampson, Archer et al. 2009). CED is beneficial in single brain tumors where drug distribution can be targeted to the tumors but in case multiple tumors, it is impractical to introduce catheter surgically into each tumor.

2.5.2 Intra-cerebroventricular injection (ICV): It is a highly invasive technique, where the drugs of interest are directly injected into the cerebrospinal fluid (CSF) present in the cerebral ventricles. Injecting directly into the ventricles, the drugs bypasses the BBB, however there are many studies suggesting complete clearance of injected drugs from CSF into the blood. Most of the studies indicate that only <10% of drug is available in brain after 1-3 h of intraventricular injection of radiolabeled sucrose (Ghersi-Egea, Finnegan et al. 1996, Ghersi-Egea, Gorevic et al. 1996). In a study performed by Nagaraja et al., they administered radiolabeled insulin like growth factor (IGF-1) into rat ventricle through ICV using stereotaxic coordinates. They found that nearly, 80% of IGF-1 was cleared with in first 30 min after administration. They also studies the concentration of IGF-1 at various distances from the ventricles and found that within 0.5 mm

from the ventricles the diffusion of IGF-1 was negligible (Fig 2.)(Nagaraja, Patel et al. 2005). ICV injection are highly invasive and only useful if the metastatic tumors are present around the ventricles, unfortunately most of the brain metastases of breast cancer form multiple tumors in the cerebrum.

2.5.3. Intracerebral Implants: FDA approved Gliadel wafer, a biodegradable polymer loaded with chemotherapy drug BCNU for implantation after surgical resection of gliomas (Perry, Chambers et al. 2007). This local delivery of the drugs eliminates side effects like fatigue and hair loss. A phase III clinical trial with gliadel wafers in patients with glioma the median survival improved from 11.6 months to 13.9 months (Westphal, Hilt et al. 2003). This study shows survival benefit with local delivery of chemotherapy. Implantation of wafers is highly invasive and this modality is good for single tumors. In case of metastatic brain tumors, surgically implanting multiple wafers into metastatic lesions is impractical.

2.5.4 Osmotic disruption of BBB: Osmotic disruption of BBB by infusing hyperosmolar agent was first reported by Rapoport et al. in 1972 (Rapoport, Hori et al. 1972). After administration of hyperosmotic agent like mannitol, the brain endothelial cells shrink resulting in dysfunction of tight junctions which will lead to increase in BBB permeability (**Fig. 2.4**) (Rapoport and Robinson 1986). This increase in BBB permeability for few hours allows a therapeutic window for administration of the chemotherapy (Rapoport and Robinson 1986). Many studies reported that there is an increase on drug concentration up to 90-folds after osmotic disruption of BBB (Williams, Henner et al. 1995). In a trail with 30 patients with primary CNS lymphoma, median survival improved from 17.8 months to 44.5 months after osmotic disruption of BBB with mannitol and chemotherapy (cyclophosphamide) before radiation therapy, when compared it to controls receiving only radiotherapy(Neuwelt, Goldman et al. 1991).

The selective opening of BBB in the tumor region (BTB) through osmotic BBB disruption is still a debate; many preclinical studies suggest that the hyperosmotic agents did not selectively open BBB in the tumor region (Nakagawa, Groothuis et al. 1984, R. Groothuis, C. Warkne et al. 1990, Zünkeler, Carson et al. 1996). The increase in BBB permeability in normal brain region may lead to CNS toxicity from chemotherapy and the patients may suffer from fading cognitive function termed as "chemo-fog" (Kemper, Boogerd et al. 2004) (Raffa 2010).

2.5.5 BBB disruption by focused ultrasound (FUS): MRI-guided FUS is a non-invasive method for precise transient BBB disruption **(Fig 2.4)** (Hynynen, McDannold et al. 2001, Hynynen, McDannold et al. 2005). FUS produces shear stress in cells and disrupt the tight junctions of BBB to increase permeability (Gonzalez-Mariscal, Tapia et al. 2008, Sheikov, McDannold et al. 2008, Shang, Wang et al. 2011). Additionally, microbubbles can be administered and lower the energy required for BBB disruption (Hynynen, McDannold et al. 2001). Microbubble induced FUS was successful in opening BBB without any major side effect in non-human primates (McDannold, Arvanitis et al. 2012). Targeted opening of BBB can be achieved by using MRI to guide FUS and real time monitoring of acoustic emissions from microbubbles (Kaye, Chen et al. 2011, Arvanitis, Livingstone et al. 2012, Jones, O'Reilly et al. 2013).

Various chemotherapeutic agents like doxorubicin, carmustine, transtuzumab, and temozolamide have been administered using FUS preclinical (Liu, Hua et al. 2010, Aryal, Vykhodtseva et al. 2013, Wei, Chu et al. 2013). Diaz et al., demonstrated the delivery of gold nanoparticles into the brain tumors, in this study they also showed anti-epidermal growth factor receptor antibody improved the uptake in glioma (Diaz, McVeigh et al. 2014). While preclinical experiments prove the effectiveness of FUS in treatment of brain tumors overcoming the BBB, a

limitation would be attenuation of ultrasound signal through human skull and its ability to reach deeper parts of human brain. FUS can only be targeted if the tumors are detected through MRI, on the contrast many of brain metastases for micro metastatic lesions which are undetectable through the aid of MRI.

2.5.6 Carrier mediated drug delivery: Carriers like liposomes, dendrimer nanoparticles and other nanoparticles are studied for drug delivery in brain tumors (Fabel, Dietrich et al. 2001, Gelperina, Maksimenko et al. 2010). Localized nanoparticle delivery into the brain tumor can be achieved by magnetic therapy, where carrier molecule with iron can be targeted using magnetic field (Saenz del Burgo, Hernandez et al. 2014). Nektar therapeutics developed a novel polyethylene glycol (PEG) based carrier system for the delivery of irinotecan and it showed significant survival benefit in preclinical breast cancer model (Adkins, Nounou et al. 2015). Doxorubicin encapsulated in a liposome was widely studied for malignant gliomas, showed disease stabilization along with low side effects.

2.5.7 BBB disruption by pharmacological agents: The peptide bradykinin is a vasodilator and upon administration increases expression of caveolin-1 and caveolin-2 at the BBB (Liu, Xue et al. 2010). Higher expression of caveolae at the BBB will lead increase in BBB permeability. Many researchers extensively studied its potential to increase dug delivery in brain (Inamura and Black 1994, Emerich, Snodgrass et al. 1998); however, this disruption is transient (Liu, Xue et al. 2010). In a clinical trial with pediatric brain tumors, a bradykinin analogue lobradimil along with anticancer agent carboplatin showed no therapeutic benefit (Warren, Jakacki et al. 2006).

Most of the chemotherapeutic agents are substrates for efflux transporters like P-gp at the BBB, unfortunately cancer cells have high expression of efflux transporters making it even more

difficult for drug delivery in brain metastases (Dombrowski, Desai et al. 2001). Many small molecules were developed for direct inhibition of efflux transporter but clinically, they showed poor efficacy and safety profile (Thomas and Coley 2003). Kreisl et al., showed greater uptake of a P-gp substrate of 11c-N-desmethylloperamide with a promising P-gp inhibitor tariquidar, which is effective at nanomolar concentration (Roe, Folkes et al. 1999, Kreisl, Liow et al. 2010).

2.5.8 New drug entities and targets for the treatment: Sagopilone, a new anti-neoplastic agent, penetrates BBB and evades from efflux transport at the BBB was evaluated in a phase 2 study of cancer patients with brain metastases from breast cancer. The overall survival after treatment with sagopilone was 5.3 months with 13% of the patients showed partial response (Hoffmann, Fichtner et al. 2009, Freedman, Bullitt et al. 2011). Peptide treated formulation of paclitaxel (GRN1005) increased the permeability of drug in to the advanced brain tumors and decreased the tumor burden (Kurzrock, Gabrail et al. 2012).

The incidence of brain metastases is as high as 40% with triple negative breast cancer (TNBC) but no targeted therapies are available for brain metastases of TNBC (Weil, Palmieri et al. 2005). Recent studies showed that high expression of PD-L1 in TNBC could be used as a targeting strategy for treating brain metastases from TNBC. In a phase I trial, targeting PD-L1 with pembrolizumab showed an overall response rate of 19% in brain metastases (Nanda, Chow et al. 2015).

Dar. M along with Smithkline Beecham corporation owns a patent for the use benzimidazole thiophene compounds for tumors in CNS (Dar 2009). Benzimidazole thiophenes showed strong anticancer and DNA binding properties along with the ability to cross the BBB (Cindric, Jambon et al. 2017). These compounds inhibit polo-like kinases, which play an

important role in mitosis (Dar 2009).

McChesney et al. and Tapestry pharmaceuticals Inc. owns a patent for taxane analogs for the treatment of brain cancer. Abeoa-taxane is an orally effective taxane, which stabilizes tubulin dimers during mitosis. These taxanes penetrate BBB and are not substrates for multi-drug resistance (MDR) proteins (McChesney, Tapolsky et al. 2011).

A Korean biotechnological company owns a patent for sodium meta arsenite for treatment of brain tumors (Jo and Yang 2011). This compound is able to cross BBB/BTB elimating the need of osmotic disruption of BBB/BTB(Jo and Yang 2011).

Myriad genetics and Laughlin own a patent for (4-Methoxy-phenyl)-methyl-(2-methyl-quinazolin-4-yl) for the treatment of metastatic brain tumors. Myriad genetics claim that (4-Methoxy-phenyl)-methyl-(2-methyl-quinazolin-4-yl) crosses BBB/BTB and reach cytotoxic concentrations (Laughlin 2010).

Zhang owns a patent on targeting brain metastases of breast cancer by inhibiting enzyme 1,6 fructose biphosphatase (FBP) which is critical in gluconeogenesis (Weihua 2013). Zhang found that the metastatic breast cancer cells survived in low glucose media while the non-metastatic cells did not. The brain interstitial spaces have low glucose and for the cancer cells to survive, they should depend on gluconeogenesis for their energy requirements. FBP inhibitors like benzimidazole derivatives, amino pyridines, tricyclic thiazoles, azaindole inhibitors will interfere with this rate-limiting step involving FBP in gluconeogenesis, which leads to inability of the cancer cells to produces their energy requirements (Weihua 2013).

Transtuzumab is already used to treat HER2 positive breast cancer but it is unable to treat

brain metastases of breast cancer, as it cannot cross the BBB/BTB. BiOasis Inc., and Hutchinson et al., own a patent for coupling P97 peptide to transtuzumab, which showed significant improvement in the therapeutic efficacy (up to 1000 times higher) in treating brain metastases of HER2 positive breast cancer (Hutchison, Vitalis et al. 2013).

Nektar therapeutics developed a novel irinotecan drug delivery system with irinotecan linked to a polymer, poly ethylene glycol (NKTR-102)(Eldon, Harite et al. 2010). In study published by Adkins et al., NKTR-102 showed increased drug accumulation of irinotecan and its active metabolite SN-38 in brain metastases, due to enhanced permeation and retention (EPR) effect through leaky brain metastases vasculature. The PEGylation is responsible for increased plasma circulation time and thereby modifying the distribution of irinotecan when compared to conventional irinotecan (Adkins, Nounou et al. 2015).

2.5.9 Clinical trials on brain metastases of breast cancer:

Chemotherapy clinical trials have typically excluded patients with brain metastases for a variety of reasons, including limited penetration of agents through the BBB/BTB, the lack of a convenient modality for tumor burden monitoring, and poor overall survival prognoses leading to negative outcomes for patients (Phillips, Jeffree et al. 2017). Some of the earliest published work in chemotherapy for brain tumors began in the 1950s and 1960s, focusing on use of systemic agents such as methotrexate, thioTEPA, nitrosoureas, and vinca alkaloids (Wilson and Delagarza 1965, Nevinny, Hall et al. 1968, Fewer, Wilson et al. 1972, Gutin, Wilson et al. 1975). Kofman *et al* noted the use of prednisolone to reduce neurological symptoms in 1957 (Kofman, Garvin et al. 1957). Though the chemotherapy field has advanced, a regimen specific for the treatment of brain metastases of breast cancer has yet to be approved and ratified by the FDA or

national and international cancer organizations. Systemic cytotoxic therapy including taxanes (docetaxel, paclitaxel), anthracyclines (doxorubicin), platinum compounds (cisplatin), and alkylating agents (cyclophosphamide) in combination with other agents have shown some efficacy in small studies (Miller, Wang et al. 2007, Miles, Chan et al. 2010, Linot, Campone et al. 2014, Isakoff, Mayer et al. 2015). The rise of novel dosage forms, immunotherapy, and small molecule inhibitors has pushed the envelope of treatment expectations and produced trials focusing specifically on brain metastases of breast cancer.

Completed clinical trials:

Cisplatin and etoposide were tested as combination agents in a Phase II for brain metastases of breast cancer patients and only one had a partial response. Penetration into the CSF is poor but it can penetrate through the blood-tumor barrier (Vinolas, Graus et al. 1997). Cisplatin and etoposide were tested as combination agents. Out of 56 patients, 7 achieved complete response, 14 achieved partial response, 12 no change, 16 progressive, 8 insufficient treatment/not assessed (BEEP NCT02185352) (Franciosi, Cocconi et al. 1999).

Doxorubicin, cisplatin, 5-fluorouracil, methotrexate cycle schedules given to patients with brain metastases of breast cancer. No improvement in overall survival was noted, with major toxicity (Lamar, Greco et al. 1994).

In a Phase II study 15 patients with brain metastases of breast cancer were treated with cyclophosphamide and cisplatin, 6 achieved partial response which is defined as, at least 50% reduction in tumor, no new lesions and no progression of brain tumors (Christodoulou, Bafaloukos et al. 2005).

In a Phase II clinical trial 25 patients with brain metastases of breast cancer treated with cisplatin and vinorelbine, with 30 Gy fractionated radiation. Complete response was seen in 3 patients, partial response in 16 patients with a total response of 76% (Cassier, Ray-Coquard et al. 2008).

In study involving 152 metastatic breast cancer patients, 78 patients responded to paclitaxel, and 6 developed CNS progression. In four brain metastases of breast cancer patients with concomitant paclitaxel and bevacizumab treatment, 3 showed partial response and 1 showed complete response, with no extra progression (Labidi, Bachelot et al. 2009). In another study, 5 brain metastases of breast cancer patients receiving similar bevacizumab and paclitaxel treatment showed partial response (2), stable disease (2), and progression (1)(Yamamoto, Iwase et al. 2012).

Vinorelbine and temozolamide was used in 6 brain metastases of breast cancer patients with only a minor response, which then progressed (Omuro, Raizer et al. 2006). In another Phase II trial of 11 brain metastases of breast cancer patients were treated with vinorelbine and temozolamide, one patient had a minor response, while the others were grouped together in stable or progressing disease (Iwamoto, Omuro et al. 2008).

In a trial liposomal doxorubicin combined with cyclophosphamide, and radiation, given in 29 patients with brain metastases from breast cancer. After 6 courses, 9 (31%) had partial response, but eventually 16 (55%) had progressive disease (Linot, Campone et al. 2014) NCT00465673.

In a study, nanoparticle albumin bound paclitaxel (nab-paclitaxel) and transtuzumab was given weekly for 14 cycles with concomitant SRS, but resulted in minimal response in brain

nodules, though the patient had progression-free survival for 13 months (Ricciardi, Russo et al. 2015).

A phase II clinical trial with ANG1005 in breast cancer patients with recurrent brain metastases was completed in September 2017 (NCT02048059). ANG1005 is novel agiopep2-paclitaxel conjugate and it showed increased drug delivery in a preclinical brain metastases of breast cancer model (Thomas, Taskar et al. 2009).

A phase I study of lapatinib with whole brain radiotherapy was completed for brain metastases for HER2-positive breast cancer (NCT00470847). Results show, 4.8 months of progression free survival with lapatinib.

GRN1005 is paclitaxel peptide conjugate, which targets low-density lipoprotein receptor-related protein 1. GRN1005 showed efficacy in metastatic brain tumors and it was well tolerated (Kurzrock, Gabrail et al. 2012). A phase II clinical trial with GRN1005 alone or with transtuzumab in patients with brain metastases was completed and yet to publish results (NCT01480583).

Ongoing clinical trials:

Currently, there are 31 clinical trial, which are active or recruiting patients for the treatment of metastatic brain tumors for breast cancer. The details of the trials are included in **Table 2.1**.

2.6 Chapter Summary

The presence of BBB is responsible for grim prognosis in patients with brain metastases of breast cancer. Current treatment strategies include whole brain radiotherapy, stereotactic radio surgery and surgical resection and most of the time these modalities are merely palliative without significantly improving the overall survival. Novel strategies are being employed for the treatment of metastatic tumors for the improved delivery of chemotherapy but unfortunately, these new strategies fail to show any beneficial improvement in overall patient survival.

2.7 References

Abbott, N. J., A. A. Patabendige, D. E. Dolman, S. R. Yusof and D. J. Begley (2010). "Structure and function of the blood-brain barrier." <u>Neurobiol Dis</u> **37**(1): 13-25.

Abbott, N. J., A. A. K. Patabendige, D. E. M. Dolman, S. R. Yusof and D. J. Begley (2010). "Structure and function of the blood–brain barrier." <u>Neurobiology of Disease</u> **37**(1): 13-25.

Adkins, C. E., M. I. Nounou, T. Hye, A. S. Mohammad, T. Terrell-Hall, N. K. Mohan, M. A. Eldon, U. Hoch and P. R. Lockman (2015). "NKTR-102 Efficacy versus irinotecan in a mouse model of brain metastases of breast cancer." <u>BMC Cancer</u> **15**: 685.

Aoyama, H., H. Shirato, M. Tago, K. Nakagawa, T. Toyoda, K. Hatano, M. Kenjyo, N. Oya, S. Hirota, H. Shioura, E. Kunieda, T. Inomata, K. Hayakawa, N. Katoh and G. Kobashi (2006). "Stereotactic radiosurgery plus whole-brain radiation therapy vs stereotactic radiosurgery alone for treatment of brain metastases: a randomized controlled trial." <u>Jama</u> **295**(21): 2483-2491.

Arvanitis, C. D., M. S. Livingstone, N. Vykhodtseva and N. McDannold (2012). "Controlled ultrasound-induced blood-brain barrier disruption using passive acoustic emissions monitoring." <u>PLoS One</u> **7**(9): e45783.

Aryal, M., N. Vykhodtseva, Y. Z. Zhang, J. Park and N. McDannold (2013). "Multiple treatments with liposomal doxorubicin and ultrasound-induced disruption of blood-tumor and blood-brain barriers improve outcomes in a rat glioma model." <u>J Control Release</u> **169**(1-2): 103-111.

Attwell, D., A. M. Buchan, S. Charpak, M. Lauritzen, B. A. Macvicar and E. A. Newman (2010). "Glial and neuronal control of brain blood flow." Nature **468**(7321): 232-243.

Ballabh, P., A. Braun and M. Nedergaard (2004). "The blood-brain barrier: an overview: structure, regulation, and clinical implications." Neurobiol Dis **16**(1): 1-13.

Bertossi, M., D. Virgintino, E. Maiorano, M. Occhiogrosso and L. Roncali (1997). "Ultrastructural and morphometric investigation of human brain capillaries in normal and peritumoral tissues." Ultrastruct Pathol **21**(1): 41-49.

Betz, C., A. Lenard, H. G. Belting and M. Affolter (2016). "Cell behaviors and dynamics during angiogenesis." **143**(13): 2249-2260.

Blasberg, R. G., J. Gazendam, C. S. Patlak, W. S. Shapiro and J. D. Fenstermacher (1980). "Changes in blood-brain transfer parameters induced by hyperosmolar intracarotid infusion and by metastatic tumor growth." Adv Exp Med Biol **131**: 307-319.

Bobo, R. H., D. W. Laske, A. Akbasak, P. F. Morrison, R. L. Dedrick and E. H. Oldfield (1994). "Convection-enhanced delivery of macromolecules in the brain." Proc Natl Acad Sci U S A **91**(6): 2076-2080.

Boccardo, F., B. Kaufman, J. Baselga, V. Dieras, J. Link, M. A. Casey, A. Fittipaldo, C. Oliva, D. Zembryki and S. D. Rubin (2008). "Evaluation of lapatinib (Lap) plus capecitabine (Cap) in patients with brain metastases (BM) from HER2+ breast cancer (BC) enrolled in the Lapatinib Expanded Access Program (LEAP) and French Authorisation Temporaire d'Utilisation (ATU)." Journal of Clinical Oncology **26**(15_suppl): 1094-1094.

Boogerd, W., O. Dalesio, E. M. Bais and J. J. van der Sande (1992). "Response of brain metastases from breast cancer to systemic chemotherapy." Cancer **69**(4): 972-980.

Bradbury, M. W., J. Stubbs, I. E. Hughes and P. Parker (1963). "The distribution of potassium, sodium, chloride and urea between lumbar cerebrospinal fluid and blood serum in human subjects." Clin Sci **25**: 97-105.

Cassier, P. A., I. Ray-Coquard, M. P. Sunyach, L. Lancry, J. P. Guastalla, C. Ferlay, F. Gomez, H. Cure, A. Lortholary, L. Claude, J. Y. Blay and T. Bachelot (2008). "A phase 2 trial of whole-brain radiotherapy combined with intravenous chemotherapy in patients with brain metastases from breast cancer." Cancer **113**(9): 2532-2538.

Chang, E. L., J. S. Wefel, K. R. Hess, P. K. Allen, F. F. Lang, D. G. Kornguth, R. B. Arbuckle, J. M. Swint, A. S. Shiu, M. H. Maor and C. A. Meyers (2009). "Neurocognition in patients with brain metastases treated with radiosurgery or radiosurgery plus whole-brain irradiation: a randomised controlled trial." Lancet Oncol **10**(11): 1037-1044.

Christodoulou, C., D. Bafaloukos, H. Linardou, G. Aravantinos, A. Bamias, M. Carina, G. Klouvas, D. Skarlos and G. Hellenic Cooperative Oncology (2005). "Temozolomide (TMZ) combined with cisplatin (CDDP) in patients with brain metastases from solid tumors: a Hellenic Cooperative Oncology Group (HeCOG) Phase II study." J Neurooncol **71**(1): 61-65.

Cindric, M., S. Jambon, A. Harej, S. Depauw, M. H. David-Cordonnier, S. Kraljevic Pavelic, G. Karminski-Zamola and M. Hranjec (2017). "Novel amidino substituted benzimidazole and benzothiazole benzo[b]thieno-2-carboxamides exert strong antiproliferative and DNA binding properties." Eur J Med Chem **136**: 468-479.

Coomber, B. L. and P. A. Stewart (1985). "Morphometric analysis of CNS microvascular endothelium." Microvasc Res **30**(1): 99-115.

Cordon-Cardo, C., J. P. O'Brien, D. Casals, L. Rittman-Grauer, J. L. Biedler, M. R. Melamed and J. R. Bertino (1989). "Multidrug-resistance gene (P-glycoprotein) is expressed by endothelial cells at blood-brain barrier sites." Proc Natl Acad Sci U S A **86**(2): 695-698.

Dar, M. (2009). Methods For The Treatment of Central Nervous System Tumors, Google Patents.

Diaz, R. J., P. Z. McVeigh, M. A. O'Reilly, K. Burrell, M. Bebenek, C. Smith, A. B. Etame, G. Zadeh, K. Hynynen, B. C. Wilson and J. T. Rutka (2014). "Focused ultrasound delivery of Raman nanoparticles across the blood-brain barrier: potential for targeting experimental brain tumors." Nanomedicine **10**(5): 1075-1087.

Dombrowski, S. M., S. Y. Desai, M. Marroni, L. Cucullo, K. Goodrich, W. Bingaman, M. R. Mayberg, L. Bengez and D. Janigro (2001). "Overexpression of multiple drug resistance genes in endothelial cells from patients with refractory epilepsy." Epilepsia **42**(12): 1501-1506.

Eldon, M. A., S. S. Harite and T. L. Barker (2010). Compositions and methods for achieving sustained therapeutic drug concentrations in a subject, Google Patents.

Emerich, D. F., P. Snodgrass, M. Pink, F. Bloom and R. T. Bartus (1998). "Central analgesic actions of loperamide following transient permeation of the blood brain barrier with Cereport (RMP-7)." Brain Res **801**(1-2): 259-266.

Fabel, K., J. Dietrich, P. Hau, C. Wismeth, B. Winner, S. Przywara, A. Steinbrecher, W. Ullrich and U. Bogdahn (2001). "Long-term stabilization in patients with malignant glioma after treatment with liposomal doxorubicin." Cancer **92**(7): 1936-1942.

Fewer, D., C. B. Wilson, E. B. Boldrey and J. K. Enot (1972). "Phase II study of 1-(2-chloroethyl)-3-cyclohexyl-1-nitrosourea (CCNU; NSC-79037) in the treatment of brain tumors." Cancer Chemother Rep **56**(3): 421-427.

Fisher, B. (2008). "Biological Research in the Evolution of Cancer Surgery: A Personal Perspective." Cancer Research **68**(24): 10007.

Folkman, J. (1971). "Tumor angiogenesis: therapeutic implications." N Engl J Med **285**(21): 1182-1186.

Franciosi, V., G. Cocconi, M. Michiara, F. Di Costanzo, V. Fosser, M. Tonato, P. Carlini, C. Boni and S. Di Sarra (1999). "Front-line chemotherapy with cisplatin and etoposide for patients with brain metastases from breast carcinoma, nonsmall cell lung carcinoma, or malignant melanoma: a prospective study." Cancer **85**(7): 1599-1605.

Freedman, R. A., E. Bullitt, L. Sun, R. Gelman, G. Harris, J. A. Ligibel, I. E. Krop, A. H. Partridge, E. Eisenberg, E. P. Winer and N. U. Lin (2011). "A phase II study of sagopilone (ZK 219477; ZK-EPO) in patients with breast cancer and brain metastases." Clin Breast Cancer **11**(6): 376-383.

Front, D., O. Israel, S. Kohn and I. Nir (1984). "The blood-tissue barrier of human brain tumors: correlation of scintigraphic and ultrastructural findings: concise communication." J Nucl Med **25**(4): 461-465.

Gelperina, S., O. Maksimenko, A. Khalansky, L. Vanchugova, E. Shipulo, K. Abbasova, R. Berdiev, S. Wohlfart, N. Chepurnova and J. Kreuter (2010). "Drug delivery to the brain using surfactant-coated poly(lactide-co-glycolide) nanoparticles: influence of the formulation parameters." <u>Eur J Pharm Biopharm</u> **74**(2): 157-163.

Ghersi-Egea, J. F., W. Finnegan, J. L. Chen and J. D. Fenstermacher (1996). "Rapid distribution of intraventricularly administered sucrose into cerebrospinal fluid cisterns via subarachnoid velae in rat." <u>Neuroscience</u> **75**(4): 1271-1288.

Ghersi-Egea, J. F., P. D. Gorevic, J. Ghiso, B. Frangione, C. S. Patlak and J. D. Fenstermacher (1996). "Fate of cerebrospinal fluid-borne amyloid beta-peptide: rapid clearance into blood and appreciable accumulation by cerebral arteries." <u>J Neurochem</u> **67**(2): 880-883.

Gingrich, M. B. and S. F. Traynelis (2000). "Serine proteases and brain damage - is there a link?" <u>Trends Neurosci</u> **23**(9): 399-407.

Gonzalez-Mariscal, L., R. Tapia and D. Chamorro (2008). "Crosstalk of tight junction components with signaling pathways." <u>Biochim Biophys Acta</u> **1778**(3): 729-756.

Gordon, G. R., C. Howarth and B. A. MacVicar (2011). "Bidirectional control of arteriole diameter by astrocytes." <u>Exp Physiol</u> **96**(4): 393-399.

Groothuis, D. R., J. M. Fischer, J. F. Pasternak, R. G. Blasberg, N. A. Vick and D. D. Bigner (1983). "Regional measurements of blood-to-tissue transport in experimental RG-2 rat gliomas." <u>Cancer Res</u> **43**(7): 3368-3373.

Gutin, P. H., C. B. Wilson, A. R. Kumar, E. B. Boldrey, V. Levin, M. Powell and K. J. Enot (1975). "Phase II study of procarbazine, CCNU, and vincristine combination chemotherapy in the treatment of malignant brain tumors." Cancer **35**(5): 1398-1404.

Hansen, A. J. (1985). "Effect of anoxia on ion distribution in the brain." Physiological Reviews **65**(1): 101-148.

Hofer, E. and B. Schweighofer (2007). "Signal transduction induced in endothelial cells by growth factor receptors involved in angiogenesis." Thromb Haemost **97**(3): 355-363.

Hoffmann, J., I. Fichtner, M. Lemm, P. Lienau, H. Hess-Stumpp, A. Rotgeri, B. Hofmann and U. Klar (2009). "Sagopilone crosses the blood-brain barrier in vivo to inhibit brain tumor growth and metastases." Neuro Oncol **11**(2): 158-166.

Hutchison, R., T. Z. Vitalis and R. Gabathuler (2013). P97-antibody conjugates and methods of use, Google Patents.

Hynynen, K., N. McDannold, N. A. Sheikov, F. A. Jolesz and N. Vykhodtseva (2005). "Local and reversible blood-brain barrier disruption by noninvasive focused ultrasound at frequencies suitable for trans-skull sonications." Neuroimage **24**(1): 12-20.

Hynynen, K., N. McDannold, N. Vykhodtseva and F. A. Jolesz (2001). "Noninvasive MR imaging-guided focal opening of the blood-brain barrier in rabbits." Radiology **220**(3): 640-646.

Inamura, T. and K. L. Black (1994). "Bradykinin selectively opens blood-tumor barrier in experimental brain tumors." J Cereb Blood Flow Metab **14**(5): 862-870.

Isakoff, S. J., E. L. Mayer, L. He, T. A. Traina, L. A. Carey, K. J. Krag, H. S. Rugo, M. C. Liu, V. Stearns, S. E. Come, K. M. Timms, A. R. Hartman, D. R. Borger, D. M. Finkelstein, J. E. Garber, P. D. Ryan, E. P. Winer, P. E. Goss and L. W. Ellisen (2015). "TBCRC009: A Multicenter Phase II Clinical Trial of Platinum Monotherapy With Biomarker Assessment in Metastatic Triple-Negative Breast Cancer." J Clin Oncol **33**(17): 1902-1909.

Iwamoto, F. M., A. M. Omuro, J. J. Raizer, C. P. Nolan, A. Hormigo, A. B. Lassman, I. T. Gavrilovic and L. E. Abrey (2008). "A phase II trial of vinorelbine and intensive temozolomide for patients with recurrent or progressive brain metastases." J Neurooncol **87**(1): 85-90.

Janzer, R. C. and M. C. Raff (1987). "Astrocytes induce blood-brain barrier properties in endothelial cells." Nature **325**(6101): 253-257.

Jo, Y. J. and Y. J. Yang (2011). Methods for treating brain tumors, Google Patents.

Jones, R. M., M. A. O'Reilly and K. Hynynen (2013). "Transcranial passive acoustic mapping with hemispherical sparse arrays using CT-based skull-specific aberration corrections: a simulation study." Phys Med Biol **58**(14): 4981-5005.

Kaye, E. A., J. Chen and K. B. Pauly (2011). "Rapid MR-ARFI method for focal spot localization during focused ultrasound therapy." Magn Reson Med **65**(3): 738-743.

Kelly, P. J., N. U. Lin, E. B. Claus, E. C. Quant, S. E. Weiss and B. M. Alexander (2012). "Salvage stereotactic radiosurgery for breast cancer brain metastases: outcomes and prognostic factors." Cancer **118**(8): 2014-2020.

Kemper, E. M., W. Boogerd, I. Thuis, J. H. Beijnen and O. van Tellingen (2004). "Modulation of the blood-brain barrier in oncology: therapeutic opportunities for the treatment of brain tumours?" Cancer Treat Rev **30**(5): 415-423.

Kioi, M., S. R. Husain, D. Croteau, S. Kunwar and R. K. Puri (2006). "Convection-enhanced delivery of interleukin-13 receptor-directed cytotoxin for malignant glioma therapy." Technol Cancer Res Treat **5**(3): 239-250.

Kocher, M., R. Soffietti, U. Abacioglu, S. Villa, F. Fauchon, B. G. Baumert, L. Fariselli, T. Tzuk-Shina, R. D. Kortmann, C. Carrie, M. Ben Hassel, M. Kouri, E. Valeinis, D. van den Berge, S. Collette, L. Collette and R. P. Mueller (2011). "Adjuvant whole-brain radiotherapy versus observation after radiosurgery or surgical resection of one to three cerebral metastases: results of the EORTC 22952-26001 study." J Clin Oncol **29**(2): 134-141.

Kofman, S., J. S. Garvin, D. Nagamani and S. G. Taylor, 3rd (1957). "Treatment of cerebral metastases from breast carcinoma with prednisolone." J Am Med Assoc **163**(16): 1473-1476.

Kreisl, W. C., J. S. Liow, N. Kimura, N. Seneca, S. S. Zoghbi, C. L. Morse, P. Herscovitch, V. W. Pike and R. B. Innis (2010). "P-glycoprotein function at the blood-brain barrier in humans can be quantified with the substrate radiotracer 11C-N-desmethyl-loperamide." J Nucl Med **51**(4): 559-566.

Kume, T. (2009). "Novel insights into the differential functions of Notch ligands in vascular formation." J Angiogenes Res **1**: 8.

Kunwar, S. (2003). "Convection enhanced delivery of IL13-PE38QQR for treatment of recurrent malignant glioma: presentation of interim findings from ongoing phase 1 studies." Acta Neurochir Suppl **88**: 105-111.

Kuo, Y. C., P. I. Lin and C. C. Wang (2011). "Targeting nevirapine delivery across human brain microvascular endothelial cells using transferrin-grafted poly(lactide-co-glycolide) nanoparticles." Nanomedicine (Lond) **6**(6): 1011-1026.

Kurzrock, R., N. Gabrail, C. Chandhasin, S. Moulder, C. Smith, A. Brenner, K. Sankhala, A. Mita, K. Elian, D. Bouchard and J. Sarantopoulos (2012). "Safety, pharmacokinetics, and activity of GRN1005, a novel conjugate of angiopep-2, a peptide facilitating brain penetration, and paclitaxel, in patients with advanced solid tumors." Mol Cancer Ther **11**(2): 308-316.

Labidi, S. I., T. Bachelot, I. Ray-Coquard, K. Mosbah, I. Treilleux, J. Fayette, B. Favier, G. Galy, J. Y. Blay and J. P. Guastalla (2009). "Bevacizumab and paclitaxel for breast cancer patients with central nervous system metastases: a case series." Clin Breast Cancer **9**(2): 118-121.

Lamar, R. E., F. A. Greco, D. H. Johnson, P. B. Murphy and J. D. Hainsworth (1994). "High-dose, brief duration, multiagent chemotherapy for metastatic breast cancer." Cancer **73**(7): 1842-1848.

Laughlin, M. (2010). Method of treating brain cancer, Google Patents.

LeBlanc, A. J., L. Krishnan, C. J. Sullivan, S. K. Williams and J. B. Hoying (2012). "Microvascular repair: post-angiogenesis vascular dynamics." Microcirculation **19**(8): 676-695.

Lin, N. U., J. R. Bellon and E. P. Winer (2004). "CNS metastases in breast cancer." J Clin Oncol **22**(17): 3608-3617.

Linot, B., M. Campone, P. Augereau, R. Delva, S. Abadie-Lacourtoisie, N. Nebout-Mesgouez and O. Capitain (2014). "Use of liposomal doxorubicin-cyclophosphamide combination in breast cancer patients with brain metastases: a monocentric retrospective study." J Neurooncol **117**(2): 253-259.

Liu, H. L., M. Y. Hua, P. Y. Chen, P. C. Chu, C. H. Pan, H. W. Yang, C. Y. Huang, J. J. Wang, T. C. Yen and K. C. Wei (2010). "Blood-brain barrier disruption with focused ultrasound enhances delivery of chemotherapeutic drugs for glioblastoma treatment." Radiology **255**(2): 415-425.

Liu, L. B., Y. X. Xue and Y. H. Liu (2010). "Bradykinin increases the permeability of the blood-tumor barrier by the caveolae-mediated transcellular pathway." J Neurooncol **99**(2): 187-194.

Liu, L. B., Y. X. Xue, Y. H. Liu and Y. B. Wang (2008). "Bradykinin increases blood-tumor barrier permeability by down-regulating the expression levels of ZO-1, occludin, and claudin-5 and rearranging actin cytoskeleton." J Neurosci Res **86**(5): 1153-1168.

Lockman, P. R., R. K. Mittapalli, K. S. Taskar, V. Rudraraju, B. Gril, K. A. Bohn, C. E. Adkins, A. Roberts, H. R. Thorsheim, J. A. Gaasch, S. Huang, D. Palmieri, P. S. Steeg and Q. R. Smith (2010). "Heterogeneous blood-tumor barrier permeability determines drug efficacy in experimental brain metastases of breast cancer." Clin Cancer Res **16**(23): 5664-5678.

Lockman, P. R., R. K. Mittapalli, K. S. Taskar, V. Rudraraju, B. Gril, K. A. Bohn, C. E. Adkins, A. Roberts, H. R. Thorsheim, J. A. Gaasch, S. Huang, D. Palmieri, P. S. Steeg and Q. R. Smith

(2010). "Heterogeneous Blood-Tumor Barrier Permeability Determines Drug Efficacy in Experimental Brain Metastases of Breast Cancer." Clinical cancer research : an official journal of the American Association for Cancer Research **16**(23): 5664-5678.

Löscher, W. and H. Potschka (2005). "Role of drug efflux transporters in the brain for drug disposition and treatment of brain diseases." Progress in Neurobiology **76**(1): 22-76.

McChesney, J. D., G. Tapolsky, D. L. Emerson, J. Marshall, T. Ahmed, A. COHN, M. KURMAN and M. MODIANO (2011). Taxane analogs for the treatment of brain cancer, Google Patents.

McDannold, N., C. D. Arvanitis, N. Vykhodtseva and M. S. Livingstone (2012). "Temporary disruption of the blood-brain barrier by use of ultrasound and microbubbles: safety and efficacy evaluation in rhesus macaques." Cancer Res **72**(14): 3652-3663.

Metro, G., J. Foglietta, M. Russillo, L. Stocchi, A. Vidiri, D. Giannarelli, L. Crino, P. Papaldo, M. Mottolese, F. Cognetti, A. Fabi and S. Gori (2011). "Clinical outcome of patients with brain metastases from HER2-positive breast cancer treated with lapatinib and capecitabine." Ann Oncol **22**(3): 625-630.

Miles, D. W., A. Chan, L. Y. Dirix, J. Cortes, X. Pivot, P. Tomczak, T. Delozier, J. H. Sohn, L. Provencher, F. Puglisi, N. Harbeck, G. G. Steger, A. Schneeweiss, A. M. Wardley, A. Chlistalla and G. Romieu (2010). "Phase III study of bevacizumab plus docetaxel compared with placebo plus docetaxel for the first-line treatment of human epidermal growth factor receptor 2-negative metastatic breast cancer." J Clin Oncol **28**(20): 3239-3247.

Miller, K., M. Wang, J. Gralow, M. Dickler, M. Cobleigh, E. A. Perez, T. Shenkier, D. Cella and N. E. Davidson (2007). "Paclitaxel plus bevacizumab versus paclitaxel alone for metastatic breast cancer." <u>N Engl J Med</u> **357**(26): 2666-2676.

Minn, A., J. F. Ghersi-Egea, R. Perrin, B. Leininger and G. Siest (1991). "Drug metabolizing enzymes in the brain and cerebral microvessels." <u>Brain Res Brain Res Rev</u> **16**(1): 65-82.

Mueller, C. B. and W. Jeffries (1975). "Cancer of the breast: Its outcome as measured by the rate of dying and causes of death." <u>Ann Surg</u> **182**(3): 334-341.

Nadal, A., E. Fuentes, J. Pastor and P. A. McNaughton (1995). "Plasma albumin is a potent trigger of calcium signals and DNA synthesis in astrocytes." <u>Proc Natl Acad Sci U S A</u> **92**(5): 1426-1430.

Nagaraja, T. N., P. Patel, M. Gorski, P. D. Gorevic, C. S. Patlak and J. D. Fenstermacher (2005). "In normal rat, intraventricularly administered insulin-like growth factor-1 is rapidly cleared from CSF with limited distribution into brain." <u>Cerebrospinal Fluid Res</u> **2**: 5.

Nakagawa, H., D. Groothuis and R. G. Blasberg (1984). "The effect of graded hypertonic intracarotid infusions on drug delivery to experimental RG-2 gliomas." <u>Neurology</u> **34**(12): 1571-1581.

Nanda, R., L. Q. Chow, E. C. Dees, R. Berger, S. Gupta, R. Geva, L. Pusztai, M. Dolled-Filhart, K. Emancipator, E. J. Gonzalez, J. Houp, K. Pathiraja, V. Karantza, R. Iannone, C. K. Gause, J. D. Cheng and L. Buisseret (2015). "Abstract S1-09: A phase Ib study of pembrolizumab (MK-3475) in patients with advanced triple-negative breast cancer." <u>Cancer Research</u> **75**(9 Supplement): S1-09.

Neuwelt, E. A., D. L. Goldman, S. A. Dahlborg, J. Crossen, F. Ramsey, S. Roman-Goldstein, R. Braziel and B. Dana (1991). "Primary CNS lymphoma treated with osmotic blood-brain barrier disruption: prolonged survival and preservation of cognitive function." <u>J Clin Oncol</u> **9**(9): 1580-1590.

Nevinny, H. B., T. C. Hall, C. Haines and M. J. Krant (1968). "Comparison of methotrexate (NSC-740) and testosterone propionate (NSC-9166) in the treatment of breast cancer." <u>J Clin Pharmacol J New Drugs</u> **8**(2): 126-129.

Oldendorf, W. H. (1974). "Blood-Brain Barrier Permeability to Drugs." <u>Annual Review of Pharmacology</u> **14**(1): 239-248.

Omuro, A. M., J. J. Raizer, A. Demopoulos, M. G. Malkin and L. E. Abrey (2006). "Vinorelbine combined with a protracted course of temozolomide for recurrent brain metastases: a phase I trial." <u>J Neurooncol</u> **78**(3): 277-280.

Ostrom, Q. T., H. Gittleman, J. Xu, C. Kromer, Y. Wolinsky, C. Kruchko and J. S. Barnholtz-Sloan (2016). "CBTRUS Statistical Report: Primary Brain and Other Central Nervous System Tumors Diagnosed in the United States in 2009-2013." <u>Neuro Oncol</u> **18**(suppl_5): v1-v75.

Paget, S. (1889). "The distribution of secondary growths in cancer of the breast." <u>The Lancet</u> **133**(3421): 571-573.

Palade, G. E. (1961). "Blood capillaries of the heart and other organs." <u>Circulation</u> **24**: 368-388.

Pathan, S. A., Z. Iqbal, S. M. Zaidi, S. Talegaonkar, D. Vohra, G. K. Jain, A. Azeem, N. Jain, J. R. Lalani, R. K. Khar and F. J. Ahmad (2009). "CNS drug delivery systems: novel approaches." Recent Pat Drug Deliv Formul **3**(1): 71-89.

Peppiatt, C. M., C. Howarth, P. Mobbs and D. Attwell (2006). "Bidirectional control of CNS capillary diameter by pericytes." Nature **443**(7112): 700-704.

Perry, J., A. Chambers, K. Spithoff and N. Laperriere (2007). "Gliadel wafers in the treatment of malignant glioma: a systematic review." Current Oncology **14**(5): 189-194.

Phillips, C., R. Jeffree and M. Khasraw (2017). "Management of breast cancer brain metastases: A practical review." Breast **31**: 90-98.

Pienta, K. J., B. A. Robertson, D. S. Coffey and R. S. Taichman (2013). "The Cancer Diaspora: Metastasis beyond the seed and soil hypothesis." Clinical cancer research : an official journal of the American Association for Cancer Research **19**(21): 10.1158/1078-0432.CCR-1113-2158.

Groothuis, D. R., P. C. Warkne, P. Molnar, G. D. Lapin and M. A. Mikhael (1990). "Effect of hyperosmotic blood-brain barrier disruption on transcapillary transport in canine brain tumors." J Neurosurg **72**(3): 441-449.

Raffa, R. B. (2010). "Is a picture worth a thousand (forgotten) words?: neuroimaging evidence for the cognitive deficits in 'chemo-fog'/'chemo-brain'." J Clin Pharm Ther **35**(1): 1-9.

Rapoport, S. I. (2001). "Advances in osmotic opening of the blood-brain barrier to enhance CNS chemotherapy." Expert Opin Investig Drugs **10**(10): 1809-1818.

Rapoport, S. I., M. Hori and I. Klatzo (1972). "Testing of a hypothesis for osmotic opening of the blood-brain barrier." Am J Physiol **223**(2): 323-331.

Rapoport, S. I. and P. J. Robinson (1986). "Tight-junctional modification as the basis of osmotic opening of the blood-brain barrier." Ann N Y Acad Sci **481**: 250-267.

Reese, T. S. and M. J. Karnovsky (1967). "Fine structural localization of a blood-brain barrier to exogenous peroxidase." J Cell Biol **34**(1): 207-217.

Ricciardi, G. R., A. Russo, T. Franchina, G. Ferraro and V. Adamo (2015). "Efficacy of nab-paclitaxel plus trastuzumab in a long-surviving heavily pretreated HER2-positive breast cancer patient with brain metastases." Onco Targets Ther **8**: 289-294.

Roe, M., A. Folkes, P. Ashworth, J. Brumwell, L. Chima, S. Hunjan, I. Pretswell, W. Dangerfield, H. Ryder and P. Charlton (1999). "Reversal of P-glycoprotein mediated multidrug resistance by novel anthranilamide derivatives." Bioorg Med Chem Lett **9**(4): 595-600.

Rosner, D., T. Nemoto and W. W. Lane (1986). "Chemotherapy induces regression of brain metastases in breast carcinoma." Cancer **58**(4): 832-839.

Saenz del Burgo, L., R. M. Hernandez, G. Orive and J. L. Pedraz (2014). "Nanotherapeutic approaches for brain cancer management." Nanomedicine **10**(5): 905-919.

Sampson, J. H., G. Akabani, A. H. Friedman, D. Bigner, S. Kunwar, M. S. Berger and K. S. Bankiewicz (2006). "Comparison of intratumoral bolus injection and convection-enhanced delivery of radiolabeled antitenascin monoclonal antibodies." Neurosurgical Focus **20**(4): E14.

Sampson, J. H., G. Archer, C. Pedain, E. Wembacher-Schröder, M. Westphal, S. Kunwar, M. A. Vogelbaum, A. Coan, J. E. Herndon, R. Raghavan, M. L. Brady, D. A. Reardon, A. H. Friedman, H. S. Friedman, M. I. Rodríguez-Ponce, S. M. Chang, S. Mittermeyer, D. Croteau and R. K. Puri (2009). "Poor drug distribution as a possible explanation for the results of the PRECISE trial." Journal of Neurosurgery **113**(2): 301-309.

Sant, M., R. Capocaccia, A. Verdecchia, J. Esteve, G. Gatta, A. Micheli, M. P. Coleman and F. Berrino (1998). "Survival of women with breast cancer in Europe: variation with age, year of diagnosis and country. The EUROCARE Working Group." Int J Cancer **77**(5): 679-683.

Shang, X., P. Wang, Y. Liu, Z. Zhang and Y. Xue (2011). "Mechanism of low-frequency ultrasound in opening blood-tumor barrier by tight junction." J Mol Neurosci **43**(3): 364-369.

Sheikov, N., N. McDannold, S. Sharma and K. Hynynen (2008). "Effect of Focused Ultrasound Applied With an Ultrasound Contrast Agent on the Tight Junctional Integrity of the Brain Microvascular Endothelium." Ultrasound in Medicine & Biology **34**(7): 1093-1104.

Somjen, G. G. (2002). "Ion regulation in the brain: implications for pathophysiology." Neuroscientist **8**(3): 254-267.

Talmadge, J. E. and I. J. Fidler (2010). "AACR Centennial Series: The Biology of Cancer Metastasis: Historical Perspective." Cancer research **70**(14): 5649-5669.

Tanner, P. G., M. Holtmannspotter, J. C. Tonn and R. Goldbrunner (2007). "Effects of drug efflux on convection-enhanced paclitaxel delivery to malignant gliomas: technical note." Neurosurgery **61**(4): E880-882; discussion E882.

Thiebaut, F., T. Tsuruo, H. Hamada, M. M. Gottesman, I. Pastan and M. C. Willingham (1989). "Immunohistochemical localization in normal tissues of different epitopes in the multidrug transport protein P170: evidence for localization in brain capillaries and crossreactivity of one antibody with a muscle protein." J Histochem Cytochem **37**(2): 159-164.

Thomas, F. C., K. Taskar, V. Rudraraju, S. Goda, H. R. Thorsheim, J. A. Gaasch, R. K. Mittapalli, D. Palmieri, P. S. Steeg, P. R. Lockman and Q. R. Smith (2009). "Uptake of ANG1005, a novel paclitaxel derivative, through the blood-brain barrier into brain and experimental brain metastases of breast cancer." Pharm Res **26**(11): 2486-2494.

Thomas, H. and H. M. Coley (2003). "Overcoming multidrug resistance in cancer: an update on the clinical strategy of inhibiting p-glycoprotein." Cancer Control **10**(2): 159-165.

Toth, A., S. Veszelka, S. Nakagawa, M. Niwa and M. A. Deli (2011). "Patented in vitro blood-brain barrier models in CNS drug discovery." Recent Pat CNS Drug Discov **6**(2): 107-118.

Tsukada, Y., A. Fouad, J. W. Pickren and W. W. Lane (1983). "Central nervous system metastasis from breast carcinoma. Autopsy study." Cancer **52**(12): 2349-2354.

Vinolas, N., F. Graus, B. Mellado, L. Caralt and J. Estape (1997). "Phase II trial of cisplatinum and etoposide in brain metastases of solid tumors." J Neurooncol **35**(2): 145-148.

Warren, K., R. Jakacki, B. Widemann, A. Aikin, M. Libucha, R. Packer, G. Vezina, G. Reaman, D. Shaw, M. Krailo, C. Osborne, J. Cehelsky, D. Caldwell, J. Stanwood, S. M. Steinberg and F. M. Balis (2006). "Phase II trial of intravenous lobradimil and carboplatin in childhood brain tumors: a report from the Children's Oncology Group." Cancer Chemother Pharmacol **58**(3): 343-347.

Wei, K. C., P. C. Chu, H. Y. Wang, C. Y. Huang, P. Y. Chen, H. C. Tsai, Y. J. Lu, P. Y. Lee, I. C. Tseng, L. Y. Feng, P. W. Hsu, T. C. Yen and H. L. Liu (2013). "Focused ultrasound-induced blood-brain barrier opening to enhance temozolomide delivery for glioblastoma treatment: a preclinical study." PLoS One **8**(3): e58995.

Weihua, Z. (2013). Fructose-1,6-biphosphatases as new targets for diagnosing and treating breast cancer brain metastasis, Google Patents.

Weil, R. J., D. C. Palmieri, J. L. Bronder, A. M. Stark and P. S. Steeg (2005). "Breast cancer metastasis to the central nervous system." Am J Pathol **167**(4): 913-920.

Westphal, M., D. C. Hilt, E. Bortey, P. Delavault, R. Olivares, P. C. Warnke, I. R. Whittle, J. Jaaskelainen and Z. Ram (2003). "A phase 3 trial of local chemotherapy with biodegradable carmustine (BCNU) wafers (Gliadel wafers) in patients with primary malignant glioma." Neuro Oncol **5**(2): 79-88.

Williams, P. C., W. D. Henner, S. Roman-Goldstein, S. A. Dahlborg, R. E. Brummett, M. Tableman, B. W. Dana and E. A. Neuwelt (1995). "Toxicity and efficacy of carboplatin and etoposide in conjunction with disruption of the blood-brain tumor barrier in the treatment of intracranial neoplasms." Neurosurgery **37**(1): 17-27; discussion 27-18.

Wilson, W. L. and J. G. Delagarza (1965). "Systemic Chemotherapy for Cns Metastases of Solid Tumors." Arch Intern Med **115**: 710-713.

Witt, K. A., T. J. Gillespie, J. D. Huber, R. D. Egleton and T. P. Davis (2001). "Peptide drug modifications to enhance bioavailability and blood-brain barrier permeability." Peptides **22**(12): 2329-2343.

Yamamoto, D., S. Iwase, Y. Tsubota, N. Sueoka, C. Yamamoto, K. Kitamura, H. Odagiri and Y. Nagumo (2012). "Bevacizumab in the treatment of five patients with breast cancer and brain metastases: Japan Breast Cancer Research Network-07 trial." Onco Targets Ther **5**: 185-189.

Zünkeler, B., R. E. Carson, J. Olson, R. G. Blasberg, H. Devroom, R. J. Lutz, S. C. Saris, D. C. Wright, W. Kammerer, N. J. Patronas, R. L. Dedrick, P. Herscovitch and E. H. Oldfield (1996). "Quantification and pharmacokinetics of blood-brain barrier disruption in humans." Journal of Neurosurgery **85**(6): 1056-1065.
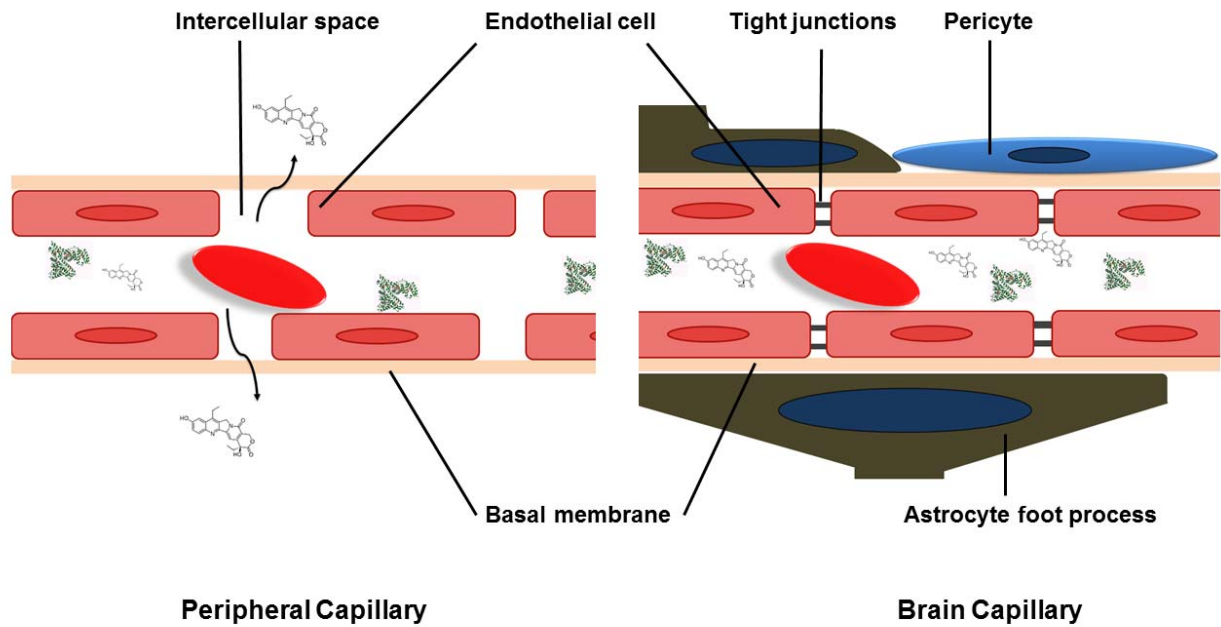
Figure 2.1: Cartoon depiction of peripheral capillary in comparison to brain capillary

Cartoon illustrating the blood-brain barrier. The structural differences between the two vessels is the presence of tight junction proteins, presence of pericytes and astrocyte foot process in brain capillary while, in peripheral capillary the endothelial cells have intercellular space and fenestrae without any additional cell structure making it more permeable when compared to brain capillary.
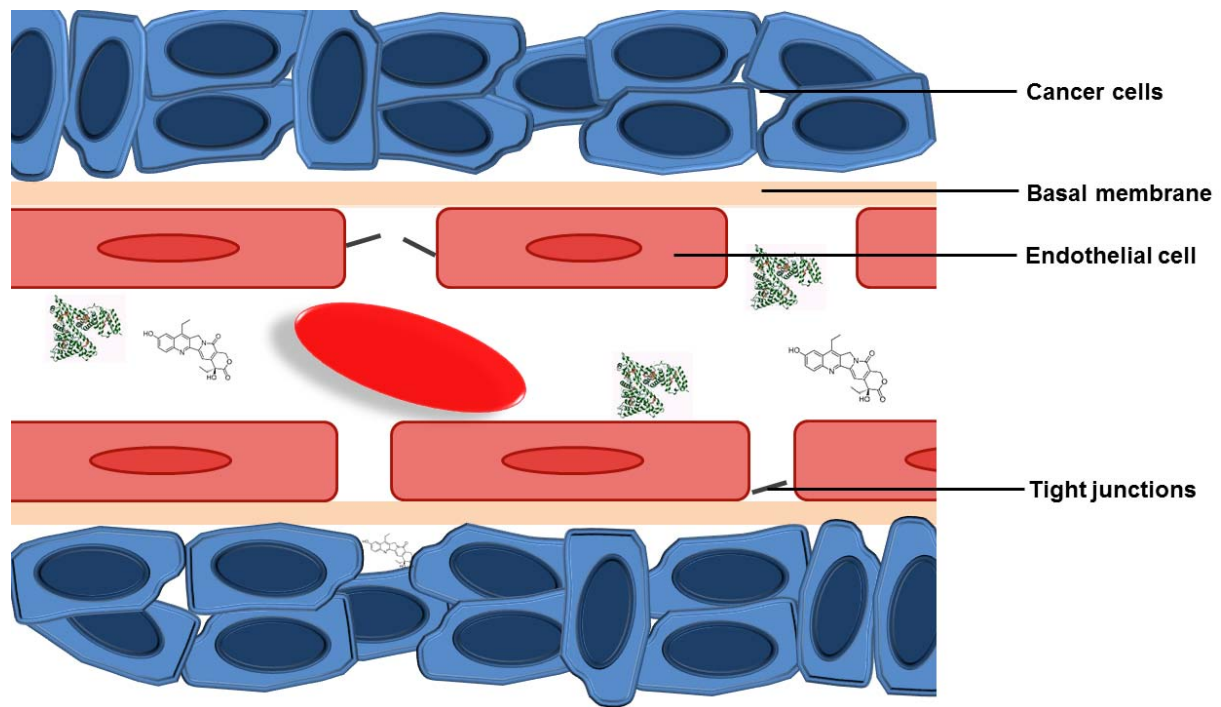
Blood-Tumor Barrier

Figure 2.2: Cartoon depicting capillary in brain tumor (Blood-tumor barrier).

Cartoon illustrating the blood-tumor barrier. A major structural difference between the Blood-tumor barrier and blood-brain barrier is decreased expression of tight junction proteins, which leads to an incomplete sealing of the vasculature in tumor, and increased permeability.
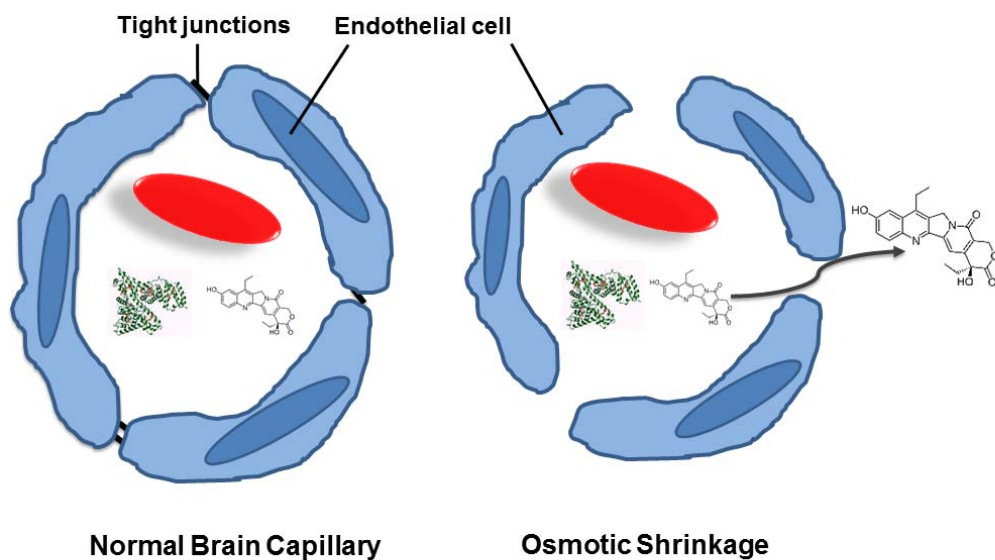
Figure 2.3: Cartoon depicting Blood-Brain Barrier disruption by osmotic shrinkage.

The figure illustrates the difference in brain capillary before and after intra-arterial

administration of hyperosmolar solution. The endothelial cells shrink due to loss of water after

administration of hyperosmolar compound, which will lead to loss of tight junctions.
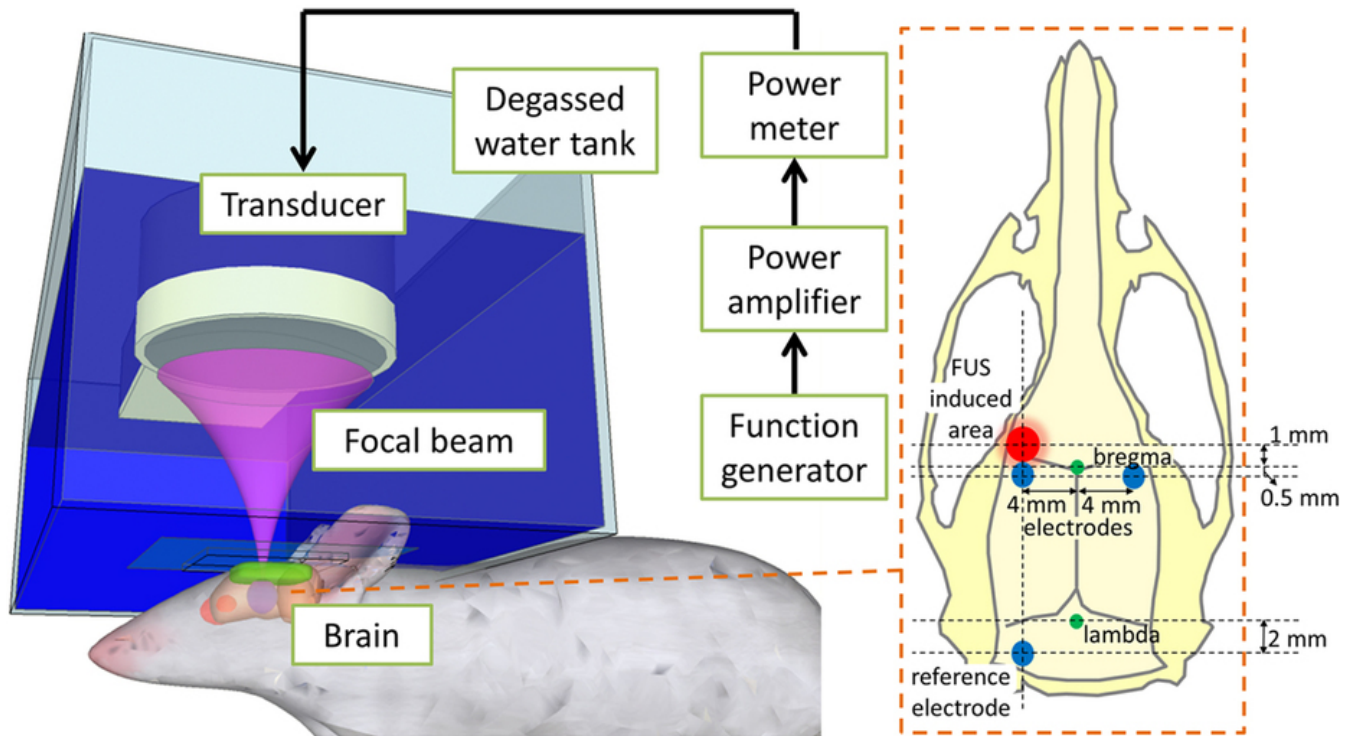
Figure 2.4: Cartoon depicting Blood-Brain Barrier disruption by osmotic shrinkage (Treat et al., 2007)

The animal is positioned with skull partially submerged in a de-gassed water tank and microbubbles are intravenously administered. A focused transducer attached to a network power and computer system delivers low frequency ultrasound, which disrupts the BBB. MRI is incorporated for targeting as well as BBB disruption visualization.

Table 2.1 On-going clinical trials in brain metastases of breast cancer

Clinical trial title	Intervention	Reference
A Study of Etirinotecan Pegol (NKTR-102) Versus Treatment of Physician's Choice (TPC) in Patients With Metastatic Breast Cancer Who Have Stable Brain Metastases and Have Been Previously Treated With an Anthracycline, a Taxane, and Capecitabine	Drug: NKTR-102 Drug: Eribulin Drug: Ixabepilone Drug: Vinorelbine Drug: Gemcitabine Dug:Paclitaxel Drug: Docetaxel Drug: Nab-paclitaxel	NCT02915744
ARRY-380 + Trastuzuamab for Breast w/ Brain Mets	Drug: ARRY-380 Twice Daily Dosage Drug: ARRY-380 Once Daily Drug: Trastuzumab	NCT01921335
A Study Of Everolimus, Trastuzumab And Vinorelbine In HER2-PositiveBreast Cancer Brain Metastases	Drug: Everolimus Drug: Vinorelbine Drug: Transtuzumab	NCT01305941
HKI-272 for HER2-Positive Breast Cancer and Brain Metastases	Drug: HKI-272 Procedure: Surgical Resection Drug: Capecitabine	NCT01494662

Clinical trial title	Intervention	Reference
Lapatinib for Brain Metastases In ErbB2-Positive Breast Cancer	Drug: Lapatinib	NCT00263588
STAR Cape+BKM120 MBC With Brain Met	Drug: BKM120	NCT02000882
	Drug: capecitabine	
	Drug: Trastuzumab	
PCI in Advanced Triple Negative Breast Cancer Patients Who Response to 1st Line Chemotherapy	Radiation: prophylactic cranial irradiation	NCT02448576
A Study of Local Therapy for the Treatment of Brain Metastases From HER2 Positive Breast Cancer	Other: Local Therapy	NCT02898727
Proteome-based Immunotherapy of Brain Metastases From Breast Cancer	Biological: Dendritic vaccine, allogeneic hematopoietic stem cells, cytotoxic lymphocytes	NCT01782274
	Biological: Dendritic vaccine, autologous hematopoietic stem cells, cytotoxic lymphocytes	

Clinical trial title	Intervention	Reference
Palbociclib in Treating Patients With Metastatic HER-2 Positive Breast Cancer With Brain Metastasis	Procedure: Cognitive Assessment Drug: Palbociclib Procedure: Quality-of-Life Assessment Biological: Transtuzumab	NCT02774681
A Study of Abemaciclib (LY2835219) in Participants With Breast Cancer, Non-small Cell Lung Cancer, or Melanoma That Has Spread to the Brain	Drug: Abemaciclib	NCT02308020
Whole-Brain Radiation Therapy or Stereotactic Radiosurgery With or Without Lapatinib Ditosylate in Treating Patients With Brain Metastasis From HER2-Positive Breast Cancer	Other: Laboratory Biomarker Analysis Drug: Lapatinib Ditosylate Radiation: Stereotactic Radiosurgery Radiation: Whole-Brain Radiotherapy	NCT01622868
Phase II Etirinotecan Pegol in Refractory Brain Metastases & Advanced Lung Cancer / Metastatic Breast Cancer	Drug: pegylated irinotecan NKTR 102 Other: laboratory biomarker analysis Stanford University, School of Medicine Stanford, California	NCT02312622
18F-FLT-PET Imaging of the Brain in Patients With Metastatic Breast Cancer to the Brain Treated With Whole Brain Radiation Therapy With or Without Sorafenib: Comparison With MR Imaging of the Brain	Device: 18F-FLT-PET Imaging	NCT01621906

Clinical trial title	Intervention	Reference
MM-398 (Nanoliposomal Irinotecan, Nal-IRI) to Determine Tumor Drug Levels and to Evaluate the Feasibility of Ferumoxytol Magnetic Resonance Imaging to Measure Tumor Associated Macrophages and to Predict Patient Response to Treatment	Drug: Ferumoxytol followed by MM-398	NCT01770353
Correlation Between Circulating Tumor Cells and Brain Disease Control After Focal Radiotherapy for Metastases of Breast Cancer	Diagnostic Test: Circulating tumor cells evaluation	NCT02941536
Stereotactic Radiation Therapy With or Without Whole-Brain Radiation Therapy in Treating Patients With Brain Metastases	Radiation: radiation therapy Radiation: stereotactic radiosurgery	NCT00377156
Cambridge Brain Mets Trial 1	Drug: Afatinib Radiation: 2 Gy targeted radiotherapy Radiation: 4 Gy targeted radiotherapy	NCT02768337
MEDI4736 (Durvalumab) in Patients With Brain Metastasis From Epithelial-derived Tumors	Drug: MEDI4736	NCT02669914
Lapatinib Plus Capecitabine Versus Trastuzumab Plus Capecitabine in ErbB2 (HER2) Positive Metastatic Breast Cancer	Drug: Capecitabine Drug: Lapatinib Drug: Trastuzumab	NCT00820222
A Pilot/Phase II Study of Gamma Knife Radiosurgery for Brain Metastases Using 3Tesla MRI and Rational Dose Selection	Procedure: Gamma Knife Radiosurgery	NCT02005614

Clinical trial title	Intervention	Reference
Phase 2 Study of Tucatinib vs Placebo in Combination With Capecitabine & Trastuzumab in Patients With Advanced HER2+ Breast Cancer	Drug: Tucatinib Drug: Capecitabine Drug: Trastuzumab Drug: Placebo	NCT02614794

CHAPTER 3

PHARMACOKINETICS OF A NANO-LIPOSOMAL FORMULATION IN AN EXPERIMENTAL BRAIN TUMOR MODEL OF TRIPLE NEGATIVE BREAST CANCER

3.1 Introduction

In spite of the progress in research for metastatic brain tumors, the primary treatment modality is whole brain radiation therapy (WBRT) and surgical resection (Lin, Amiri-Kordestani et al. 2013). Treatment with anticancer agents is particularly challenging because of presence of BBB/BTB and its related low permeability of various drugs (Pardridge 2003). Many new approaches are under investigation for CNS drug delivery but the unique issue with metastatic brain tumors is its randomness in spatial location within the brain. Most often, these metastatic brain tumors form multiple tumors and making it harder to surgically remove (Ramakrishna, Temin et al. 2014).

Nanoparticles like liposomes can be used to deliver anticancer agents and currently approved agents include Marqibo (liposomal vincristine, Talon Therapeutics, CA), Doxil (liposomal doxorubicin, Alza Pharmaceuticals Inc., CA), DaunoXome (liposomal daunorubicin, Gilead Inc., CA) (Rifkin, Gregory et al. 2006, Gibson, Alzghari et al. 2013, Andriyanov, Koren et al. 2014). In our previous studies, we demonstrated that irinotecan administered as Etirinotecan pegol (NKTR-102), not only improved the pharmacokinetics of irinotecan and its active

metabolite SN-38, it also improved the median survival in our preclinical metastases model (Adkins, Nounou et al. 2015). Irinotecan shows cytotoxic activity against many cancer types including breast cancer and malignant gliomas (Taguchi, Tominaga et al. 1994, Adkins, Nounou et al. 2015, Sengupta, Rojas et al. 2015). Irinotecan is a prodrug and it is converted SN-38 which is a potent topoisomerase I inhibitor and this conversion is dependent on carboxylesterase II (Kaneda, Nagata et al. 1990). This makes it a great case for drug delivery through carriers like liposomes as it evades premature conversion to SN-38 until it is delivered to brain metastases.

The BBB serves as a functional and structural barrier for the entry of most of the chemotherapeutic agents but growth of the intracranial tumors will alter the permeability characteristics. The BTB has increased permeability when compared to normal BBB due to reduced expression of tight junction proteins and increased angiogenic factor (Ballabh, Braun et al. 2004). Nanoparticles like liposomes with sizes in the range of 80-200 nm take the advantage of leaky tumor vasculature and distribute due to enhanced permeation and retention (EPR) effect (Drummond, Meyer et al. 2000). We hypothesize that liposomal irinotecan will have better brain tumor distribution than non-liposomal irinotecan by 1) increased passive diffusion from blood to tumor due to EPR effect 2) bypassing various efflux transporters present at the BBB/BTB and 3) increased plasma mean residence time (Kemper, Cleypool et al. 2004, Amzerin, Mokrim et al. 2015).

Here, we present encouraging pharmacokinetic (PK) results for liposomal irinotecan in an experimental brain tumor model when compared to non-liposomal irinotecan. Liposomal irinotecan showed prolonged plasma drug exposure with mean residence time (MRT) of 17.7 ± 3.8 h for SN-38, whereas MRT was 3.67 ± 1.2 for non-liposomal irinotecan. Further, liposomal irinotecan accumulated in metastatic lesions and demonstrated prolonged exposure of SN-38

compared to non-liposomal irinotecan. Liposomal irinotecan achieved AUC values of 6883 ± 4149 ng-h/g for SN-38, whereas non-liposomal irinotecan showed significantly lower AUC values of 982 ± 256 ng-h/g for SN-38.

3.2 Materials and Methods

Chemicals

Irinotecan HCl and nal-IRI were supplied by Merrimack Pharmaceuticals (Cambridge, US), which were prepared as reported by Noble et al. and Kalra et al. (Kalra, Kim et al. 2014, Noble, Krauze et al. 2014). The lipid mixture of nal-IRI consisting of distearoylphosphatidylcholine, cholesterol, and polyethyleneglycol-distearoylphosphatidyl-ethanolamine at the molar ration of 3:2:0.015 (Noble, Krauze et al. 2014). Irinotecan HCl was in the liposomes at a ratio of 750 g irinotecan HCl / mol phospholipid (Noble, Krauze et al. 2014). All other chemicals were analytical grade purchased from Sigma-Aldrich (St. Louis, MO).

Animals

Female athymic nude mice (Charles River Laboratories, Kingston, NY) were used for all experiments in the study. Mice were 6-8 weeks of age and weighed 22-28 g before injecting with cancer cells and were housed under 12-hour light/dark conditions with food and water *ad libitum,* and mice were acclimated for 1 week prior to use. All animal work was approved by West Virginia University Institutional Animal care and Use Committee (IACUC protocols 13-1207). All animal experiments were performed according to the principles of the *Guide for the Care and use of Laboratory animals.*

Cell Culture

Brain-seeking human triple negative breast cancer cells, transfected to express firefly luciferase (MDA-MB-231Br-Luc), were cultured in Dulbecco's Modified Eagle's Medium (DMEM) with 10% fetal bovine serum (FBS). Dr. Patricia Steeg, of the National Institute of Health Center for Cancer Research, kindly provided MDA-MB-231Br-Luc cells. All cell work was performed under aseptic conditions, and cells were cultured at 37°C with 5% CO_2.

Pharmacokinetic study of irinotecan and liposomal irinotecan in brain tumors

MDA-MB-231Br-Luc cells (5×10^5) cells were injected intra-cranially as described previously (Adkins, Nounou et al. 2015). Tumors were allowed to grow until neurological symptoms developed, and the animals were intravenously administered Non-liposomal irinotecan (50 mg/kg, IRN-50), and two different doses of liposomal irinotecan, 10 mg/kg (nal-IRI-10) and 50 mg/kg (nal-IRI-50). Non-liposomal irinotecan-treated animals (n=5/time point) were sacrificed at 0.083, 0.5, 1, 2, 6, 12 and 24 h after administration, and liposomal irinotecan treated animals (n=5/time point) were sacrificed at 0.5, 2, 6, 24, 72, 48 and 168 h after administration. The animals were anesthetized (ketamine/xylazine; 100 mg/kg and 8 mg/kg respectively) and then blood samples were collected before a washout with phosphate buffer saline at 5 ml/min flow rate. The animal was sacrificed by decapitation to collect brain and tumor samples. The blood was centrifuged at 13600 RPM for 5 minutes at 4°C and the plasma was separated and stored along with tumor samples at -80°C until analysis. Irinotecan and SN-38 concentrations in normal brain and brain tumor samples were analyzed by liquid chromatography-tandem mass spectrometry (LC/MS). Metabolite levels in plasma samples were measured using high performance liquid

chromatography (HPLC) methods reported previously (Kalra, Kim et al. 2014). The limit of quantification for irinotecan was 25 ng/ml and for its active metabolite, SN-38 was 2 ng/ml.

Pharmacokinetic analysis

Pharmacokinetic parameters of irinotecan and its active metabolite SN-38 were characterized by non-compartmental analysis (NCA)(Huang and Zheng 2010). NCA applies to linear pharmacokinetic models and it doesn't not assume specific compartmental model for drug or metabolite. In this method area under plasma concentration- time curve was calculated by the application of trapezoidal rule and this is often called as area under zero moment curve (AUC). The area under first moment curve (AUMC) refers to area under the product of time and the concentration versus time curve (**Figure 3.1**). AUC is express as concentration times time for example mg.hr/L (Gabrielsson and Weiner 2012).

The mean residence time (MRT) is the average of the total number of molecules dosed reside in the body. MRT is a function of distribution and elimination like half-life. MRT calculation after I.V administration is provides a quantitative estimate of persistence in the body. MRT is calculated by the ratio of AUMC to AUC. The units for MRT are time and expressed as hours or minutes(Gabrielsson and Weiner 2012).

$$\text{MRT} = \frac{\text{AUMC}}{\text{AUC}}$$

Drug clearance is the ability of certain organs like kidneys and liver to excrete and metabolize drugs. Clearance is defined as the volume of fluid cleared of the drug in a unit time and is expressed as ml/min or L/h. The rate of elimination of drug is proportional to plasma concertation (Gibaldi and Levy 1976).

$$\text{Rate of elimination } (\frac{dX}{dt}) \ \alpha \text{ plasma concentration } (C_p)$$

55

$$\frac{dX}{dt} = \text{Cl. } C_p$$

$$\int_0^\infty dX = \text{Cl. } \int_0^\infty \text{Cp dt}$$

Total amount eliminated = Cl. $[AUC]_0^\infty$

$$\text{Cl} = \frac{\text{Total amount eliminated}}{[AUC]_0^\infty}$$

$$\text{Cl} = \frac{I.V\ Dose}{[AUC]_0^\infty}$$

Apparent volume of distribution (Vd) is the most useful volume term in pharmacokinetics. Vd is the hypothetical volume within which a drug is distributed and Vd does not refers to the physiological fluid volume. Vd solely demonstrates the space occupied by the drug and relative degree of drug distribution in blood and extravascular space and expressed as ml or L. Vd can be calculated by the following equation (Gibaldi and Levy 1976, Huang and Zheng 2010);

$$\text{Vd} = \frac{IV\ dose\ (AUMC)}{(AUC)^2}$$

Which can be re-written as,

$$\text{Vd} = \frac{IV\ dose}{AUC} \frac{AUMC}{AUC}$$

But, Cl$= \frac{IV\ dose}{AUC}$ and MRT $= \frac{AUMC}{AUC}$

Therefore, **Vd= Cl. MRT**

Data Analysis

Differences among treatment groups in the pharmacokinetic study were compared GraphPad® Prism 6.0, San Diego, CA and were considered statistically significant at p<0.05.

3.3 Results

Liposomal irinotecan increased plasma half-life and total exposure of both irinotecan and its active metabolite SN-38

Initially, we set out to study the plasma concentration time profile of irinotecan and its active metabolite, SN-38, after the administration of IRN-50, nal-IRI-10, and nal-IRI-50. We observed the plasma half-life of irinotecan significantly increased in liposomal formulations, nal-IRI-10 and nal-IRI-50 with half-lives of 12.7 ± 0.5 h and 10.9 ± 0.3 h respectively, when compared to that of IRN-50 with a half-life of 3.3 ± 0.1 h. Plasma half-life of SN-38 was also significantly increased for nal-IRI with 21 ± 2.9 h in nal-IRI-10 group and 18 ± 1.3 h in nal-IRI-50 group when compared to that of IRN-50 with a half-life of 3.17 ± 0.43 h (**Table 3.1, Fig 3.4**). We also observed that the mean residence time (MRT) for liposomal formulation significantly increased with 4.5 ± 0.4 h for nal-IRI-10 and 7.3 ± 2.6 h for nal-IRI-50, whereas IRI-50 showed MRT of 2 ± 0.5 h for plasma irinotecan. We found similar trend for its active metabolite SN-38 with MRT of 16.7 ± 8.3 h and 17.7 ± 3.8 h for nal-IRI-10 and nal-IRI-50 respectively, while MRT for IRI-50 was 3.67 ± 1.2 (**Table 3.1, Fig 3.5**). Clearance (Cl) of irinotecan for IRI-50 was 85.7 ± 22.8 ml/h with apparent volume of distribution (Vd) 178.6 ± 64.7. Whereas for liposomal irinotecan clearance and volume of distribution significantly decreased with values 0.6 ± 0.2 ml/h and 2.9 ± 0.5 ml respectively for nal-IRI-10 and clearance value of 0.3 ± 0.1 ml/h and volume of distribution of 2.2 ± 1.1 ml for nal-IRI-50. We have seen the similar trend for plasma SN-38

clearance and volume of distribution values, for liposomal irinotecan, both clearance and volume

of distribution values were significantly lower than that of IRI-150 values (**Table 3.1, Fig 3.6 and**

3.7).

We also observed the area under the curve (AUC) significantly increased with nal-IRI,

3.20 ± 0.94 ng-hr/ml $\times 10^5$ for nal-IRI-10 and 45.05 ± 5.52 ng-hr/ml $\times 10^5$ for nal-IRI-50 compared

with IRN-50, which had an AUC of 0.15 ± 0.02 ng-hr/ml $\times 10^5$ (**Fig. 3.2B**). With the increase in

AUC for free irinotecan from nal-IRI formulations, we also observed significant increase in AUC

for the active metabolite SN-38 from the liposomal formulations with 2.56 ± 0.63 ng-hr/ml $\times 10^3$

for nal-IRI-10 and 9.66 ± 0.44 ng-hr/ml $\times 10^3$ for nal-IRI-50, compared to the AUC for IRN-50 at

0.55 ± 0.08 ng-hr/ml $\times 10^3$ (**Fig. 3.3B**). These results confirm the increased plasma exposure of

irinotecan and its active metabolite SN-38 from nal-IRI-10 and nal-IRI-50 formulations when

compared to IRN-50 (**Fig. 3.3B**).

Liposomal irinotecan acts as reservoir and increase the exposure of irinotecan and SN-38 in

brain tumors

After studying the plasma pharmacokinetics, we set out to assess the concentrations of

irinotecan, and its active metabolite, SN-38, in brain tumors and normal brain tissue after the

administration of liposomal formulations and conventional irinotecan. After the administration of

IRN-50, irinotecan and SN-38 concentrations in brain tumors peaked at 0.5 to 2 h post-

administration (**Fig. 3.8A and 3.9A**). Both irinotecan and SN-38 were cleared rapidly after 6 h

with tumor-to-plasma ratios ranged from 3.0 to 10 for irinotecan and 0.62-5.1 for SN-38 (**Table**

3.2). After administration of nal-IRI-50, irinotecan and SN-38 concentrations continue to

accumulate in brain tumors over 168 h with tumor-to-plasma ratios of 0.05-90 and 0.59-39 for

irinotecan and SN-38, respectively. Tumor SN-38 concentration in mice treated with nal-IRI-50 at

168 h was found to be 50 ± 30 ng/g, whereas SN-38 concentration in non-liposomal irinotecan treated group was undetectable (<10 ng/g) at 12 h post-administration (**Fig. 3.9A**). The AUC of both irinotecan and SN-38 from nal-IRI-50 in brain tumors was found to be significantly higher than that of IRN-50 (**Fig. 3.8B** and **3.9B**). These results suggest that nal-IRI prolonged drug exposure in brain tumors compared to conventional irinotecan.

3.4 Discussion

The results of this study show that nal-IRI penetrates the BTB and accumulates within brain tumors in a preclinical model of MDA-MB-231Br-Luc. Upon accumulation in brain tumors, the liposomes appear to act as reservoir for the release of irinotecan. The local release of irinotecan improved free drug exposure irinotecan and its active metabolite SN-38 to tumor.

In general, nanoparticles with sizes ranging from 80 to 200 nm are expected to have optimal tumor distribution and accumulation due to enhanced permeation and retention (EPR) through the leaky vasculature of tumors (Yuan, Dellian et al. 1995, Greish 2010, Raza, Shareef et al. 2014). It has been posited, based upon liver and renal clearance of nanoparticles, that ideal size of liposomes for maximum distribution and to maintain prolonged plasma residence times is approximately 100 nm (Drummond, Meyer et al. 1999). The liposomal irinotecan formulation described in this study were between 100-110 nm (Noble, Krauze et al. 2014). Once liposomes accumulate in tumors due to EPR effect, the clearance from the tumor is limited because of its size and impaired lymphatic system, which results in prolonged drug exposure (Abrams 1964, Iwai, Maeda et al. 1984). On the other hand, non-liposomal irinotecan is rapidly cleared from the tumor due to its smaller size, leading to sub-therapeutic drug levels in tumor between the cycles of treatment. These observations support that liposomal irinotecan accumulates in brain metastases via the EPR effect, as reported for other solid tumor types (Kalra, Kim et al. 2014).

Further mechanistic possibilities for the increased drug uptake and accumulation from liposomal irinotecan is that it may avoid efflux by multidrug resistant proteins like P-gp and BCRP (Michieli, Damiani et al. 1999, Bansal, Mishra et al. 2009, Adkins, Mittapalli et al. 2013, Lo and Tu 2015). The uptake of conventional anticancer agents is limited by multidrug resistant protein present on membranes of cancer cells (Bansal, Mishra et al. 2009). In addition to efflux mechanisms on cancer cells, the BBB and BTB also express variety of multidrug resistant proteins, which further limits the uptake of chemotherapy (Mittapalli, Chung et al. 2016). Uptake of conventional irinotecan is also restricted by P-gp efflux (Bansal, Mishra et al. 2009, Adkins, Mittapalli et al. 2013, Mittapalli, Manda et al. 2013), but we hypothesize that the liposomal irinotecan formulation bypasses multidrug resistant proteins both at the BBB/BTB.

We observed that clearance rates for both irinotecan and its active metabolite SN-38 was significantly lower in liposomal irinotecan groups when compared to non-liposomal irinotecan group and this lower clearance rates for liposomes are responsible for prolonged plasma halves and mean residence times for both irinotecan and SN-38 with liposomal irinotecan formulation. The rate of clearance for liposomes are determined by both drug release and also uptake of liposomes by mononuclear phagocyte system (MPS) (Patel 1992, Patel and Moghimi 1998). The liposomes used for this study are "PEGylated" with approximately one polyethyleneglycol (PEG) molecule for 200 phospholipid molecules and PEGylated liposomes have long circulation time(Gabizon, Catane et al. 1994, Bayever, Fitzgerald et al. 2016). This increase in circulation time also accounts for the decrease in volume of distribution of both irinotecan and SN-38 from liposomal formulations when compared to non-liposomal irinotecan formulation (**Table 3.1**). This increased plasma MRT with decreased volume of distribution ultimately lead to increased exposure for the drug to penetrate BBB/BTB.

Irinotecan is mostly converted to SN-38 in liver, whereas, liposomal irinotecan formulation leads to local conversion of irinotecan to SN-38 upon accumulation in the tumor (Wang, Rao et al. 2016). Tissue pharmacokinetics reveal that liposomal irinotecan resulted in significantly higher drug exposure for both irinotecan and its active metabolite SN-38. Non-liposomal irinotecan (IRI-50) has showed AUC values of 27575 ± 4042 ng-h/g which is significantly lower than nal-IRI-50 with 250253 ± 74682 ng-he/g. Similar trend was observed in AUC of active metabolite SN-38 where, nal-IRI-50 showed AUC values of 6883 ± 4149 ng-h/g for SN-38, whereas IRI-50 showed significantly lower AUC values of 982 ± 256 ng-h/g for SN-38. In addition to drug exposure, tumor-to-plasma ratio of SN-38 in IRN-50 group was highest at 2 h with 5.1 but at 4 h it decreased to 0.6. The tumor-to-plasma ratio of SN-38 in liposomal irinotecan groups increased over time and reached 38.6 at 168 h in nal-IRI-50 groups (**Table 3.2**). The increase in tumor-to-plasma SN-38 ratio may be attributed to local conversion of irinotecan to SN-38 in the brain tumors following liposome accumulation via the EPR effect.

In summary, our data suggests that liposomal irinotecan significantly improved tumor exposure of irinotecan and its active metabolite SN-38 when compared to non-liposomal irinotecan in our preclinical brain tumor model. We also demonstrated that improved plasma pharmacokinetic profile with liposomal irinotecan compared to non-liposomal irinotecan.

3.5. References

Abrams, H. L. (1964). "The response of neoplastic renal vessels to epinephrine in man." Radiology **82**: 217-224.

Adkins, C. E., R. K. Mittapalli, V. K. Manda, M. I. Nounou, A. S. Mohammad, T. B. Terrell, K. A. Bohn, C. Yasemin, T. R. Grothe, J. A. Lockman and P. R. Lockman (2013). "P-glycoprotein mediated efflux limits substrate and drug uptake in a preclinical brain metastases of breast cancer model." Front Pharmacol **4**: 136.

Adkins, C. E., M. I. Nounou, T. Hye, A. S. Mohammad, T. Terrell-Hall, N. K. Mohan, M. A. Eldon, U. Hoch and P. R. Lockman (2015). "NKTR-102 Efficacy versus irinotecan in a mouse model of brain metastases of breast cancer." BMC Cancer **15**: 685.

Adkins, C. E., M. I. Nounou, R. K. Mittapalli, T. B. Terrell-Hall, A. S. Mohammad, R. Jagannathan and P. R. Lockman (2015). "A Novel Preclinical Method to Quantitatively Evaluate Early-Stage Metastatic Events at the Murine Blood–Brain Barrier." Cancer Prevention Research **8**(1): 68-76.

Amzerin, M., M. Mokrim, H. Errihani and M. J. Piccart (2015). "Iterative and prolonged remission in metastatic breast cancer using pegylated irinotecan: a case report." Journal of Medical Case Reports **9**(1): 5.

Andriyanov, A. V., E. Koren, Y. Barenholz and S. N. Goldberg (2014). "Therapeutic Efficacy of Combining PEGylated Liposomal Doxorubicin and Radiofrequency (RF) Ablation: Comparison between Slow-Drug-Releasing, Non-Thermosensitive and Fast-Drug-Releasing, Thermosensitive Nano-Liposomes." PLoS ONE **9**(5): e92555.

Ballabh, P., A. Braun and M. Nedergaard (2004). "The blood-brain barrier: an overview: structure, regulation, and clinical implications." Neurobiol Dis **16**(1): 1-13.

Bansal, T., G. Mishra, M. Jaggi, R. K. Khar and S. Talegaonkar (2009). "Effect of P-glycoprotein inhibitor, verapamil, on oral bioavailability and pharmacokinetics of irinotecan in rats." Eur J Pharm Sci **36**(4-5): 580-590.

Bayever, E., J. B. Fitzgerald, J. Kim and S. Klinz (2016). Treatment of breast cancer with liposomal irinotecan, Google Patents.

Drummond, D., O. Meyer, K. L. Hong, D. Kirpotin and D. Papahadjopoulos (2000). Optimizing Liposomes for Delivery of Chemotherapeutic Agents to Solid Tumors.

Drummond, D. C., O. Meyer, K. Hong, D. B. Kirpotin and D. Papahadjopoulos (1999). "Optimizing liposomes for delivery of chemotherapeutic agents to solid tumors." Pharmacol Rev **51**(4): 691-743.

Gabizon, A., R. Catane, B. Uziely, B. Kaufman, T. Safra, R. Cohen, F. Martin, A. Huang and Y. Barenholz (1994). "Prolonged circulation time and enhanced accumulation in malignant exudates of doxorubicin encapsulated in polyethylene-glycol coated liposomes." Cancer Res **54**(4): 987-992.

Gabrielsson, J. and D. Weiner (2012). Non-compartmental Analysis. Computational Toxicology: Volume I. B. Reisfeld and A. N. Mayeno. Totowa, NJ, Humana Press**:** 377-389.

Gibaldi, M. and G. Levy (1976). "Pharmacokinetics in clinical practice. 2. Applications." Jama **235**(18): 1987-1992.

Gibson, J.-M., S. Alzghari, C. Ahn, H. Trantham and N. M. La-Beck (2013). "The Role of Pegylated Liposomal Doxorubicin in Ovarian Cancer: A Meta-Analysis of Randomized Clinical Trials." The Oncologist **18**(9): 1022-1031.

Greish, K. (2010). "Enhanced permeability and retention (EPR) effect for anticancer nanomedicine drug targeting." Methods Mol Biol **624**: 25-37.

Huang, X. H. and Q. S. Zheng (2010). "Pharmacokinetic and Pharmacodynamic Data Analysis: Concepts and Applications." American Journal of Pharmaceutical Education **74**(3): 53b.

Iwai, K., H. Maeda and T. Konno (1984). "Use of oily contrast medium for selective drug targeting to tumor: enhanced therapeutic effect and X-ray image." Cancer Res **44**(5): 2115-2121.

Kalra, A. V., J. Kim, S. G. Klinz, N. Paz, J. Cain, D. C. Drummond, U. B. Nielsen and J. B. Fitzgerald (2014). "Preclinical activity of nanoliposomal irinotecan is governed by tumor deposition and intratumor prodrug conversion." Cancer Res **74**(23): 7003-7013.

Kaneda, N., H. Nagata, T. Furuta and T. Yokokura (1990). "Metabolism and pharmacokinetics of the camptothecin analogue CPT-11 in the mouse." Cancer Res **50**(6): 1715-1720.

Kemper, E. M., C. Cleypool, W. Boogerd, J. H. Beijnen and O. van Tellingen (2004). "The influence of the P-glycoprotein inhibitor zosuquidar trihydrochloride (LY335979) on the brain penetration of paclitaxel in mice." Cancer Chemother Pharmacol **53**(2): 173-178.

Lin, N. U., L. Amiri-Kordestani, D. Palmieri, D. J. Liewehr and P. S. Steeg (2013). "CNS metastases in breast cancer: old challenge, new frontiers." Clin Cancer Res **19**(23): 6404-6418.

Lo, Y. L. and W. C. Tu (2015). "Co-encapsulation of chrysophsin-1 and epirubicin in PEGylated liposomes circumvents multidrug resistance in HeLa cells." <u>Chem Biol Interact</u> **242**: 13-23.

Michieli, M., D. Damiani, A. Ermacora, P. Masolini, A. Michelutti, T. Michelutti, D. Russo, F. Pea and M. Baccarani (1999). "Liposome-encapsulated daunorubicin for PGP-related multidrug resistance." <u>Br J Haematol</u> **106**(1): 92-99.

Mittapalli, R. K., A. H. Chung, K. E. Parrish, D. Crabtree, K. G. Halvorson, G. Hu, W. F. Elmquist and O. J. Becher (2016). "ABCG2 and ABCB1 Limit the Efficacy of Dasatinib in a PDGF-B-Driven Brainstem Glioma Model." <u>Mol Cancer Ther</u> **15**(5): 819-829.

Mittapalli, R. K., V. K. Manda, K. A. Bohn, C. E. Adkins and P. R. Lockman (2013). "Quantitative fluorescence microscopy provides high resolution imaging of passive diffusion and P-gp mediated efflux at the in vivo blood-brain barrier." <u>J Neurosci Methods</u> **219**(1): 188-195.

Noble, C. O., M. T. Krauze, D. C. Drummond, J. Forsayeth, M. E. Hayes, J. Beyer, P. Hadaczek, M. S. Berger, D. B. Kirpotin, K. S. Bankiewicz and J. W. Park (2014). "Pharmacokinetics, tumor accumulation and antitumor activity of nanoliposomal irinotecan following systemic treatment of intracranial tumors." <u>Nanomedicine (Lond)</u> **9**(14): 2099-2108.

Pardridge, W. M. (2003). Molecular Biology of the Blood-Brain Barrier. <u>The Blood-Brain Barrier: Biology and Research Protocols</u>. S. Nag. Totowa, NJ, Humana Press**:** 385-399.

Patel, H. M. (1992). "Serum opsonins and liposomes: their interaction and opsonophagocytosis." <u>Crit Rev Ther Drug Carrier Syst</u> **9**(1): 39-90.

Patel, H. M. and S. M. Moghimi (1998). "Serum-mediated recognition of liposomes by phagocytic cells of the reticuloendothelial system - The concept of tissue specificity." Adv Drug Deliv Rev **32**(1-2): 45-60.

Ramakrishna, N., S. Temin, S. Chandarlapaty, J. R. Crews, N. E. Davidson, F. J. Esteva, S. H. Giordano, A. M. Gonzalez-Angulo, J. J. Kirshner, I. Krop, J. Levinson, S. Modi, D. A. Patt, E. A. Perez, J. Perlmutter, E. P. Winer and N. U. Lin (2014). "Recommendations on Disease Management for Patients With Advanced Human Epidermal Growth Factor Receptor 2–Positive Breast Cancer and Brain Metastases: American Society of Clinical Oncology Clinical Practice Guideline." Journal of Clinical Oncology **32**(19): 2100-2108.

Raza, K., M. A. Shareef, P. Singal, G. Sharma, P. Negi and O. P. Katare (2014). "Lipid-based capsaicin-loaded nano-colloidal biocompatible topical carriers with enhanced analgesic potential and decreased dermal irritation." J Liposome Res **24**(4): 290-296.

Rifkin, R. M., S. A. Gregory, A. Mohrbacher and M. A. Hussein (2006). "Pegylated liposomal doxorubicin, vincristine, and dexamethasone provide significant reduction in toxicity compared with doxorubicin, vincristine, and dexamethasone in patients with newly diagnosed multiple myeloma." Cancer **106**(4): 848-858.

Sengupta, S., R. Rojas, A. Mahadevan, E. Kasper and S. Jeyapalan (2015). "CPT-11/bevacizumab for the treatment of refractory brain metastases in patients with HER2-neu-positive breast cancer." Oxf Med Case Reports **2015**(4): 254-257.

Taguchi, T., T. Tominaga, M. Ogawa, T. Ishida, K. Morimoto and N. Ogawa (1994). "[A late phase II study of CPT-11 (irinotecan) in advanced breast cancer. CPT-11 Study Group on Breast Cancer]." Gan To Kagaku Ryoho **21**(7): 1017-1024.

Wang, X., Z. Rao, H. Qin, G. Zhang, Y. Ma, Y. Jin, M. Han, A. Shi, Y. Wang and X. Wu (2016). "Effect of hesperidin on the pharmacokinetics of CPT-11 and its active metabolite SN-38 by regulating hepatic Mrp2 in rats." Biopharm Drug Dispos **37**(7): 421-432.

Yuan, F., M. Dellian, D. Fukumura, M. Leunig, D. A. Berk, V. P. Torchilin and R. K. Jain (1995). "Vascular permeability in a human tumor xenograft: molecular size dependence and cutoff size." Cancer Res **55**(17): 3752-3756.

Table 3.1: Plasma pharmacokinetics of non-liposomal irinotecan and liposomal irinotecan.

Treatment	AUC$_{0-\alpha}$ (ng-hr/mL) $\times 10^5$	t$_{1/2}$ (h)	MRT (h)	Cl (ml/h)	Vd (ml)
Plasma Irinotecan					
IRI-50	0.2 ± 0.02	3.3 ± 0.1	2 ± 0.5	85.7 ± 22.8	178.6 ± 64.7
nal-IRI-10	3.2 ± 0.9	12.7 ± 0.5	4.5 ± 0.4	0.6 ± 0.2	2.9 ± 0.5
nal-IRI-50	45 ± 5.5	10.9 ± 0.3	7.3 ± 2.6	0.3 ± 0.1	2.2 ± 1.1

Treatment	AUC$_{0-\alpha}$ (ng-hr/mL) $\times 10^3$	t$_{1/2}$ (h)	MRT (h)	Cl (ml/h)	Vd (ml)
Plasma SN-38					
IRI-50	0.6 ± 0.08	4.32 ± 3.2	3.67 ± 1.2	2472 ± 881	7845.6 ± 2023
nal-IRI-10	2.6 ± 0.6	21 ± 2.9	16.7 ± 8.3	80.9 ± 13.5	1327.5 ± 678
nal-IRI-50	9.7 ± 0.4	18 ± 1.3	17.7 ± 3.8	130.2 ± 11.9	1990.3 ± 329

AUC$_{0-\alpha}$: Area under the time-concentration cure; Cl: Clearance; MRT: Mean residence time; t$_{1/2:}$ plasma half-life of the drug; Vd: Apparent volume of distribution

Table 3.2: Plasma and Brain Tumor Concentrations of Irinotecan and SN-38 after Administration of IRN-50 and nal-IRI -50.

Time (hr)	Conventional Irinotecan (50 mg/kg)				Liposomal Irinotecan (50 mg/kg)			
	2	6	12	24	6	24	72	168
Irinotecan concentration ± SEM (ng/mL or ng/g)								
Plasma	1470±159	239± 101	78.0±21.3	12.6±3.9	248000±60000	49800±24800	5.8±2.3	2.3±0.5
Tumor	4370±622	841±393	807±327	102±26.1	11300±6650	2760±1180	523±343	123±72.5
Tumor/Plasma	2.97	3.52	10.35	8.08	0.05	0.06	90.1	52.9
SN-38 concentration ± SEM (ng/mL or ng/g)								
Plasma	35.9±3.7	14.3±6.5	9.0±6.0	1.6±0.8	197±50.6	185±61.7	5.3±1.5	1.28±0.6
Tumor	184±71.1	18.5±18.5	5.6±5.6	1±1	116±57.8	68.8±24.5	7.1±7.1	49.5±30.4
Tumor/Plasma	5.13	1.29	0.62	0.63	0.59	0.37	1.33	38.66
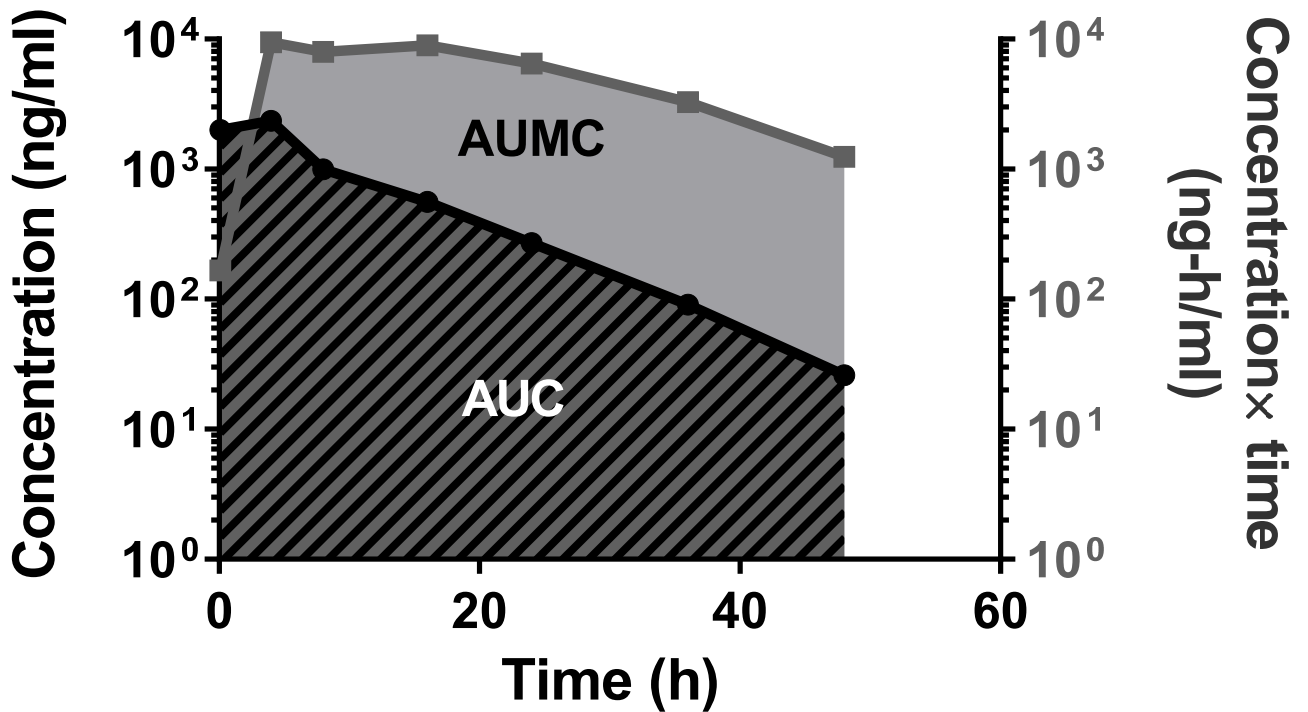
Figure 3.1: Image representing the calculation of AUC and AUMC by trapezoidal rule.

Plasma concentration (left y-axis) and time (x -axis) curve is used for calculation of AUC by trapezoidal rule. Plasma concentration-time (right y-axis) and time (x -axis) curve is used for calculation of AUMC by trapezoidal rule.
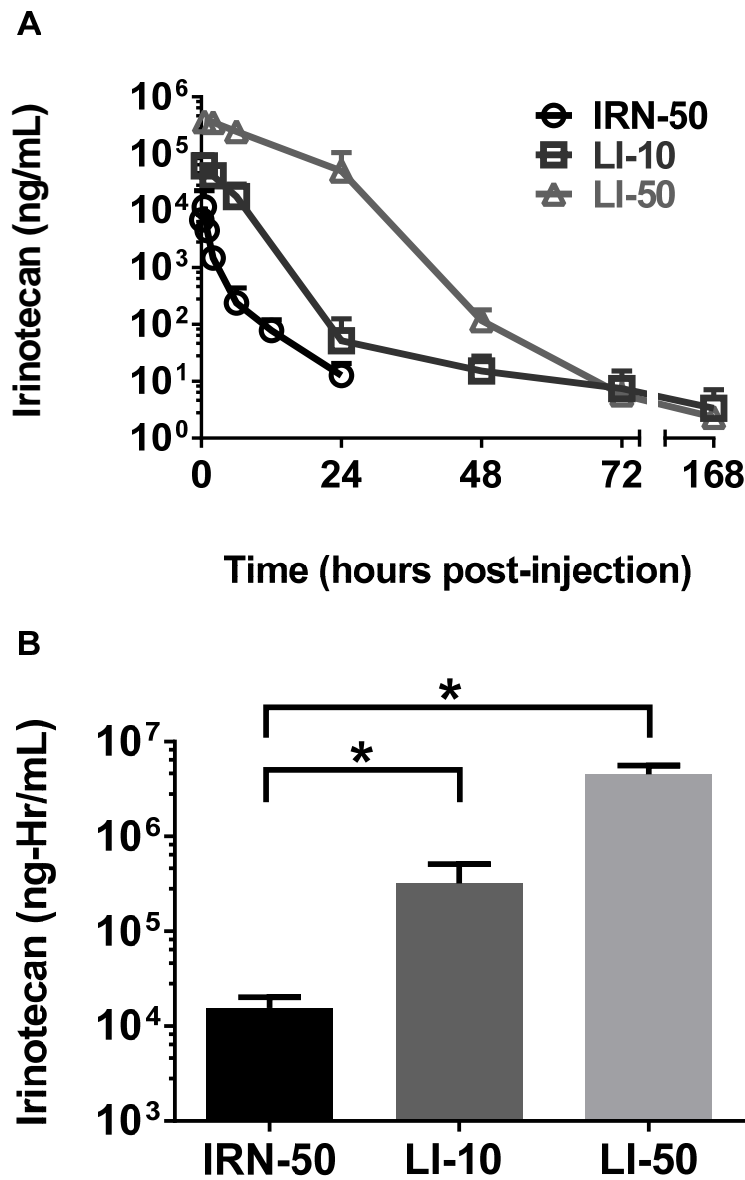
Figure 3.2: Plasma time profile of irinotecan after administration of liposomal and non-liposomal irinotecan formulations and their exposures.
(A) Plasma concentration-time profile of irinotecan after IV bolus administration of IRN-50, nal-IRI-10 and nal-IRI -50. Irinotecan essentially cleared from circulation within 24 hr from IRN-50, whereas in nal-IRI-10 and nal-IRI -50 formulations, we observed a prolonged exposure of both irinotecan and SN-38 until 168 hr. **(B)** Plasma drug exposure of irinotecan expressed by area under the curve (AUC) after IV bolus administration of IRN-50, nal-IRI -10 and nal-IRI -50. Irinotecan AUCs for nal-IRI -10 and nal-IRI -50 were significantly higher than that of IRN-50 ($p<0.05$). Data represents mean $\pm$ SD for n=4 animals per time point.

Figure 3.3: Plasma time profile of SN-38 after administration of liposomal and non-liposomal irinotecan formulations and their exposures
(**A**) Plasma concentration-time profile of SN-38 after IV bolus administration of IRN-50, nal-IRI-10 and nal-IRI -50. SN-38 essentially cleared from circulation within 24 hr from IRN-50, whereas in nal-IRI-10 and nal-IRI -50 formulations, we observed a prolonged exposure of SN-38 until 168 hr. (**B**) Plasma drug exposure of SN-38 expressed by area under the curve (AUC) after IV bolus administration of IRN-50, nal-IRI -10 and nal-IRI -50. SN-38 AUCs for nal-IRI -10 and nal-IRI -50 were significantly higher than that of IRN-50 ($p<0.05$). Data represents mean ± SD for n=4 animals per time point.

Figure 3.3: Plasma half-lives of irinotecan and SN-38 after administration of liposomal and non-liposomal irinotecan formulations.

(A) Plasma half-lives of irinotecan after administration of IR-50, nal-IRI-10 and nal-IRI-50. Irinotecan half-lives for nal-IRI -10 and nal-IRI -50 were significantly higher than that of IRN-50 ($p < 0.05$). Data represents mean ± SD for n=4 animals per time point.

(B) Plasma half-life of Plasma half-lives of SN-38 after administration of IR-50, nal-IRI-10 and nal-IRI-50. SN-38 half-lives for nal-IRI -10 and nal-IRI -50 were significantly higher than that of IRN-50 ($p < 0.05$). Data represents mean ± SD for n=4 animals per time point.
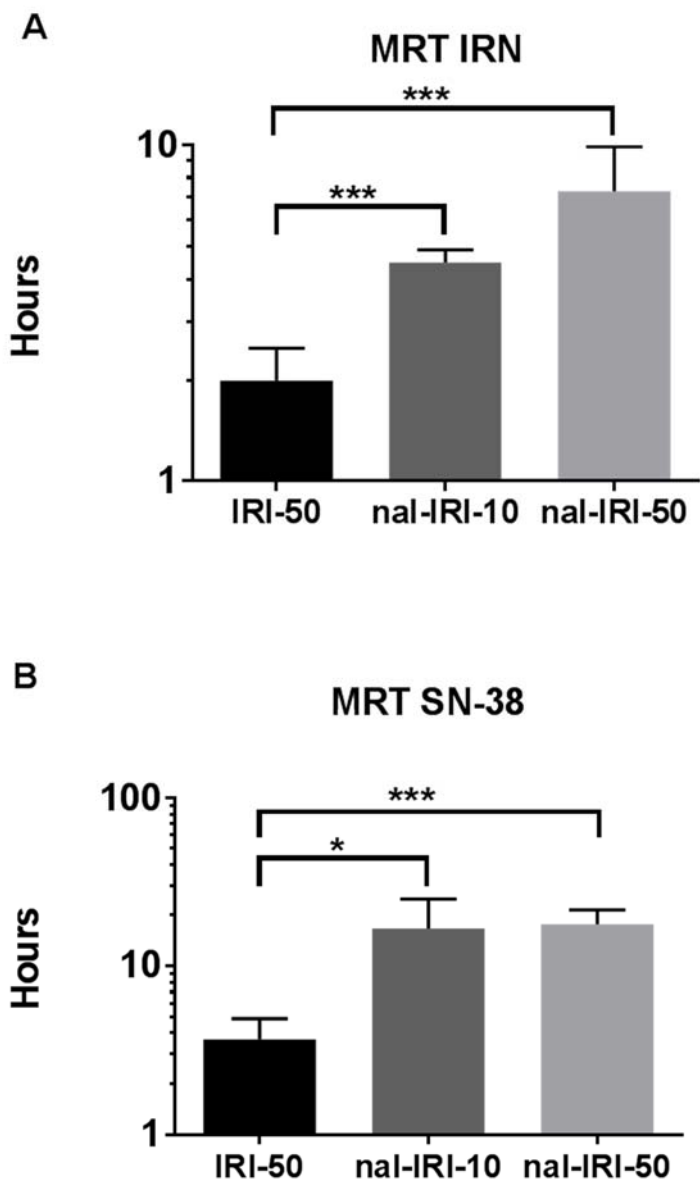
Figure 3.4: Plasma mean residence time (MRT) of irinotecan and SN-38 after administration of liposomal and non-liposomal irinotecan formulations.

(A) Plasma MRT of irinotecan after administration of IR-50, nal-IRI-10 and nal-IRI-50. Irinotecan MRT for nal-IRI -10 and nal-IRI -50 were significantly higher than that of IRN-50 ($p<0.05$). Data represents mean ± SD for n=4 animals per time point.

(B) Plasma MRT of Plasma half-lives of SN-38 after administration of IR-50, nal-IRI-10 and nal-IRI-50. SN-38 MRT for nal-IRI -10 and nal-IRI -50 were significantly higher than that of IRN-50 ($p<0.05$). Data represents mean ± SD for n=4 animals per time point.
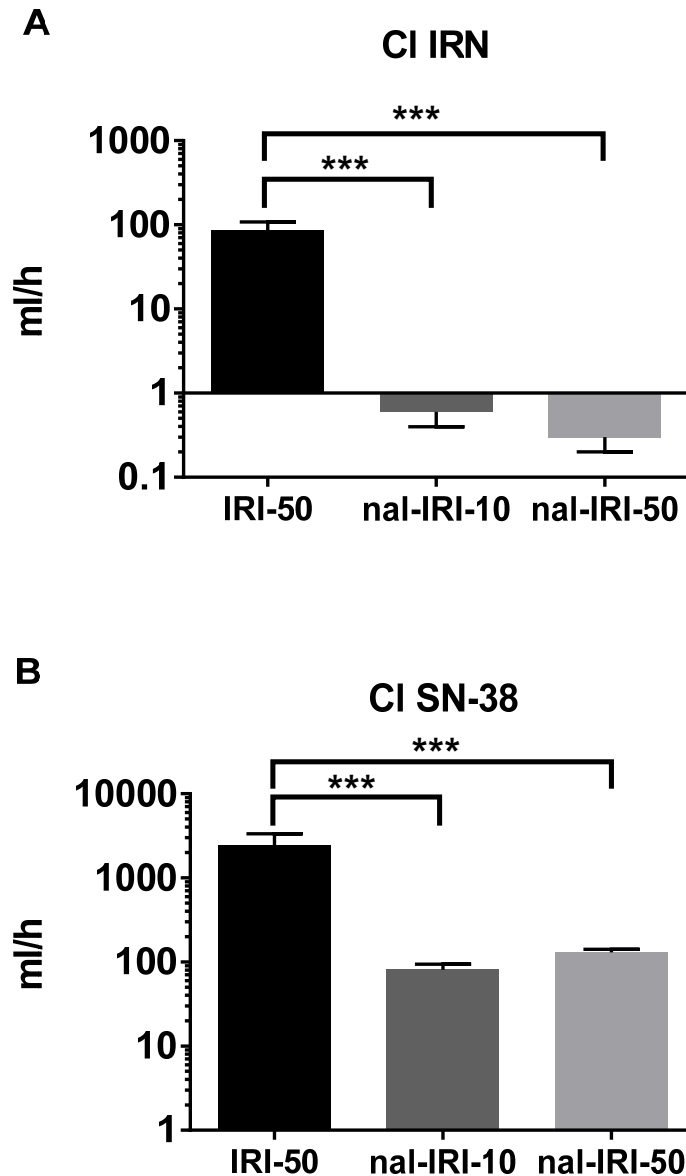
Figure 3.5: Plasma clearance (Cl) of irinotecan and SN-38 after administration of liposomal and non-liposomal irinotecan formulations.

(A) Plasma Cl of irinotecan after administration of IR-50, nal-IRI-10 and nal-IRI-50. Irinotecan Cl for nal-IRI -10 and nal-IRI -50 were significantly higher than that of IRN-50 ($p < 0.05$). Data represents mean $\pm$ SD for n=4 animals per time point.

(B) Plasma Cl of Plasma half-lives of SN-38 after administration of IR-50, nal-IRI-10 and nal-IRI-50. SN-38 Cl for nal-IRI -10 and nal-IRI -50 were significantly higher than that of IRN-50 ($p < 0.05$). Data represents mean $\pm$ SD for n=4 animals per time point.
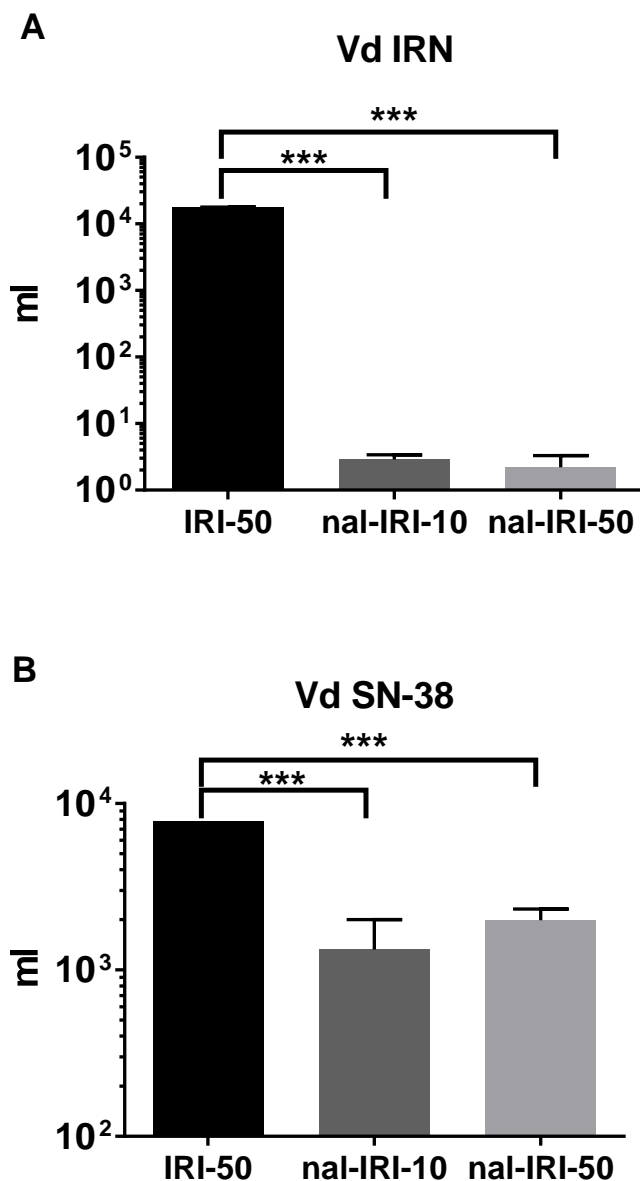
Figure 3.6: Plasma volume of distribution (Vd) of irinotecan and SN-38 after administration of liposomal and non-liposomal irinotecan formulations.

(A) Plasma Vd of irinotecan after administration of IR-50, nal-IRI-10 and nal-IRI-50. Irinotecan Vd for nal-IRI -10 and nal-IRI -50 were significantly higher than that of IRN-50 (p<0.05). Data represents mean ± SD for n=4 animals per time point.

(B) Plasma Vd of Plasma half-lives of SN-38 after administration of IR-50, nal-IRI-10 and nal-IRI-50. SN-38 Vd for nal-IRI -10 and nal-IRI -50 were significantly higher than that of IRN-50 (p<0.05). Data represents mean ± SD for n=4 animals per time point.

Figure 3.7: Tumor time profile of irinotecan after administration of liposomal and non-liposomal irinotecan formulation and their exposures.
(A) Brain tumor concentration-time profile of irinotecan after IV bolus administration of IRN-50, nal-IRI-10 and nal-IRI -50. Irinotecan essentially cleared from circulation within 24 hr from IRN-50, whereas in nal-IRI-10 and nal-IRI -50 formulations, we observed a prolonged exposure of both irinotecan and SN-38 until 168 hr. **(B)** Brain tumor drug exposure of irinotecan expressed by area under the curve (AUC) after IV bolus administration of IRN-50, nal-IRI -10 and nal-IRI -50. Irinotecan AUCs for nal-IRI -10 and nal-IRI -50 were significantly higher than that of IRN-50 ($p < 0.05$). Data represents mean $\pm$ SD for n=4 animals per time point.
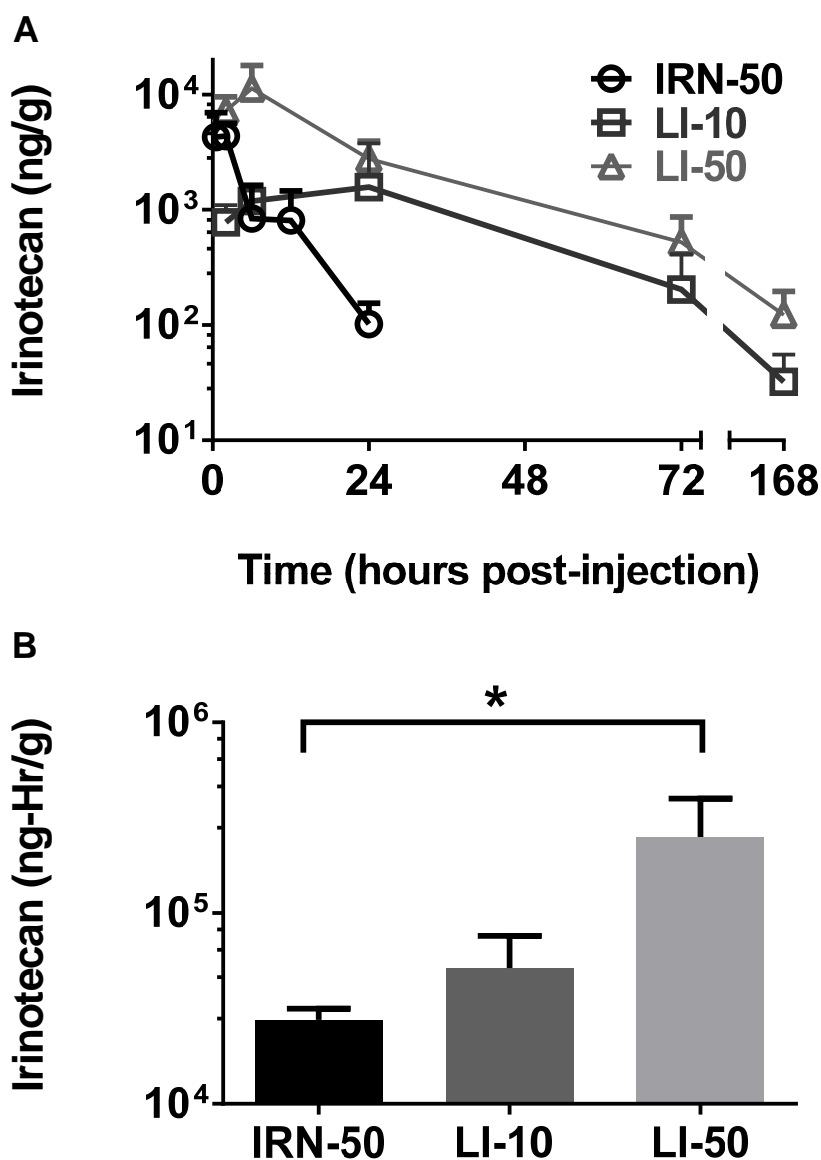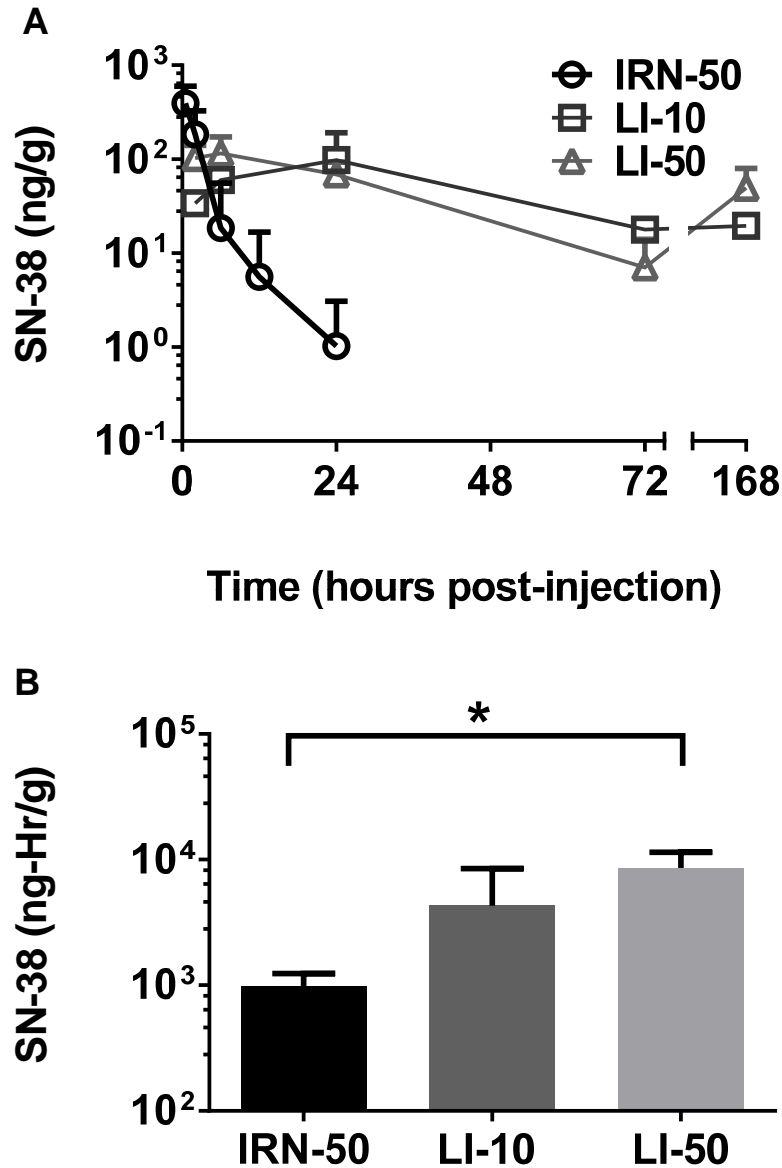
Figure 3.8: Brain tumor time profile of SN-38 after administration of liposomal and non-liposomal irinotecan formulation and their exposures
(**A**) Tumor concentration-time profile of SN-38 after IV bolus administration of IRN-50, nal-IRI-10 and nal-IRI -50. SN-38 essentially cleared from circulation within 24 hr from IRN-50, whereas in nal-IRI-10 and nal-IRI -50 formulations, we observed a prolonged exposure of SN-38 until 168 hr. (**B**) Brain tumor drug exposure of SN-38 expressed by area under the curve (AUC) after IV bolus administration of IRN-50, nal-IRI -10 and nal-IRI -50. SN-38 AUCs for nal-IRI - 50 was significantly higher than that of IRN-50 ($p<0.05$). Data represents mean ± SD for n=4 animals per time point.

CHAPTER 4

LIPOSOMAL IRINOTECAN ACCUMULATES IN METASTATIC LESIONS, CROSSES THE BLOOD-TUMOR BARRIER (BTB), AND PROLONGS SURVIVAL IN AN EXPERIMENTAL MODEL OF BRAIN METASTASES OF TRIPLE NEGATIVE BREAST CANCER

4.1 Introduction

More than 230,000 women are diagnosed with breast cancer every year (Society 2015). Of this general population of women with breast cancer, 6% present with distant metastases at the time of diagnosis, and 10-15% will develop brain metastases at some period during their lifetime. After diagnosis of a brain metastasis, survival is approximately 3-25 months depending on breast cancer subtype, total body burden, and treatment regimen (Sperduto, Kased et al. 2012, Siegel, Miller et al. 2015). Brain metastases are common in human epidermal growth factor receptor 2 overexpressing (HER2+) cancers and triple negative breast cancer (Bachelot, Romieu et al. 2013, Bohn, Adkins et al. 2016, H. Nitta 2016). While the HER2 receptor can be targeted to treat primary breast cancer, unfortunately these therapies (e.g., trastuzumab and lapatinib) have limited distribution to HER2+ brain metastases and accordingly have poor efficacy (Taskar, Rudraraju et al. 2012, Morikawa, Peereboom et al. 2015, Bohn, Adkins et al. 2016). There are no such targeted therapies for the treatment of basal-like triple negative breast cancer (TNBC). Triple negative breast cancer is characterized by the absence of the oncogenic overexpression of HER2, estrogen receptors (ER) and progesterone receptors (PR). Of significance is the fact that brain metastases are a major sequelae of TNBC, as one study found that as many as 36% of

women with TNBC will develop metastatic CNS lesions over their lifetime (Lin, Vanderplas et al. 2012).

A major impediment in effectively treating brain metastases of breast cancer is the distribution of chemotherapeutics past the blood-brain barrier (BBB). The BBB, which remains intact to a large degree in metastatic brain lesions of breast cancer (blood-tumor barrier; BTB), significantly limits the passive permeation of drugs from blood to tumor (Lockmanet al. 2010, Mittapalli et al. 2017) and continues to actively extrude and limit lesion accumulation of substrates subject to drug-resistance efflux transporters. For example, paclitaxel, which is used in treating breast cancer, is unable to permeate the BTB at rates to achieve a therapeutically relevant concentration (Lockman et al. 2010, Adkins et al. 2013, Geldenhuys et al. 2015). Approaches to treatment of brain metastases include stereotactic radiosurgery (SRS) or whole brain radiation therapy (WBRT) in combination with systemic therapy, though these therapies are largely palliative and may result in neurocognitive degeneration (El-Habashy et al. 2014, Halasz et al. 2016).

Nanoparticles and other polymeric drug formulations have shown promise for the delivery of chemotherapeutics, primarily through extravasation across the BTB (Mittapalli et al. 2013, Adkins et al. 2015, Mittapalli et al. 2017). This strategy has been particularly effective in fast-growing, aggressive metastases, which produce more growth factors associated with angiogenesis and have a resultant vasculature that is more permeable than BBB (Greish 2010). In addition, nanoparticles have prolonged residence times within lesions due to increased circulation half-life, while small molecules leave the tumor interstitial space

much faster. Consequently, the increased residence time of the nanoparticles results in significantly greater total drug exposure (area under the curve) (Sambade et al. 2016). Improvements in pharmacokinetics and reduced toxicity are evident with nano-liposome encapsulated anticancer agents such as vinorelbine, docetaxel and doxorubicin (Drummond, et al. 2009, Maeda et al. 2013).

Recently, Nobel et al. demonstrated that a liposomal nanoparticle increased concentration of irinotecan by 3.1-fold in glioblastoma xenograft tumors compared to non-liposomal irinotecan (Noble et al. 2014). The 3-fold increase in C_{max} was mirrored by similar increases observed for the active metabolite of irinotecan, SN-38, in the tumor (Noble et al. 2014). The liposomes preferentially accumulated in tumor tissues, with a 35-fold increase in irinotecan concentration from normal brain concentration, whereas non-liposomal irinotecan showed 9.5 fold increase in irinotecan concentration in tumor tissue compared to normal brain (Noble et al. 2014). Consistent with previous work showing nanoparticles increase total tumor exposure (area under the curve), the 3.1-fold increased peak concentrations were reached at 12 h in comparison to 15 min with non-liposomal irinotecan (Noble et al. 2014).

In the clinical setting, delivery of liposomes to brain lesions was previously observed with multiple methods. Detectable and variable uptake of ^{111}In labelled non-PEGylated liposomes at 72 h was observed in brain tumors across multiple patients with malignant glioma using single photon emission tomography(Khalifa et al. 1997). In another study, delivery of ^{99m}Tc labelled liposomal doxorubicin to glioblastomas and metastatic brain tumors of various origin was also observed using planar and SPECT scintigraphy (Koukourakis et al. 2000). Most recently, delivery of ^{64}Cu labelled HER2-targeted liposomal doxorubicin was noted by PET/CT in breast

cancer brain metastases (Lee et al. 2017). These studies highlight the potential for liposomes to enable drug delivery to brain metastases.

We hypothesize that liposomal irinotecan (nal-IRI, irinotecan liposome injection) will effectively deliver irinotecan and SN-38 resulting in efficacy and prolonged survival in a preclinical model of brain metastases of TNBC. nal-IRI, in combination with 5-fluorouracil and leucovorin, has recently been approved in the US and EU for the treatment of patients with advanced metastatic pancreatic adenocarcinoma after disease progression following gemcitabine-based therapy.

4.2 Materials and Methods
Chemicals

Irinotecan HCl, nal-IRI were supplied by Merrimack Pharmaceuticals (Cambridge, US), which were prepared as reported by Noble et al. and Kalra et al. (Kalra et al. 2014, Noble et al. 2014). Fluorescently-labeled liposomal irinotecan (DiI5-liposomal irinotecan) was also provided by Merrimack Pharmaceuticals, which was prepared following previously reported methods (Espelin, Leonard et al. 2016). The lipid mixture of nal-IRI consisting of distearoylphosphatidylcholine, cholesterol, and polyethyleneglycol-distearoylphosphatidyl-ethanolamine at the molar ration of 3:2:0.015(Noble et al. 2014). Irinotecan HCl was in the liposomes at a ratio of 750 g irinotecan HCl / mol phospholipid (Noble et al. 2014). Carbocyanine tracer DiIC18 (5)-DS (D12730; Life Technologies) was incorporated into the lipid bilayer of the liposome prior to drug loading. All other chemicals were analytical grade purchased from Sigma-Aldrich (St. Louis, MO).

Animals

Female athymic nude mice (22-28 g) were obrained from Charles River Laboratories (Kingston, NY) were used for all experiments in the study. Mice were 6-8 weeks of age before injecting with cancer cells and were housed under 12-hour light/dark conditions with food and water *ad libitum,* and mice were acclimated for 1 week prior to use. All animal work was approved by West Virginia University Institutional Animal care and Use Committee (IACUC protocols 13-1207). All animal experiments were performed according to the principles of the *Guide for the Care and use of Laboratory animals.*

Cell Culture

Brain-seeking human triple negative breast cancer cells, transfected to express firefly luciferase (MDA-MB-231Br-Luc), were cultured in Dulbecco's Modified Eagle's Medium (DMEM) with 10% fetal bovine serum (FBS). MDA-MB-231Br-Luc cells were kindly provided by Dr. Patricia Steeg, of the National Institute of Health Center for Cancer Research. All cell work was performed under aseptic conditions, and cells were cultured at 37°C with 5% CO_2.

Survival of animals with brain metastases after treatment

MDA-MB-231Br-Luc cells (1.75×10^5) cells were injected intracardially into the left ventricle and allowed to develop into CNS metastases for 21 days. The presence of metastases was confirmed by bioluminescence imaging (BLI) using the IVIS Lumina *in vivo* imaging system (PerkinElmer, Waltham, MA) after 15 min intraperitoneal administration of D-luciferin

potassium salt (150 mg/kg; PerkinElmer). Animals were then randomized into treatment groups (Saline, n=10), IRN-50 (n=10), nal-IRI-10 (n=10), and nal-IRI-50 (n=10). Drugs were administered intravenously via tail vein injection. Treatments were repeated once weekly, and BLI data was gathered twice weekly to quantify tumor burden and progression in different groups, similar to our previous work (Adkins et al. 2015). Once animals developed neurological symptoms or showed weight loss of ≥20 %, they were sacrificed under anesthesia. Euthanasia upon development of neurological symptoms was blinded and performed based on the recommendation of OLAR staff at WVU.

Uptake and accumulation of liposomal irinotecan formulation

Animals from the liposomal irinotecan group (nal-IRI-10 and nal-IRI-50) were administered with Dil5-labelled liposomes intravenously. After 24 h, animals were sacrificed under anesthesia as described above. The brain was immediately harvested, frozen in 2-methylbutane at -50°C, and sectioned into 20 μm thick sections (Leica CM3050 S cryostat). The sections were imaged with an Olympus MVX10 microscope with a 2x objective (NA=0.5) using the Cy5 channel. The same sections were then stained with cresyl violet and compared to fluorescent images to confirm the accumulation of Dil-5 labeled liposomes within the metastatic tumors. Sections were also stained for cytokeratin and DAPI, a fluorescent stain that binds to DNA to visualize the accumulation of liposomes within the cancer cell using Nikon N-Storm super-resolution microscope system.

Data Analysis

Differences among treatment groups in the survival study were compared by log-rank test (GraphPad® Prism 6.0, San Diego, CA) and were considered statistically significant at $p < 0.05$.

Living Image V4.0 software (PerkinElmer, Waltham, MA) was used to quantify tumor burden in different groups.

4.3 Results
Dil-5 labelled liposomes cross the BTB and accumulate in brain metastases

To understand tumor localization of nal-IRI, we studied the spatial distribution of the liposomal formulation incorporated with a fluorescent dye (Dil-5). After confirmation of the presence of metastatic lesions by BLI (**Fig. 4.1A, 4.2A and 4.3A**), Dil5-labelled liposomes were administered at equivalent dose of nal-IRI-10(**Fig 4.3**) and nal-IRI-50 (**Fig 4.2 and 4.3**). The liposomes were allowed to circulate for 24 hr, the animals were anesthetized (ketamine/xylazine; 100 mg/kg and 8 mg/kg respectively) and a washout with phosphate buffer saline at 5 ml/min flow rate for two minutes was performed in animals (**Fig 4.2 and 4.3**). For visualizing the brain vasculature, a mouse injected with Dil5-labelled liposomes was washed out with Texas red dextran 70 k (50 μg/ml) at 5 ml/min flow rate for 2 minutes (**Fig 4.3**)   The animals were sacrificed by decapitation to collect brain and tumor samples and then brain tissues were harvested and sectioned to allow for microscopic distribution visualization (**Fig. 4.1B, 4.2B and 4.3B**). Brain sections corresponding to regions 1, 2, 3 and 4, as shown in **Fig. 4.1B, 4.2B and 4.3B**, were also imaged for visualization of Dil-5 liposomes (**Fig. 4.**1, **4.2 and 4.3 (D1-D4)**). The same sections were stained with cresyl violet and imaged for histopathologic visualization of lesions (**Fig. 4.1, 4.2 (C1-C4) and 4.3 (C1-C3)**). Cresyl violet images (**Fig. 4.1, 4.2 (C1-C4) and 4.3 (C1-C3)**) and their corresponding fluorescent images (**Fig. 4.1**, **4.2 (D1-D4) and 4.3 (D1-D3)**) show that there is localization of Dil-5 liposomes within metastatic lesions (i.e. cresyl violet positive regions). We also confirmed normal brain tissue (i.e. brain regions devoid of any

metastases) has undetectable amounts of Dil-5 labelled liposomes (**Fig. 4.1 C4** and **Fig. 4.1 D4**). Figures 4.3 (E1-E3) show the vasculature in the brain.

The sections were then stained for cytokeratin and DAPI for high-resolution visualization within the metastatic lesions using Nikon N-Storm super-resolution microscope system (**Fig. 4.4**). We found that the Dil5 labelled liposomes not only crossed the BTB, but also localized within the cancer cells in the perinuclear regions, as shown in **Fig. 4.4**.

Liposomal irinotecan reduces tumor burden and prolongs survival in animals with brain metastases of breast cancer

Lastly, we set out to determine if the increased accumulation of DiI5-liposomal irinotecan and prolonged drug exposure would result in increased median survival in our experimental model. To evaluate this, mice injected with TNBC cells intracardially for metastases development; after 21 days, mice were randomized to receive different therapeutic treatment regimens (Saline, IRN-50, nal-IRI-10 and nal-IRI-50). We observed that progression of tumor burden in liposomal irinotecan-treated groups (nal-IRI-10 and nal-IRI-50) was significantly lowered when compared to vehicle and IRN-50 groups (**Fig. 4.5A** and **B**). We also noted that liposomal irinotecan formulations significantly improved survival when compared to both the vehicle group and conventional irinotecan group (**Fig. 4.6**). The median survival for liposomal irinotecan groups were 48 and 50 days for nal-IRI-10 and nal-IRI-50 respectively, while for vehicle and non-liposomal irinotecan (50 mg/kg) group's median survival were 37 and 35 days, respectively (**Fig. 4.6**).

4.4 Discussion

The results of this study show that nal-IRI penetrates the BTB and accumulates within metastases in a preclinical model of MDA-MB-231Br-Luc brain metastases. Upon accumulation in metastatic tumors, the liposomes appear to act as reservoir for the release of irinotecan. The local release of irinotecan improved free drug exposure to tumor and presumably delayed the progression of tumor burden, which ultimately corresponded to significant prolonged survival.

Irinotecan is a widely used chemotherapeutic agent, upon administration it is converted to its active metabolite7-ethyly-10hydroxy-camptothecin (SN-38), which is a potent topoisomerase I inhibitor (Adkins et al. 2015). Inhibition of topoisomerase I activity by SN-38 and irinotecan prevents DNA from unwinding. This results in DNA damage leading to inhibition of DNA replication ultimately triggering apoptosis in the tumor cells (Chabot 1996). Irinotecan is mostly converted to SN-38 in liver, whereas, liposomal irinotecan formulation leads to local conversion of irinotecan to SN-38 upon accumulation in the tumor (Wang et al. 2016). Adkins et al., previously reported that polyethylene glycol (PEG)- coupled irinotecan (NKTR-102) showed superior drug distribution in a preclinical brain metastases of breast cancer model. They also found that the survival with this novel formulation significantly improved with complete regression of brain metastases in 50% of the mice treated with NKTR-102 by the end of the study (Adkins et al. 2015). A phase III study of NKTR-102 versus treatment of physician's choice (TPC) in patients with brain metastases of breast cancer is currently recruiting participants (NCT02915744). Liposomal irinotecan has already proved to beneficial both preclinically and clinically for treating metastatic pancreatic cancer (Carnevale and Ko 2016, Chiang et al. 2016). FDA approved ONIVYDE®, irinotecan liposomal injection in combination

of 5-Flurouracil/ leucovorin (5-FU/LV) for metastatic pancreatic cancer patients(Kipps et al. 2017).

The accumulation of Dil-5 labelled liposomes in brain metastases, and the increased concentrations of drug payload over a period align with previous observations of passive targeting in tumors with nanoparticles like liposomes (Jain and Stylianopoulos 2010, Liu et al. 2013). These observations support that liposomal irinotecan accumulates in brain metastases via the EPR effect, as reported for other solid tumor types (Kalra et al. 2014). This maintenance of prolonged SN-38 cytotoxic concentrations and high tumor-to-normal tissue ratio **(Chapter 3)** are likely responsible for the prolonged survival observed in our animal model. Irinotecan is also substrate for efflux transporters present at the BBB/BTB. The pharmacokinetic data presented in Chapter 3 confirms the increased plasma mean residence time for both SN-38 and irinotecan,

In addition to preferential accumulation of liposomal irinotecan in metastatic lesions, we observed that the progression of tumor burden was significantly delayed in liposomal irinotecan groups, which correlated with prolonged survival. The median survival of the vehicle group was found to be 37 days (Adkins et al. 2015, Adkins et al. 2016). Treatment with conventional irinotecan (50 mg/kg) showed no improvement in survival (median survival of 35 days). However, liposomal irinotecan-treated groups significantly prolonged median survival to 50 days in 50 mg/kg group and 48 days in 10 mg/kg group (**Fig.6**). We hypothesize that after accumulation of liposomal irinotecan formulation in brain tumors, they act as reservoir for the release of irinotecan as described in other previous studies (Ostrowski et al. 2012, Liu et al. 2013). The prolonged release of the chemotherapy from the liposomes provides sustained tumor

drug concentration, as shown in the pharmacokinetic results (**Chapter 3**). Maintenance of the irinotecan concentration in between cycles of treatments in liposomal irinotecan groups may be responsible for the prolonged survival when compared to vehicle and conventional irinotecan groups. We have demonstrated that nal-IRI permeates the BTB and accumulates in metastatic brain tumors due to the EPR effect, prolonged systemic circulation, and potentially bypassing the efflux mechanisms. We also observed accumulation of liposomes in lesions with sustained release of irinotecan. We believe this is responsible for the increase in survival in liposomal irinotecan groups compared to non-liposomal irinotecan group. Clinically, the chemotherapy used for the management of brain metastases of breast cancer are conventional cytotoxic agents such as cyclophosphamide, fluorouracil, methotrexate, and doxorubicin based upon their increased permeability through tumor vasculature (Boogerd et al. 1992, Lin, Bellon et al. 2004). Collectively, results presented herein support the on-going clinical study of nal-IRI in patients with breast cancer brain metastases (NCT01770353) and indicates its potential for treatment of brain metastases of breast cancer.

In summary, we demonstrated efficacy of liposomal irinotecan in a preclinical model of a metastatic brain tumors. We observed the preferential uptake and accumulation of liposomal irinotecan into the brain tumors, ultimately correlating with increased survival.

4.5 References

Adkins, C. E., R. K. Mittapalli, V. K. Manda, M. I. Nounou, A. S. Mohammad, T. B. Terrell, K. A. Bohn, C. Yasemin, T. R. Grothe, J. A. Lockman and P. R. Lockman (2013). "P-glycoprotein mediated efflux limits substrate and drug uptake in a preclinical brain metastases of breast cancer model." Front Pharmacol **4**: 136.

Adkins, C. E., A. S. Mohammad, T. B. Terrell-Hall, E. L. Dolan, N. Shah, E. Sechrest, J. Griffith and P. R. Lockman (2016). "Characterization of passive permeability at the blood-tumor barrier in five preclinical models of brain metastases of breast cancer." Clin Exp Metastasis **33**(4): 373-383.

Adkins, C. E., M. I. Nounou, T. Hye, A. S. Mohammad, T. Terrell-Hall, N. K. Mohan, M. A. Eldon, U. Hoch and P. R. Lockman (2015). "NKTR-102 Efficacy versus irinotecan in a mouse model of brain metastases of breast cancer." BMC Cancer **15**: 685.

Bachelot, T., G. Romieu, M. Campone, V. Dieras, C. Cropet, F. Dalenc, M. Jimenez, E. Le Rhun, J. Y. Pierga, A. Goncalves, M. Leheurteur, J. Domont, M. Gutierrez, H. Cure, J. M. Ferrero and C. Labbe-Devilliers (2013). "Lapatinib plus capecitabine in patients with previously untreated brain metastases from HER2-positive metastatic breast cancer (LANDSCAPE): a single-group phase 2 study." Lancet Oncol **14**(1): 64-71.

Bohn, K. A., C. E. Adkins, R. K. Mittapalli, T. B. Terrell-Hall, A. S. Mohammad, N. Shah, E. L. Dolan, M. I. Nounou and P. R. Lockman (2016). "Semi-automated Rapid Quantification of Brain Vessel Density Utilizing Fluorescent Microscopy." J Neurosci Methods.

Boogerd, W., O. Dalesio, E. M. Bais and J. J. van der Sande (1992). "Response of brain metastases from breast cancer to systemic chemotherapy." Cancer **69**(4): 972-980.

Carnevale, J. and A. H. Ko (2016). "MM-398 (nanoliposomal irinotecan): emergence of a novel therapy for the treatment of advanced pancreatic cancer." Future Oncol **12**(4): 453-464.

Chabot, G. G. (1996). "Clinical pharmacology and pharmacodynamics of irinotecan. A review." Ann N Y Acad Sci **803**: 164-172.

Chiang, N. J., J. Y. Chang, Y. S. Shan and L. T. Chen (2016). "Development of nanoliposomal irinotecan (nal-IRI, MM-398, PEP02) in the management of metastatic pancreatic cancer." Expert Opin Pharmacother **17**(10): 1413-1420.

Drummond, D. C., C. O. Noble, Z. Guo, M. E. Hayes, J. W. Park, C. J. Ou, Y. L. Tseng, K. Hong and D. B. Kirpotin (2009). "Improved pharmacokinetics and efficacy of a highly stable nanoliposomal vinorelbine." J Pharmacol Exp Ther **328**(1): 321-330.

El-Habashy, S. E., A. M. Nazief, C. E. Adkins, M. M. Wen, A. H. El-Kamel, A. M. Hamdan, A. S. Hanafy, T. O. Terrell, A. S. Mohammad, P. R. Lockman and M. I. Nounou (2014). "Novel treatment strategies for brain tumors and metastases." Pharm Pat Anal **3**(3): 279-296.

Espelin, C. W., S. C. Leonard, E. Geretti, T. J. Wickham and B. S. Hendriks (2016). "Dual HER2 Targeting with Trastuzumab and Liposomal-Encapsulated Doxorubicin (MM-302) Demonstrates Synergistic Antitumor Activity in Breast and Gastric Cancer." Cancer Res **76**(6): 1517-1527.

Geldenhuys, W. J., A. S. Mohammad, C. E. Adkins and P. R. Lockman (2015). "Molecular determinants of blood-brain barrier permeation." Ther Deliv **6**(8): 961-971.

Greish, K. (2010). "Enhanced permeability and retention (EPR) effect for anticancer nanomedicine drug targeting." Methods Mol Biol **624**: 25-37.

H. Nitta, B. D. K., C. Alfred, S. Jewell, P. Banks, E. Dennis, T.M. Grogan (2016). "The assessment of HER2 status in breast cancer: the past, the present, and the future." Pathology International.

Halasz, L. M., H. Uno, M. Hughes, T. D'Amico, E. U. Dexter, S. B. Edge, J. A. Hayman, J. C. Niland, G. A. Otterson, K. M. Pisters, R. Theriault, J. C. Weeks and R. S. Punglia (2016). "Comparative effectiveness of stereotactic radiosurgery versus whole-brain radiation therapy for patients with brain metastases from breast or non-small cell lung cancer." Cancer **122**(13): 2091-2100.

Jain, R. K. and T. Stylianopoulos (2010). "Delivering nanomedicine to solid tumors." Nat Rev Clin Oncol **7**(11): 653-664.

Kalra, A. V., J. Kim, S. G. Klinz, N. Paz, J. Cain, D. C. Drummond, U. B. Nielsen and J. B. Fitzgerald (2014). "Preclinical activity of nanoliposomal irinotecan is governed by tumor deposition and intratumor prodrug conversion." Cancer Res **74**(23): 7003-7013.

Khalifa, A., D. Dodds, R. Rampling, J. Paterson and T. Murray (1997). "Liposomal distribution in malignant glioma: possibilities for therapy." Nucl Med Commun **18**(1): 17-23.

Kipps, E., K. Young and N. Starling (2017). "Liposomal irinotecan in gemcitabine-refractory metastatic pancreatic cancer: efficacy, safety and place in therapy." Therapeutic Advances in Medical Oncology **9**(3): 159-170.

Koukourakis, M. I., S. Koukouraki, I. Fezoulidis, N. Kelekis, G. Kyrias, S. Archimandritis and N. Karkavitsas (2000). "High intratumoural accumulation of stealth liposomal doxorubicin (Caelyx) in glioblastomas and in metastatic brain tumours." Br J Cancer **83**(10): 1281-1286.

Lee, H., A. F. Shields, B. A. Siegel, K. D. Miller, I. Krop, C. X. Ma, P. M. LoRusso, P. N. Munster, K. Campbell, D. F. Gaddy, S. C. Leonard, E. Geretti, S. J. Blocker, D. B. Kirpotin, V. Moyo, T. J. Wickham and B. S. Hendriks (2017). "64Cu-MM-302 Positron Emission Tomography Quantifies Variability of Enhanced Permeability and Retention of Nanoparticles in Relation to Treatment Response in Patients with Metastatic Breast Cancer." Clin Cancer Res.

Lin, N. U., J. R. Bellon and E. P. Winer (2004). "CNS metastases in breast cancer." J Clin Oncol **22**(17): 3608-3617.

Lin, N. U., A. Vanderplas, M. E. Hughes, R. L. Theriault, S. B. Edge, Y. N. Wong, D. W. Blayney, J. C. Niland, E. P. Winer and J. C. Weeks (2012). "Clinicopathologic features, patterns of recurrence, and survival among women with triple-negative breast cancer in the National Comprehensive Cancer Network." Cancer **118**(22): 5463-5472.

Liu, D., P. Yang, D. Hu and F. Liu (2013). "[Minocycline hydrochloride liposome controlled-release gel improves rat experimental periodontitis]." Hua Xi Kou Qiang Yi Xue Za Zhi **31**(6): 592-596.

Liu, J., M. Yu, C. Zhou, S. Yang, X. Ning and J. Zheng (2013). "Passive tumor targeting of renal-clearable luminescent gold nanoparticles: long tumor retention and fast normal tissue clearance." J Am Chem Soc **135**(13): 4978-4981.

Lockman, P. R., R. K. Mittapalli, K. S. Taskar, V. Rudraraju, B. Gril, K. A. Bohn, C. E. Adkins, A. Roberts, H. R. Thorsheim, J. A. Gaasch, S. Huang, D. Palmieri, P. S. Steeg and Q. R. Smith (2010). "Heterogeneous blood-tumor barrier permeability determines drug efficacy in experimental brain metastases of breast cancer." Clin Cancer Res **16**(23): 5664-5678.

Maeda, H., H. Nakamura and J. Fang (2013). "The EPR effect for macromolecular drug delivery to solid tumors: Improvement of tumor uptake, lowering of systemic toxicity, and distinct tumor imaging in vivo." Adv Drug Deliv Rev **65**(1): 71-79.

Mittapalli, R. K., C. E. Adkins, K. A. Bohn, A. S. Mohammad, J. A. Lockman and P. R. Lockman (2017). "Quantitative Fluorescence Microscopy Measures Vascular Pore Size in Primary and Metastatic Brain Tumors." Cancer Res **77**(2): 238-246.

Mittapalli, R. K., X. Liu, C. E. Adkins, M. I. Nounou, K. A. Bohn, T. B. Terrell, H. S. Qhattal, W. J. Geldenhuys, D. Palmieri, P. S. Steeg, Q. R. Smith and P. R. Lockman (2013). "Paclitaxel-hyaluronic nanoconjugates prolong overall survival in a preclinical brain metastases of breast cancer model." Mol Cancer Ther **12**(11): 2389-2399.

Morikawa, A., D. M. Peereboom, H. R. Thorsheim, R. Samala, R. Balyan, C. G. Murphy, P. R. Lockman, A. Simmons, R. J. Weil, V. Tabar, P. S. Steeg, Q. R. Smith and A. D. Seidman (2015). "Capecitabine and lapatinib uptake in surgically resected brain metastases from metastatic breast cancer patients: a prospective study." Neuro Oncol **17**(2): 289-295.

94

Noble, C. O., M. T. Krauze, D. C. Drummond, J. Forsayeth, M. E. Hayes, J. Beyer, P. Hadaczek, M. S. Berger, D. B. Kirpotin, K. S. Bankiewicz and J. W. Park (2014). "Pharmacokinetics, tumor accumulation and antitumor activity of nanoliposomal irinotecan following systemic treatment of intracranial tumors." Nanomedicine (Lond) **9**(14): 2099-2108.

Ostrowski, A. D., B. F. Lin, M. V. Tirrell and P. C. Ford (2012). "Liposome encapsulation of a photochemical NO precursor for controlled nitric oxide release and simultaneous fluorescence imaging." Mol Pharm **9**(10): 2950-2955.

Sambade, M., A. Deal, A. Schorzman, J. C. Luft, C. Bowerman, K. Chu, O. Karginova, A. V. Swearingen, W. Zamboni, J. DeSimone and C. K. Anders (2016). "Efficacy and pharmacokinetics of a modified acid-labile docetaxel-PRINT((R)) nanoparticle formulation against non-small-cell lung cancer brain metastases." Nanomedicine (Lond) **11**(15): 1947-1955.

Siegel, R. L., K. D. Miller and A. Jemal (2015). "Cancer statistics, 2015." CA Cancer J Clin **65**(1): 5-29.

Society, A. C. (2015). "Breast Cancer Facts & Figures 2015-2016."

Sperduto, P. W., N. Kased, D. Roberge, Z. Xu, R. Shanley, X. Luo, P. K. Sneed, S. T. Chao, R. J. Weil, J. Suh, A. Bhatt, A. W. Jensen, P. D. Brown, H. A. Shih, J. Kirkpatrick, L. E. Gaspar, J. B. Fiveash, V. Chiang, J. P. Knisely, C. M. Sperduto, N. Lin and M. Mehta (2012). "Summary report on the graded prognostic assessment: an accurate and facile diagnosis-specific tool to estimate survival for patients with brain metastases." J Clin Oncol **30**(4): 419-425.

Taskar, K. S., V. Rudraraju, R. K. Mittapalli, R. Samala, H. R. Thorsheim, J. Lockman, B. Gril, E. Hua, D. Palmieri, J. W. Polli, S. Castellino, S. D. Rubin, P. R. Lockman, P. S. Steeg and Q. R.

Smith (2012). "Lapatinib distribution in HER2 overexpressing experimental brain metastases of breast cancer." Pharm Res **29**(3): 770-781.

Wang, X., Z. Rao, H. Qin, G. Zhang, Y. Ma, Y. Jin, M. Han, A. Shi, Y. Wang and X. Wu (2016). "Effect of hesperidin on the pharmacokinetics of CPT-11 and its active metabolite SN-38 by regulating hepatic Mrp2 in rats." Biopharm Drug Dispos **37**(7): 421-432.
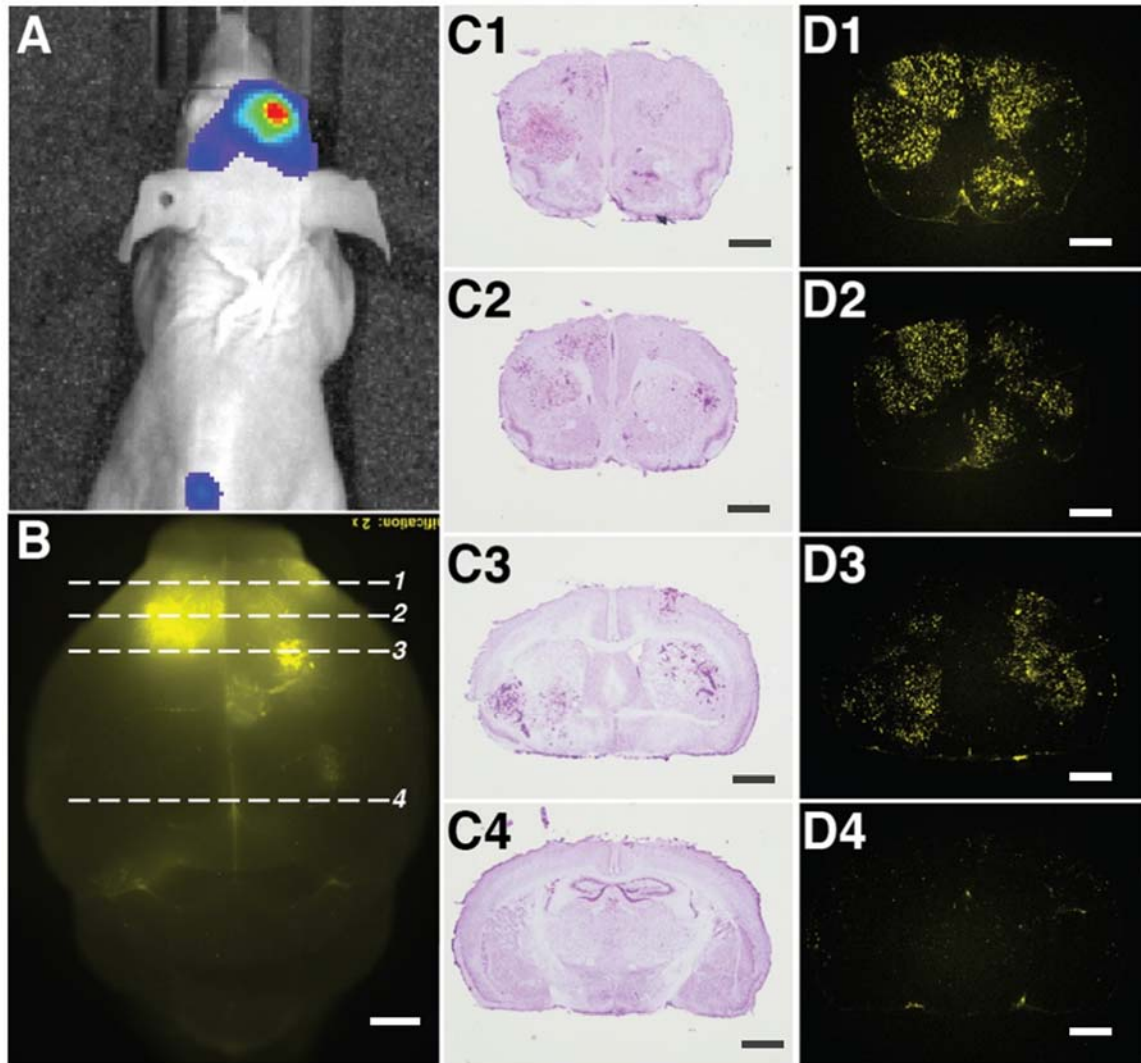
Figure 4.1: nal-IRI-50 accumulates in metastatic lesions in preclinical brain metastases of breast cancer model after 24 hour intravenous administration.

A. Image showing MDA MB 231Br-Luc brain metastases Bio-luminescence image (BLI) signal

B. Image showing accumulation of fluorescent liposomes. The numbered dashed lines 1,2,3 and 4 corresponds to the numbered coronal sections (C and D panels).

C. Cresyl violet stained images corresponding to tumors in brain sections. (C1= Bregma 2.24 mm; C2=1.54 mm; C3= 0.5 mm; C4= -0.7 mm)

D. Florescent liposomes accumulation in the corresponding brain tumors. . (D1= Bregma 2.24 mm; D2=1.54 mm; D3= 0.5 mm; D4= -0.7 mm).
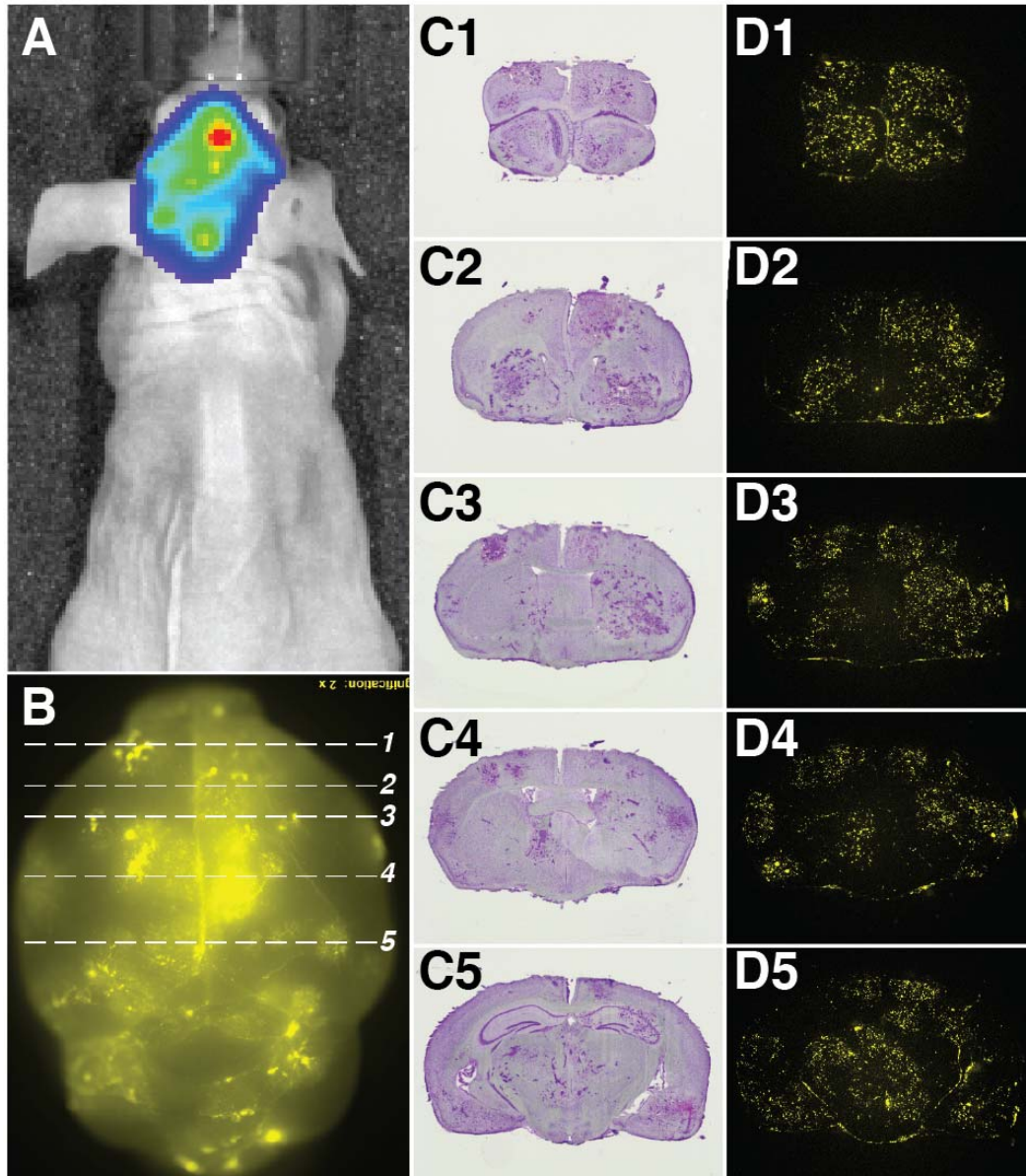
Figure 4.2: nal-IRI-50 accumulates in metastatic lesions in preclinical brain metastases of breast cancer model after 24 hour intravenous administration.

A. Image showing MDA MB 231Br-Luc brain metastases Bio-luminescence image (BLI) signal

B. Image showing accumulation of fluorescent liposomes. The numbered dashed lines 1,2,3 and 4 corresponds to the numbered coronal sections (C and D panels).

C. Cresyl violet stained images corresponding to tumors in brain sections. (C1= Bregma 2.8 mm; C2=1.18 mm; C3= 0.5 mm; C4= -0.7 mm; C5= -2.18 mm)

D. Florescent liposomes accumulation in the corresponding brain tumors. (D1= Bregma 2.8 mm; D2=1.18 mm; D3= 0.5 mm; D4= -0.7 mm; D5= -2.18 mm)

Figure 4.3: nal-IRI-10 accumulates in metastatic lesions in preclinical brain metastases of breast cancer model after 24 hour intravenous administration.
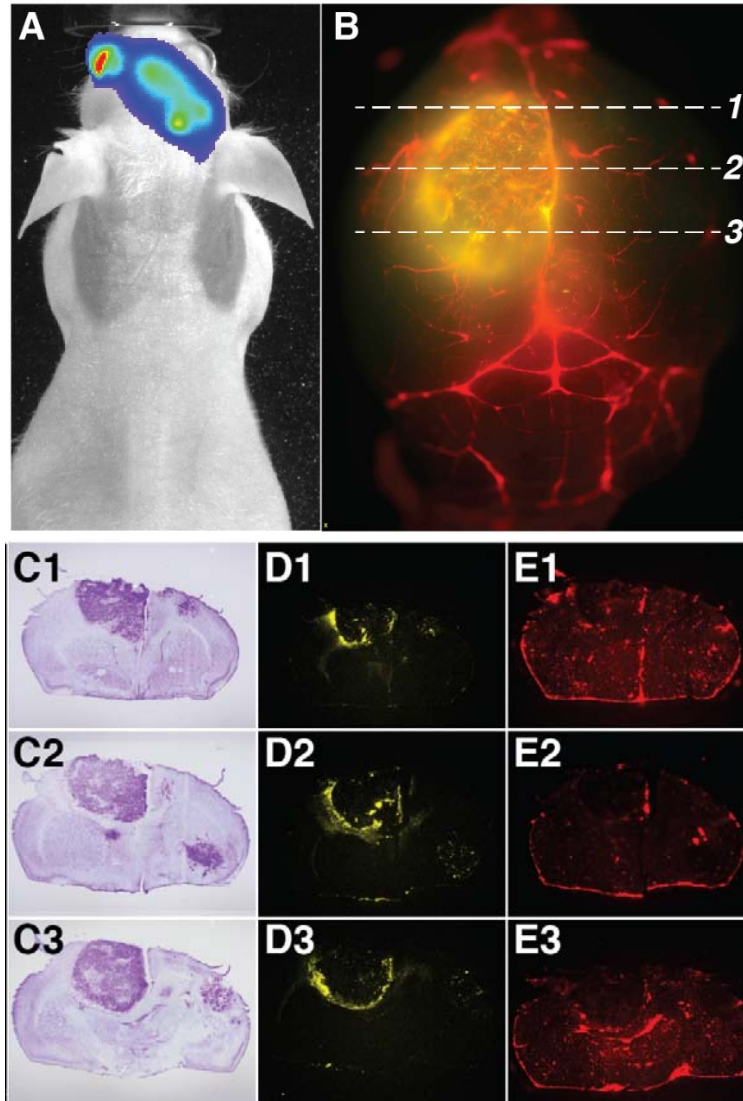
A. Image showing MDA MB 231Br-Luc brain metastases Bio-luminescence image (BLI) signal

B. Image showing accumulation of fluorescent liposomes. The numbered dashed lines 1,2,3 and 4 corresponds to the numbered coronal sections (C, D and E panels).

C. Cresyl violet stained images corresponding to tumors in brain sections. (C1= Bregma 1.10 mm; C2=0.02 mm; C3= -1.06 mm)

D. Florescent liposomes accumulation in the corresponding brain tumors. (D1= Bregma 1.10 mm; D2=0.02 mm; D3= -1.06 mm)

E. Image showing vasculature in brain sections. (E1= Bregma 1.10 mm; E2=0.02 mm; E3= -1.06 mm)

Figure 4.4: Dil5-labelled liposomes accumulate in metastatic lesions in preclinical brain metastases of breast cancer model 24 hr after intravenous administration.
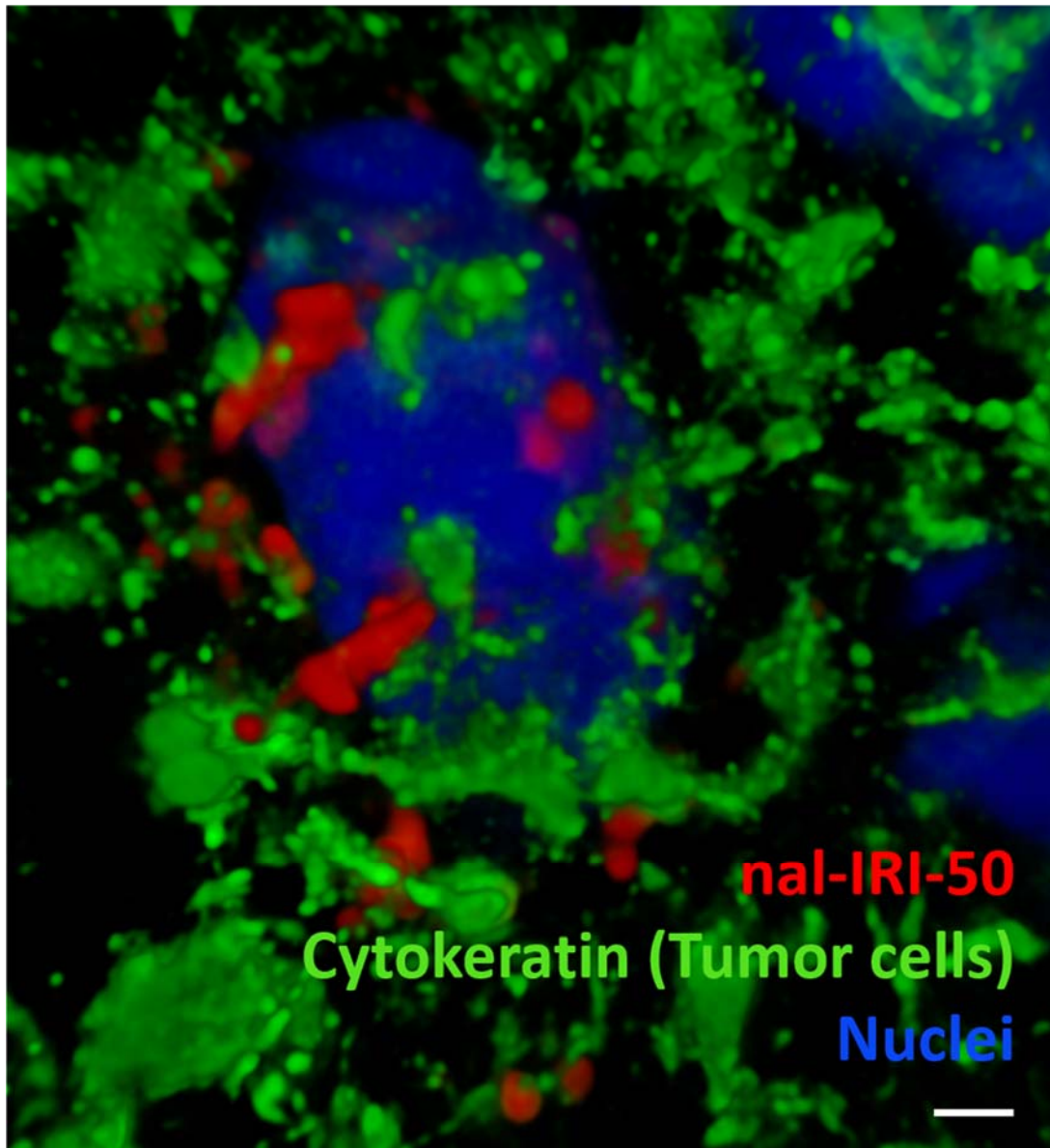
Mouse brain tissue sections were stained for DAPI (blue) and cytokeratin (green) after 24 hr circulation of Dil5-labelled liposomes. DAPI highlights the nucleus and cytokeratin highlights MDA-MB-231Br-Luc brain metastases. We observed Dil5-labelled liposomes (red) accumulated in the MDA-MB-231Br-Luc cancer cell (green) around the nucleus (blue). Images were acquired from Nikon N-Storm super-resolution microscope system. Scale bar =1 µm.
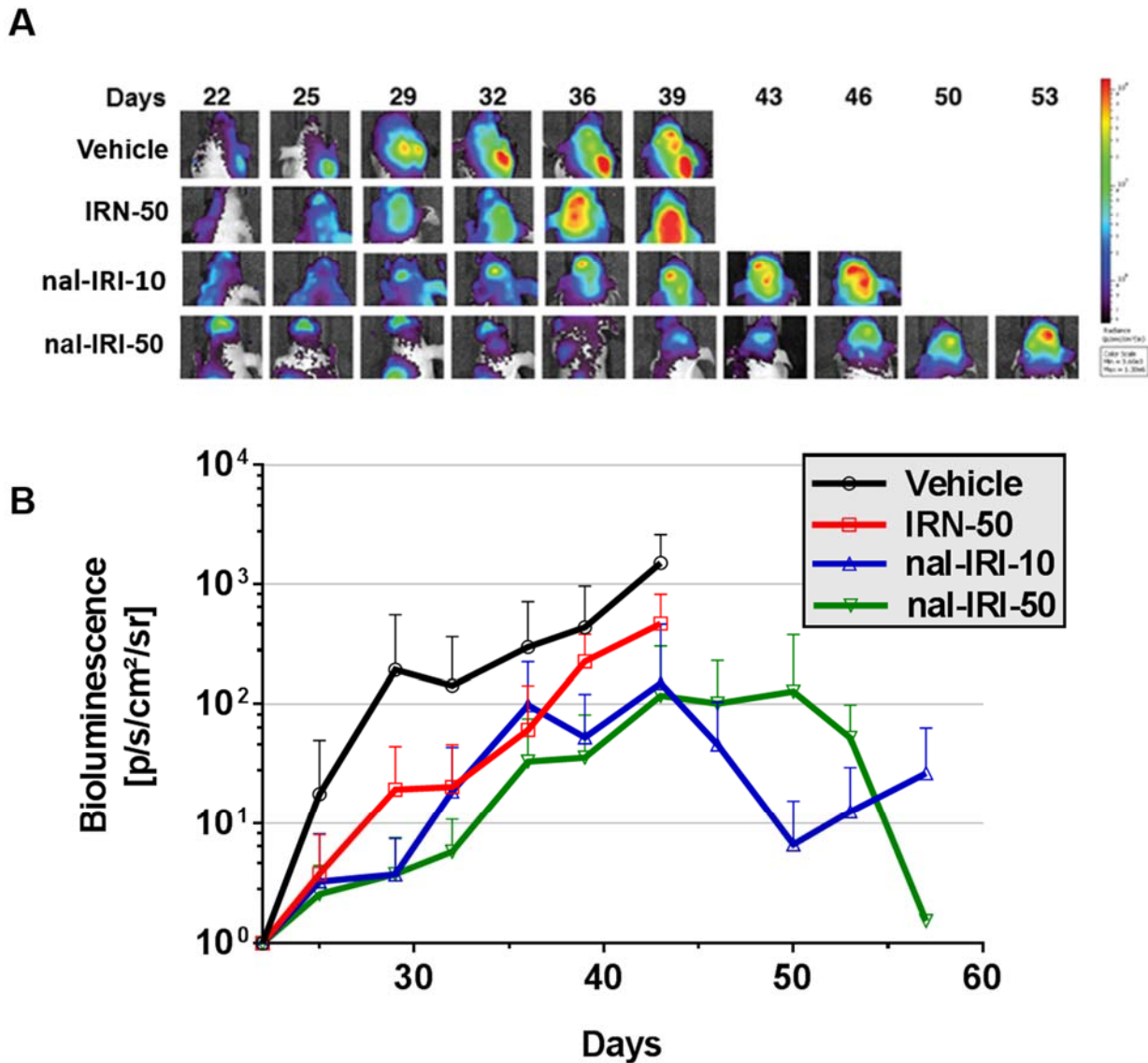
Figure 4.5: Liposomal irinotecan decreases tumor burden compared to non-liposomal irinotecan and vehicle.

(A) *In vivo* optical imagining (IVIS Lumina) was used to confirm and monitor the metastatic tumor growth after intracardiac injection. Increase in BLI signal in brain reflects the pattern of metastatic tumor growth in different treatment groups. Images acquired are of same animal sequentially over time. **(B)** Mean BLI signal versus time in mice exhibiting brain metastases. Treatment was initiated on day 21. Each data point represents mean ± SD. Tumor burden in groups treated with liposomal irinotecan were significantly lower ($P<0.05$)
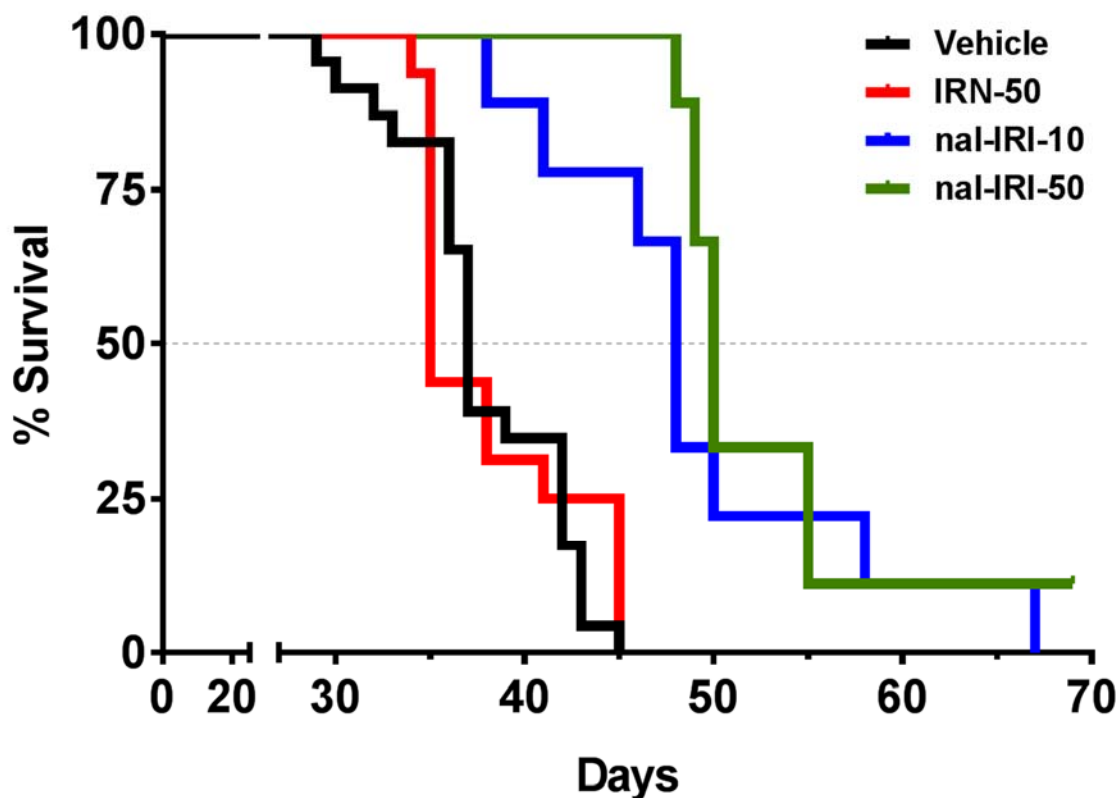
Figure 4.6: Kaplan-Meier Survival Plot of mice bearing metastatic brain tumors from human triple negative breast cancer.

The mice were treated weekly via IV bolus with vehicle (n=23), IRN-50 (n = 16), nal-IRI -10 (n=8) and nal-IRI -50 (n=9) starting 21 days after intracardiac injection of MDA-MB-231Br-Luc cancer cells. The median survival time was 37 days for vehicle, 35 days for IRN-50, 48 and 50 days for nal-IRI -10 and nal-IRI -50 respectively. The median survival for liposomal irinotecan groups (nal-IRI -10 and nal-IRI -50) significantly increased ($P< 0.05$) when compared to vehicle group. The groups were compared to vehicle by Log-rank statistical analysis.

CHAPTER 5

NOTCH-4 INHIBITION FOLLOWED BY CHEMOTHERAPY ADMINISTRATION DECREASES TUMOR BURDEN AND INCREASES SURVIVAL IN A MOUSE MODEL OF BRAIN METASTASES OF BREAST CANCER.

5.1 Introduction

Drugs used in the treatment of CNS disorders like psychosis, Parkinson's disease, Alzheimer's disease, affective mood disorders, pain and brain tumors experience a peculiar hurdle of passing into the brain because of a selective barrier between brain and blood (Oldendorf 1974). Entry of the molecules into the brain is regulated by this selective barrier and it is called the Blood Brain Barrier (BBB). Many drugs that act on the CNS disorders should be delivered at the site of action, which are often invasive because of intact BBB (Pardridge 1997).

Blood capillaries in the brain are not structurally similar to that of other tissues. The unique structural characteristic of the BBB is complete sealing of vascular endothelium with tight junction protein complexes like occludins, claudins, and intercellular junctional adhesion molecules making BBB devoid of any paracellular diffusion of drugs from blood to brain(Ballabh, Braun et al. 2004). In addition to the compact endothelium in the cerebral capillaries, it also contains pericytes and astrocytes. Pericytes share common basement membrane with endothelial cells and they are on the brain side of the endothelium. Astrocytes are specialized glial cells supporting the neurons. The extensions of these cell are called foot processes or limbs which are closely associated with cerebral endothelial cells encapsulating the capillaries. This physically uncompromised structure is also complemented with various active

efflux mechanisms and highly active enzymes secreted by endothelial cells, pericytes and astrocytes represent diffusion of drugs across the BBB is also curtailed metabolically. The active efflux mechanisms include P-glycoprotein, breast cancer resistance proteins and the family of multi drug resistance proteins which decrease the BBB permeability considerably despite their lipophilicity. The drugs that undergo active efflux mechanism include anti-cancer drugs like doxorubicin and vincristine. (Sun et al. 2003, Noble et al. 2014) (Löscher and Potschka 2005). Several families of active enzymes like phosphatases secreted by brain parenchyma and microvessel endothelial cells inactivate several drugs including peptides and neuropeptides.(Minn et al. 1991) (Brownlees and Williams 1993).

20-40% of the patients with advanced breast cancer will develop symptomatic brain metastases (Ostrom, Gittleman et al. 2016). Once the patients develop metastatic brain tumor from breast cancer, there is 80% mortality within one year in the patients (Ostrom, Gittleman et al. 2016). Current modalities for treatment of metastatic brain tumors from breast cancer include radiotherapy and surgical resection (Kocher, Soffietti et al. 2011). Chemotherapy fails to cross the blood-brain barrier and show optimum efficacy in metastatic brain tumors (Lockman, Mittapalli et al. 2010). There is a need for developing new strategies to increase the permeability of the vasculature in brain metastases specifically.

In our previous studies we found that the vasculature in the tumor (BTB) is leakier compared normal brain vasculature (BBB) (Adkins et al. 2016). The increased permeability of blood vessels in the tumor (BTB) can be accounted for angiogenic process in the tumor(Dvorak et al. 1988, Jain 2000). Many studied antiangiogenic therapy for brain tumors but the results demonstrated that these therapies resulted in sustained tumor progression and also increased local invasion of the tumor cells (Leenders et al. 2004, Pàez-Ribes et al. 2009). One approach to

104

improve chemotherapeutic permeability into the tumors is to increase angiogenesis as angiogenic vessels are leakier compared to normal brain vessels (Carmeliet and Jain 2000, Jain and Munn 2000). Notch-4 plays an important role in angiogenesis and in quiescence of brain endothelium. The brain endothelium is a dormant and an inactive tissue and activated Notch-4 is responsible for its stabilization of mature endothelium because activated Notch-4 inhibits apoptosis and downregulates the VEGF-2 receptors making it very quiescent **(Fig. 5.1)**(Williams et al. 2006). We hypothesized that inhibiting Notch-4 will upregulate the VEGF-2 receptors, which leads to increased angiogenesis ultimately leading to increased permeability. We also hypothesized that, concurrent chemotherapy administration with Notch-4 inhibition will decrease the tumor burden and increase overall survival in mouse model of brain metastases of breast cancer.

5.2 Material and Methods

Chemicals

Irinotecan HCl, DAPT (GSI-IX) were purchased from APExBIO (Boston, MA). Irinotecan HCl was dissolved in 5% dextrose before administration into the mice intravenously and DAPT was dissolved in corn oil, 5 % (V/V) ethanol before its administration intraperitoneally. ^{14}C-labelled aminoisobutyric acid (AIB) was purchased from American Radiolabelled Chemicals (St. Louis, MO). Cresyl violet acetate (0.1%) was purchased from Sigma-Aldrich (St. Louis, MO). Firefly D-luciferase potassium salt was purchased from Caliper-PerkinElmer (Waltham, MA). All chemicals and reagents used were of analytical grade and were purchased from Sigma-Aldrich (St. Louis, MO)

Animals

All experiments in the study were conducted in female athymic nude mice (Charles River Laboratories, Kinston, NY). Mice weighed 23-28 g and were 6-8 weeks of age before the start of the experiments and were acclimated for 1 week prior to use. Mice were housed under 12-hour light/dark conditions with food and water *ad libitum*. All Experiments were performed under approved institutional Animal Care and Use Committee protocols (WVU #13-1207) and all work followed internationally recognized animal welfare guidelines.

Cell Culture

Human brain endothelial cells (CRL-3245) were purchased from ATCC (Manassas, VA) and cells were cultured in Dulbecco's Modified Eagle's Medium (DMEM) with 10% fetal bovine serum (FBS) and supplemented by 40 µg/ml endothelial growth supplement (ECGS). MDA-MB-231Br-Luc cells were kindly provided by Dr. Patricia Steeg, were cultured in Dulbecco's Modified Eagle's Medium (DMEM) with 10% fetal bovine serum (FBS). All cell work was performed under aseptic conditions, and cells were cultured at 37˚C with 5% CO_2.

Determination of Vascular endothelial growth factor receptor-2 (VEGFR-2) mRNA and protein levels

Human brain endothelial cells were treated with different concentrations of Notch-4 inhibitor DAPT, cells are collected after treatments and RNA was isolated from samples using RNeasy Plus Mini Kit (QIAGEN, Germantown, MD) according to the manufacturer's instruction. NanoDrop 1,000 spectrophotometer (Thermo Scientific, Wilmington, DE) was used assess the concentration and purity of RNA. 1 µg of RNA was reverse transcribed to cDNA with

random primers and then cDNA was diluted to the concentration of 50 ng/ml. qPCR was performed on cDNA using oligo nucleotide primer for VEGFR-2, HES-1 and GAPDH (endogenous control) by 7300 Real Time PCR (Applied Biosystems, CA) in 96 well microtiter plates with amplification mixture SYBER Green master mix (Fermentas, MA). Changes in mRNA levels were analyzed by the ΔΔCt method.

VEGFR-2 and HES-1 protein levels are determined by dissolving the cells in RIPA buffer and western blot analysis was performed as previously described (Logsdon, Lucke-Wold et al. 2017). A rabbit anit-VEGR-2 antibody (1:1000), a rabbit anti-HES-1 (1:1000), and a rabbit anti-GAPDH antibody (1:1000) (Cell signaling, Denvers, CA) were used with a secondary IRDye 800 CW (goat anti-rabbit) (LI-COR Biosciences).

Determination of Blood-Brain Barrier Permeability

Mice were anesthetized under 2% isoflurane and injected with 175,000 MDA MB 231Br-Luc cells intracardially into the left ventricle using stereotaxic device (Stoelting, Wood Dale, IL). After the injection metastases were allowed to develop and presence of brain metastases was confirmed by the presence of bio-luminescence imaging (BLI) on the mice on day 21. Once the confirmation of metastases the mice were randomized into 3 different groups and treated with control (Corn oil, 5 % (V/V) ethanol), 50 mg/kg DAPT and 100 mg/kg DAPT intraperitoneally daily until the mice showed neurological symptoms. The mice were anesthetized with ketamine/xylazine (100mg/kg and 8mg/kg respectively) and administered with 10 µCi/animal ^{14}C-labelled aminoisobutyric acid (AIB) intravenously and allowed it to circulate for 10 minutes, then animals were euthanized. Brains were rapidly removed and flash frozen in isopentane and then stored at negative 80°C.

Brains were sliced at 20 μm thickness using cryotome (Leica CM3050S; Leica Microsystems, Wetzlar, Germany) and transferred to slides. The slides were placed in quantitative autoradiography (QAR) cassettes (GE Healthcare, Piscataway, NJ) and then a phosphor screen (FujiFilm Life Sciences, 20×40 super-resolution) was placed over the slides and allowed to develop for 20 days. High resolution phosphor imager (FUJI FLA-7000, FujiFilm Life Sciences) was used develop QAR phosphor screens and the images were converted to digital images which were calibrated with ^{14}C standards and analyzed using MCID Analysis software (InterFocus Imaging LTD, Linton, Cambridge, England). The permeability of ^{14}C-labelled aminoisobutyric acid (AIB) in brain metastases were determined by overlaying cresyl violet stained images of the same brain slice.

Survival of animals with brain metastases

Brain seeking breast cancer cell were injected intracardially and allowed to metastasize. The presence of metastases was confirmed on day 21 by BLI and then the mice were randomized and divided into 4 different groups (n=10), Vehicle group, Irinotecan group, DAPT group and DAPT+ irinotecan group and treated according with vehicle or DAPT (50mg/kg I.P, once daily) or irinotecan (50 mg/kg I.V, once a week). The treatment were continued with BLI to monitor tumor burden. Once animals developed neurological symptoms or showed weight loss of ≥20 %, they were sacrificed under anesthesia. Euthanasia upon development of neurological symptoms was blinded and performed based on the recommendation of OLAR staff at WVU. BLI data was gathered twice weekly to quantify tumor burden and progression in different groups, similar to our previous work (Adkins et al. 2015).

Data Analysis

A long-rank test (GraphPad® Prism 6.0, San Diego, CA) was used to compare difference among different groups and groups were considered statistically different at p<0.05. Living Image V4.0 software (PerkinElmer, Waltham, MA) was used to quantify tumor burden in different groups.

5.3 Results:

Increase in VEGFR-2 mRNA and protein levels in human brain endothelial cells after Notch-4 inhibition

First, we investigated mRNA levels in human brain endothelial cells after treating with Notch-4 inhibitor DAPT at different concentration; 0 µM (Control), 5 µM, 10 µM, 20 µM, 50 µM, and 100 µM. Cells were treated with DAPT treated for 48 hours before quantitative PCR was performed. We then determined mRNA levels of VEGFR-2 after Notch-4 inhibition. We found that with increase in DAPT concentrations the VEGFR-2 mRNA expression increased. The mRNA expression levels significantly increased more than two-folds in the groups treated at 10 µM, 20 µM, 50 µM DAPT. 20 µM and 50 µM of DAPT treatment showed highest fold increase (q= 2.5; p<0.05) in mRNA expression (**Fig 5.2A**). We also confirmed the inhibition of Notch-4 expression by investigating mRNA expression of HES-1 from the same samples and we found that with increase in DAPT concentration the mRNA expression of HES-1 decreased (**Fig 5.2B**).

After investigating VEGFR-2 mRNA expression levels, we studied VEGFR-2 protein levels in human brain endothelial cells after treatment with DAPT at concentration similar concentrations (0 µM (Control), 5 µM, 10 µM, 20 µM, 50 µM, and 100 µM. DAPT). We found

that the expression VEGFR-2 protein levels increased with decrease in HES-1 protein levels (**Fig 5.3**).

Notch-4 inhibition increased blood-tumor barrier permeability in animals with brain metastases of breast cancer

After studying the expression of VEGFR-2 mRNA and protein levels, we investigated the permeability of blood-tumor barrier in brain metastases. After development of brain metastases, animals were randomized into three groups, control, DAPT (50 mg/kg) and DAPT (100 mg/kg). The permeability was determined by ^{14}C-labelled aminoisobutyric acid (AIB) as discussed in methods section. We found that the permeability of ^{14}C-labelled aminoisobutyric acid (AIB) significantly increased in DAPT treated group when compared to vehicle group. DAPT (50 mg/kg) group showed the highest ^{14}C-labelled aminoisobutyric acid (AIB) levels in the tumor with the mean values of 280 ± 31 nCi/g, the values observed from DAPT (100 mg/kg) was 204 ± 24 nCi/g whereas, the control group showed the mean values of 93.5 ± 10 nCi/g (**Figure 5.4 A and B**). We also found that ^{14}C-labelled aminoisobutyric acid (AIB) levels in normal brain region did not show any differences with control group values of 5 ± 0.9 nCi/g, DAPT (50 mg/kg) showed the values of 5.6 ± 0.6 nCi/g and DAPT (100 mg/kg) showed the values of 7.9 ± 0.4 nCi/g. We also observed that there was no difference in [14]C- (AIB) permeation in brain distant from tumor.

After investigating the permeability of the tumors from different groups we want to evaluate if there is any correlation between the size of the tumor and the permeability of ^{14}C-labelled aminoisobutyric acid (AIB). We stained the brain sections with 0.1% cresyl violet acetate (Sigma-Aldrich, St. Louis, MO) to localize brain metastases. Cell sense software (Olympus,

Center Valley, PA) was used to measure the area of the metastases. Tumor size and metastases were plotted on XY plots and the XY plots were analyzed by linear regression (Graph pad prism). We found that there is no correlation between size of the tumor and the permeability of 14C-labelled aminoisobutyric acid (AIB). The R^2 value for Control group found to be 0.1, similarly for DAPT (50 mg/kg) and DAPT (100 mg/kg) the R^2 values were found to be 0.17 and 0.18 respectively (**Fig 5.5**).

Chemotherapy administration with concurrent Notch-4 inhibition reduces tumor burden and prolongs survival in animals with brain metastases of breast cancer

Lastly, we set out to determine if this increase in VEGFR-2 and increase in BTB permeability in Notch-4 treated groups would result in increased median survival in our experimental model of brain metastases of breast cancer. To investigate this, mice were injected with MDA MB 231Br-Luc cells and allowed to metastasize. Once the metastasis was confirmed in mice after 21 days, mice were randomized into four groups (n=10) into control, irinotecan (50 mg/kg), DAPT (50 mg/kg) and irinotecan (50 mg/kg) + DAPT (50 mg/kg) groups. BLI imaging was performed twice a week to monitor tumor burden in 4 groups. We found that the tumor burden progression in DAPT + Irinotecan group is delayed when compared to vehicle and other groups (**Fig. 5.6 A and B**). DAPT group and the irinotecan group showed similar trend to that of vehicle group. This decrease in tumor burden progression correlated with that of survival in different groups. The median survival of irinotecan + DAPT group significantly increased when compared to vehicle and other groups. We found that the median survival from DAPT + irinotecan group improved by 20% when compared to vehicle group. The survival from irinotecan and DAPT groups did not significantly improved when compared to the vehicle. The

median survival for vehicle group was found to be 28.5 days, whereas the median survival for irinotecan and DAPT group were found to be 29 days and the median survival for irinotecan + DAPT group was found to be 35 days **(Fig. 5.7).**

5.4 Discussion

The results of this study shows that Notch-4 inhibition increases the permeability in the brain tumors and this increased permeability also resulted in the decreased progression of tumor burden with increase in median survival when treated with chemotherapy with concurrent Notch-4 inhibition by DAPT in an experimental model of brain metastases of breast cancer.

As tumors grow, they secrete various proangiogenic growth factors such as vascular endothelial growth factor (VEGF) for their vascular supply and inhibition of angiogenesis may suppress tumor growth (Folkman 1971). Based on this many antiangiogenic therapies were developed but antiangiogenic drugs such as bevacizumab, sunitinib and afliberecept targeting VEGF pathways slowed disease progression in some patients but the results are modest and limited to certain settings (Hurwitz et al. 2004, Carmeliet and Jain 2011, Raymond et al. 2011, Jayson et al. 2016). Preclinical and clinical data suggests that brain tumors becomes more infiltrative when the VEGF pathways are inhibited by facilitating vessel co-option.(Leenders et al. 2004, de Groot et al. 2010, di Tomaso et al. 2011). We have previously showed that brain metastases are leaky compared to normal brain vasculature and here we want to take advantage of leaky vasculature in the tumor due to angiogenesis and instead of taking an antiangiogenic approach we want to investigate if proangiogenic approach would result in increase in permeation and ultimately leading increased survival in this study (Lockman et al. 2010).

Notch signaling is short range communication system between the adjacent cells by ligand gated receptors to coordinate development.(Ables et al. 2011). Notch is fully activated

112

after proteolytic cleavage of intracellular domain (ICD) of Notch receptor by gamma secretase, then intracellular domain will translocate to nucleus for further downstream events (**Fig 5.1**) (De Strooper et al. 1999). Notch signaling pathway is inhibited by inhibiting the activity of gamma secretase. Notch (Notch-1 and Notch-4 receptors) plays many roles during vascular development in vertebrates which include differentiation of both endothelial cells and vascular smooth muscle cells and it also plays a vital role in influencing angiogenesis (Gridley 2010). The role of Notch-4 in vasculogeneis and angiogenesis is crucial as activated Notch-4 downregulates the VEGF-2 thereby regulating VEGF pathways for angiogenesis (Shibuya and Claesson-Welsh 2006, Williams, Li et al. 2006). During angiogenesis, the formation of new capillaries take place from particular endothelial cells and the Notch pathway has a key role in formation and function of this endothelial tip. Inhibition of Notch signaling increases the endothelial tip cell division and branching by vessel bifurcation ultimately leading to leakier angiogenic vessel (Sainson and Harris 2007). We observed that permeability of ^{14}C-labelled aminoisobutyric acid (AIB) significantly increased after Notch-4 inhibition by a gamma secretase inhibitor, DAPT in our experimental metastatic model. We also observed that there was no difference in the permeability of brain distant from tumor after Notch-4 inhibition by DAPT when compared to vehicle group.

After studying the permeation of tumors after Notch-4 inhibition we investigated survival with chemotherapy and concurrent Notch-4 inhibition in an experimental model of metastases. We found that tumor burden progression decreased in DAPT + Irinotecan group compared to vehicle and other groups. This also correlated with the survival study, where the median survival was significantly increased in DAPT + Irinotecan group in our experimental model. We found that there was 20% increase in median survival when compared to both vehicle and irinotecan

113

group. The data suggests that increase in permeability of BTB is responsible for increased drug efficacy in the metastatic brain tumors.

In this study Notch-4 is inhibited by a gamma secretase inhibitor, DAPT (N-[N-(3, 5-difluorophenacetyl-*L*-alanyl)]-*S*-phenylglycine t-butyl ester). DAPT is investigated in other diseases like Alzheimer's disease, where they found certain isoforms of amyloid beta levels decreased upon treatment with DAPT in a mouse model of Alzheimer's disease (Portelius et al. 2010). But with chronic Notch inhibition some toxicities were observed. In a mouse study, necropsy analysis various organ revealed that Notch was active in the liver endothelium and they observed benign tumors of endothelial tumors on histopathological examination (Liu et al. 2011, Ryeom 2011). However, there is not enough data about the gamma secretase inhibitor related toxicities and the dose at which it causes toxicity(D'Onofrio et al. 2012).

In summary, we found that Notch-4 inhibition increased the expression of VEGFR-2 mRNA and protein levels. DAPT treated animals also showed increased permeability of ^{14}C-AIB in an experimental mouse model. We also observed that chemotherapy administration with concurrent Notch-4 inhibition decreased the tumor burden progression and significantly increasing the survival in a preclinical model of brain metastases of breast cancer.

5.5 References

Ables, J. L., J. J. Breunig, A. J. Eisch and P. Rakic (2011). "Not(ch) just development: Notch signalling in the adult brain." <u>Nature Reviews Neuroscience</u> **12**(5): 269-283.

Adkins, C. E., A. S. Mohammad, T. B. Terrell-Hall, E. L. Dolan, N. Shah, E. Sechrest, J. Griffith and P. R. Lockman (2016). "Characterization of passive permeability at the blood-tumor barrier in five preclinical models of brain metastases of breast cancer." <u>Clin Exp Metastasis</u> **33**(4): 373-383.

Adkins, C. E., M. I. Nounou, T. Hye, A. S. Mohammad, T. Terrell-Hall, N. K. Mohan, M. A. Eldon, U. Hoch and P. R. Lockman (2015). "NKTR-102 Efficacy versus irinotecan in a mouse model of brain metastases of breast cancer." <u>BMC Cancer</u> **15**: 685.

Ballabh, P., A. Braun and M. Nedergaard (2004). "The blood–brain barrier: an overview: Structure, regulation, and clinical implications." <u>Neurobiology of Disease</u> **16**(1): 1-13.

Brownlees, J. and C. H. Williams (1993). "Peptidases, peptides, and the mammalian blood-brain barrier." <u>J Neurochem</u> **60**(3): 793-803.

Carmeliet, P. and R. K. Jain (2000). "Angiogenesis in cancer and other diseases." <u>Nature</u> **407**(6801): 249-257.

Carmeliet, P. and R. K. Jain (2011). "Molecular mechanisms and clinical applications of angiogenesis." <u>Nature</u> **473**(7347): 298-307.

D'Onofrio, G., F. Panza, V. Frisardi, V. Solfrizzi, B. P. Imbimbo, G. Paroni, L. Cascavilla, D. Seripa and A. Pilotto (2012). "Advances in the identification of γ-secretase inhibitors for the treatment of Alzheimer's disease." Expert Opinion on Drug Discovery **7**(1): 19-37.

de Groot, J. F., G. Fuller, A. J. Kumar, Y. Piao, K. Eterovic, Y. Ji and C. A. Conrad (2010). "Tumor invasion after treatment of glioblastoma with bevacizumab: radiographic and pathologic correlation in humans and mice." Neuro Oncol **12**(3): 233-242.

De Strooper, B., W. Annaert, P. Cupers, P. Saftig, K. Craessaerts, J. Mumm, E. Schroeter, V. Schrijvers, M. Wolfe, W. Ray, A. Goate and R. Kopan (1999). "A presenilin-1-dependent gamma-secretase-like protease mediates release of Notch intracellular domain." Nature **398**(6727): 518-522.

di Tomaso, E., M. Snuderl, W. S. Kamoun, D. G. Duda, P. K. Auluck, L. Fazlollahi, O. C. Andronesi, M. P. Frosch, P. Y. Wen, S. R. Plotkin, E. T. Hedley-Whyte, A. G. Sorensen, T. T. Batchelor and R. K. Jain (2011). "Glioblastoma recurrence after cediranib therapy in patients: lack of "rebound" revascularization as mode of escape." Cancer Res **71**(1): 19-28.

Dvorak, H. F., J. A. Nagy, J. T. Dvorak and A. M. Dvorak (1988). "Identification and characterization of the blood vessels of solid tumors that are leaky to circulating macromolecules." The American Journal of Pathology **133**(1): 95-109.

Folkman, J. (1971). "Tumor angiogenesis: therapeutic implications." N Engl J Med **285**(21): 1182-1186.

Gridley, T. (2010). "Notch Signaling in the Vasculature." Curr Top Dev Biol **92**: 277-309.

Hurwitz, H., L. Fehrenbacher, W. Novotny, T. Cartwright, J. Hainsworth, W. Heim, J. Berlin, A. Baron, S. Griffing, E. Holmgren, N. Ferrara, G. Fyfe, B. Rogers, R. Ross and F. Kabbinavar (2004). "Bevacizumab plus irinotecan, fluorouracil, and leucovorin for metastatic colorectal cancer." N Engl J Med **350**(23): 2335-2342.

Jain, R. K. and L. L. Munn (2000). "Leaky vessels? Call Ang1 [??]." Nature medicine **6**(2): 131-133.

Jayson, G. C., R. Kerbel, L. M. Ellis and A. L. Harris (2016). "Antiangiogenic therapy in oncology: current status and future directions." The Lancet **388**(10043): 518-529.

Kocher, M., R. Soffietti, U. Abacioglu, S. Villà, F. Fauchon, B. G. Baumert, L. Fariselli, T. Tzuk-Shina, R.-D. Kortmann, C. Carrie, M. B. Hassel, M. Kouri, E. Valeinis, D. van den Berge, S. Collette, L. Collette and R.-P. Mueller (2011). "Adjuvant Whole-Brain Radiotherapy Versus Observation After Radiosurgery or Surgical Resection of One to Three Cerebral Metastases: Results of the EORTC 22952-26001 Study." Journal of Clinical Oncology **29**(2): 134-141.

Leenders, W. P., B. Kusters, K. Verrijp, C. Maass, P. Wesseling, A. Heerschap, D. Ruiter, A. Ryan and R. de Waal (2004). "Antiangiogenic therapy of cerebral melanoma metastases results in sustained tumor progression via vessel co-option." Clin Cancer Res **10**(18 Pt 1): 6222-6230.

Leenders, W. P. J., B. Küsters, K. Verrijp, C. Maass, P. Wesseling, A. Heerschap, D. Ruiter, A. Ryan and R. de Waal (2004). "Antiangiogenic Therapy of Cerebral Melanoma Metastases Results in Sustained Tumor Progression via Vessel Co-Option." Clinical Cancer Research **10**(18): 6222.

Liu, Z., A. Turkoz, E. N. Jackson, J. C. Corbo, J. A. Engelbach, J. R. Garbow, D. R. Piwnica-Worms and R. Kopan (2011). "Notch1 loss of heterozygosity causes vascular tumors and lethal hemorrhage in mice." The Journal of Clinical Investigation **121**(2): 800-808.

Lockman, P. R., R. K. Mittapalli, K. S. Taskar, V. Rudraraju, B. Gril, K. A. Bohn, C. E. Adkins, A. Roberts, H. R. Thorsheim, J. A. Gaasch, S. Huang, D. Palmieri, P. S. Steeg and Q. R. Smith (2010). "Heterogeneous Blood-Tumor Barrier Permeability Determines Drug Efficacy in Experimental Brain Metastases of Breast Cancer." Clinical cancer research : an official journal of the American Association for Cancer Research **16**(23): 5664-5678.

Logsdon, A. F., B. P. Lucke-Wold, R. C. Turner, X. Li, C. E. Adkins, A. S. Mohammad, J. D. Huber, C. L. Rosen and P. R. Lockman (2017). "A mouse Model of Focal Vascular Injury Induces Astrocyte Reactivity, Tau Oligomers, and Aberrant Behavior." Archives of neuroscience **4**(2): e44254.

Löscher, W. and H. Potschka (2005). "Role of drug efflux transporters in the brain for drug disposition and treatment of brain diseases." Progress in Neurobiology **76**(1): 22-76.

Minn, A., J. F. Ghersi-Egea, R. Perrin, B. Leininger and G. Siest (1991). "Drug metabolizing enzymes in the brain and cerebral microvessels." Brain Res Brain Res Rev **16**(1): 65-82.

Noble, C. O., M. T. Krauze, D. C. Drummond, J. Forsayeth, M. E. Hayes, J. Beyer, P. Hadaczek, M. S. Berger, D. B. Kirpotin, K. S. Bankiewicz and J. W. Park (2014). "Pharmacokinetics, tumor accumulation and antitumor activity of nanoliposomal irinotecan following systemic treatment of intracranial tumors." Nanomedicine (Lond) **9**(14): 2099-2108.

Oldendorf, W. H. (1974). "Blood-Brain Barrier Permeability to Drugs." Annual Review of Pharmacology **14**(1): 239-248.

Ostrom, Q. T., H. Gittleman, J. Xu, C. Kromer, Y. Wolinsky, C. Kruchko and J. S. Barnholtz-Sloan (2016). "CBTRUS Statistical Report: Primary Brain and Other Central Nervous System Tumors Diagnosed in the United States in 2009–2013." Neuro-Oncology **18**(suppl_5): v1-v75.

Pàez-Ribes, M., E. Allen, J. Hudock, T. Takeda, H. Okuyama, F. Viñals, M. Inoue, G. Bergers, D. Hanahan and O. Casanovas (2009). "Antiangiogenic Therapy Elicits Malignant Progression of Tumors to Increased Local Invasion and Distant Metastasis." Cancer Cell **15**(3): 220-231.

Pardridge, W. M. (1997). "Drug delivery to the brain." J Cereb Blood Flow Metab **17**(7): 713-731.

Portelius, E., B. Zhang, M. K. Gustavsson, G. Brinkmalm, A. Westman-Brinkmalm, H. Zetterberg, V. M. Y. Lee, J. Q. Trojanowski and K. Blennow (2010). "Effects of γ-Secretase Inhibition on the Amyloid β Isoform Pattern in a Mouse Model of Alzheimer's Disease." Neuro-Degenerative Diseases **6**(5-6): 258-262.

Raymond, E., L. Dahan, J. L. Raoul, Y. J. Bang, I. Borbath, C. Lombard-Bohas, J. Valle, P. Metrakos, D. Smith, A. Vinik, J. S. Chen, D. Horsch, P. Hammel, B. Wiedenmann, E. Van Cutsem, S. Patyna, D. R. Lu, C. Blanckmeister, R. Chao and P. Ruszniewski (2011). "Sunitinib malate for the treatment of pancreatic neuroendocrine tumors." N Engl J Med **364**(6): 501-513.

Ryeom, S. W. (2011). "The cautionary tale of side effects of chronic Notch1 inhibition." The Journal of Clinical Investigation **121**(2): 508-509.

Sainson, R. C. A. and A. L. Harris (2007). "Anti-Dll4 therapy: can we block tumour growth by increasing angiogenesis?" Trends in Molecular Medicine **13**(9): 389-395.

Shibuya, M. and L. Claesson-Welsh (2006). "Signal transduction by VEGF receptors in regulation of angiogenesis and lymphangiogenesis." Experimental Cell Research **312**(5): 549-560.

Sun, H., H. Dai, N. Shaik and W. F. Elmquist (2003). "Drug efflux transporters in the CNS." Advanced Drug Delivery Reviews **55**(1): 83-105.

Williams, C. K., J. L. Li, M. Murga, A. L. Harris and G. Tosato (2006). "Up-regulation of the Notch ligand Delta-like 4 inhibits VEGF-induced endothelial cell function." Blood **107**(3): 931-939.
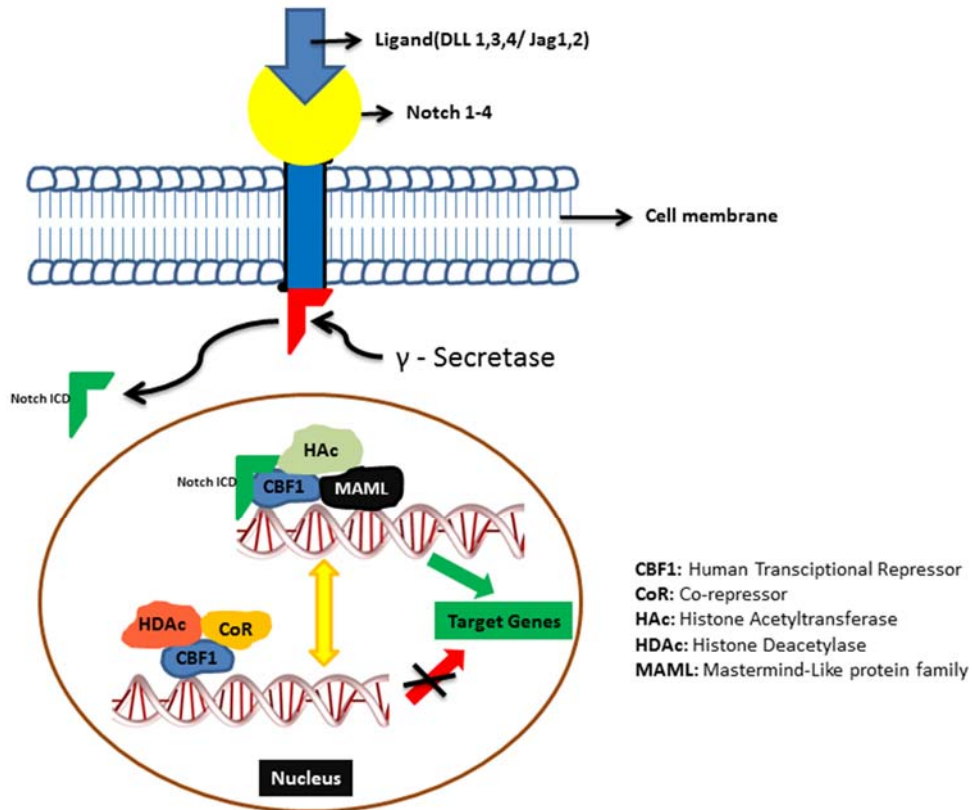
**Fig 5.1. Schematic representation of NOTCH signaling pathway.**

Notch is transmembrane proteins which act as receptor for DSL (Delta, Serrate and Lag-2) group of ligands and there are four types of Notch receptors (Notch 1, 2, 3 and 4). Notch receptor consisting of large extracellular domain (ECD), small transmembrane and intracellular domain (ICD). When the ligands bind to the ECD of the Notch receptors it initiates the S2 cleavage of the ECD domain and also internalization of both ECD and the ligand occurs. Notch is fully activated when gamma secretase cleaves ICD from the membrane. The cleaved ICD translocates to the nucleus and binds to the transcriptional repressor CBF1. The multi-protein complex of ICD, CBF1 and proteins of mastermind-like family (MAML) decreases the trascriptional repressor activity of CBF1 by displacement of co-repressor (SMRT) and Histone Deacetylase (HDAc) and with simultaneous binding of Histone acetyltransferase (HAc) and Ski-interacting protein (SKIP) ultimately causing the transcriptional initiation of HES-1.

121

A

VEGFR-2

B

HES-1
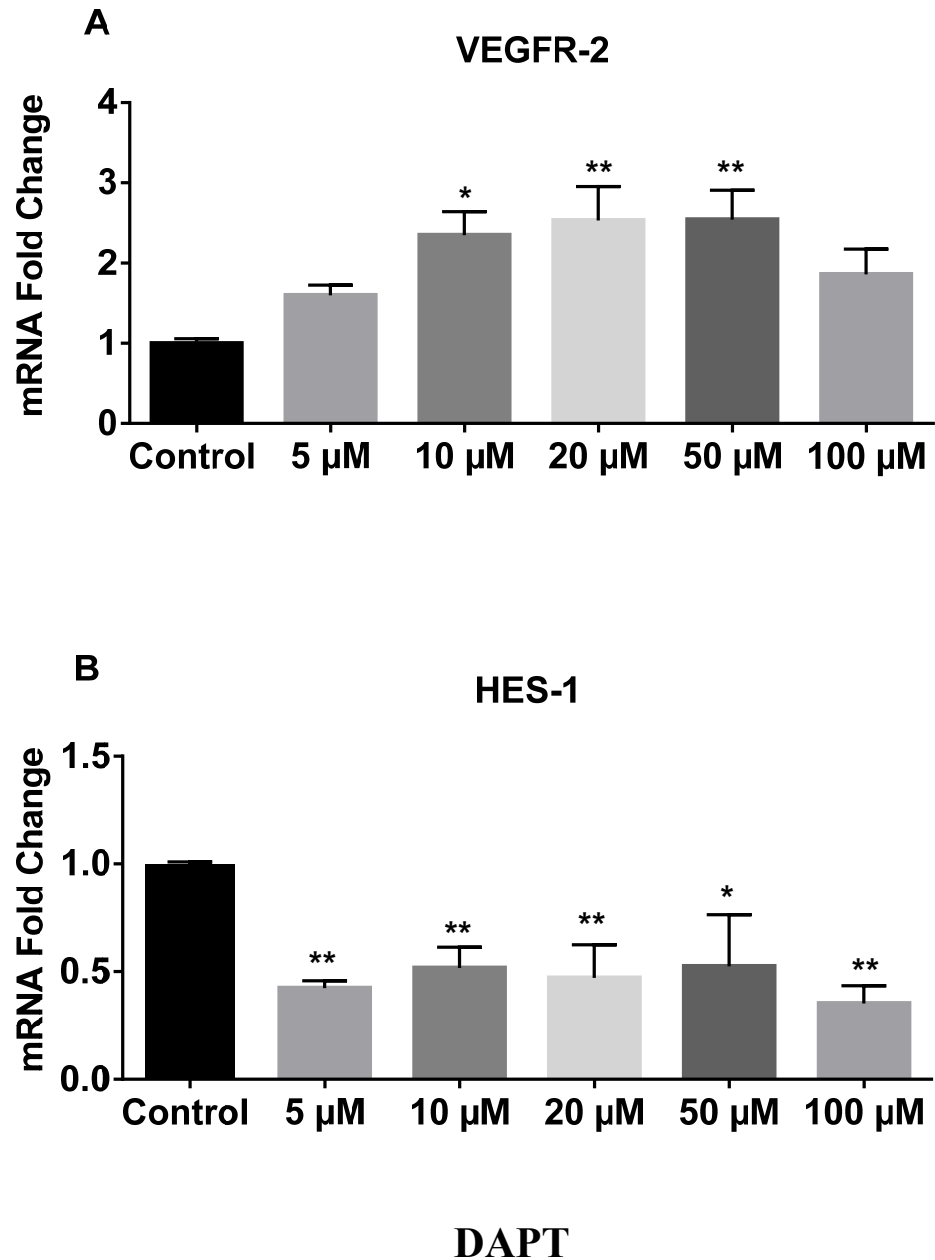
DAPT

Figure 5.2 Notch-4 inhibition increases the expression of VEGFR-2 mRNA in human brain endothelial cells

(A) A significant increase in VEGFR-2 mRNA was observed in human brain endothelial cells after treatment with DAPT at different concentration for 48 hours. (*$P < 0.05$ vs control, **$P < 0.01$ vs control). (B) A significant decrease in HES-1 mRNA was observed in human brain endothelial cells after treatment with DAPT at different concentration for 48 hours confirming Notch inhibition. (*$P < 0.05$ vs control, **$P < 0.01$ vs control)
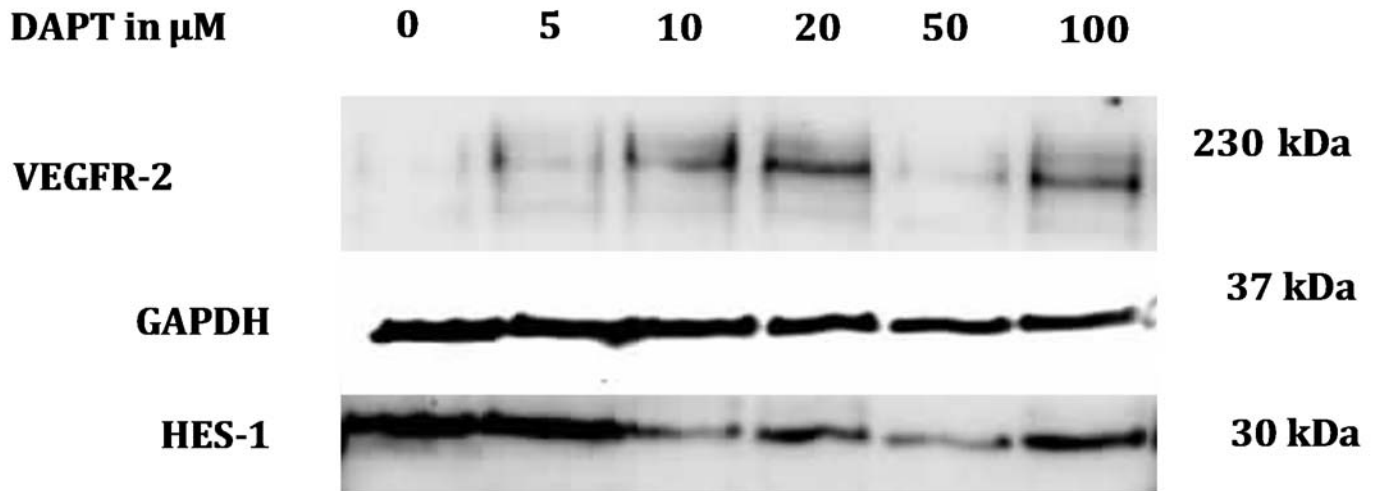
Figure 5.3 Notch-4 increases the expression of VEGFR-2 protein levels in human brain endothelial cells

Increase in VEGFR-2 protein levels was observed in human brain endothelial cells after treatment with DAPT at different concentration for 48 hours. Maximum expression of VEGFR-2 protein levels was found at 20 µM of DAPT treatment. Decrease in HES-1 protein levels was observed in human brain endothelial cells after treatment with DAPT at different concentration for 48 hours confirming Notch inhibition.
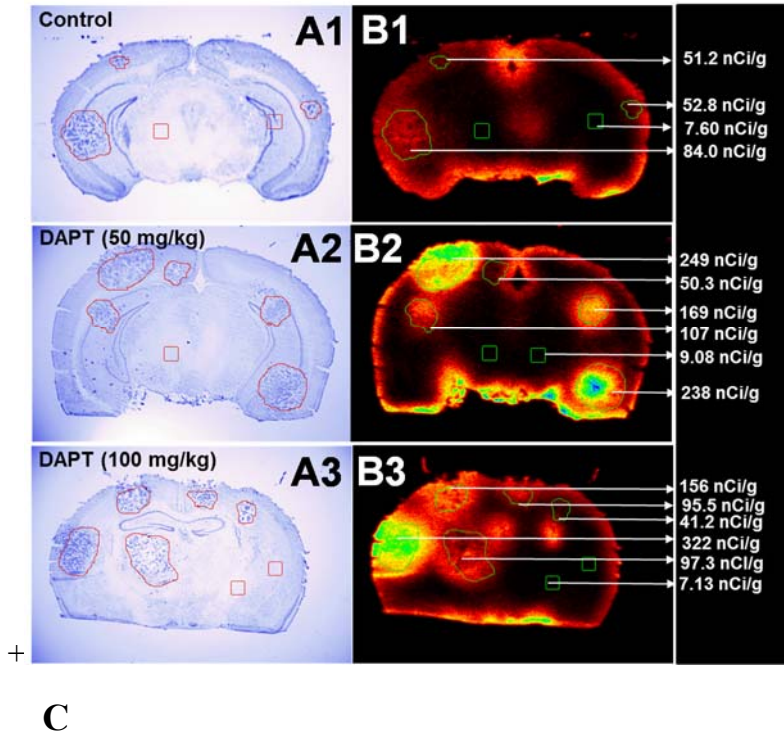
Figure 5.4 Notch-4 Inhibition Increases the permeability of ^{14}C-AIB in a Mouse Model

(A1-A3) Brain metastases identification of coronal sections based on cresyl violet staining. (B1-B3) Autoradiograms of corresponding cresyl violet sections showing the intensity of ^{14}C-AIB. (C) Image representing amount of ^{14}C-AIB accumulation in brain metastases in animals treated with saline (Control), DAPT (50mg/kg) and DAPT (100mg/kg) (****$P < 0.0001$). Each column represents mean $\pm$ SEM
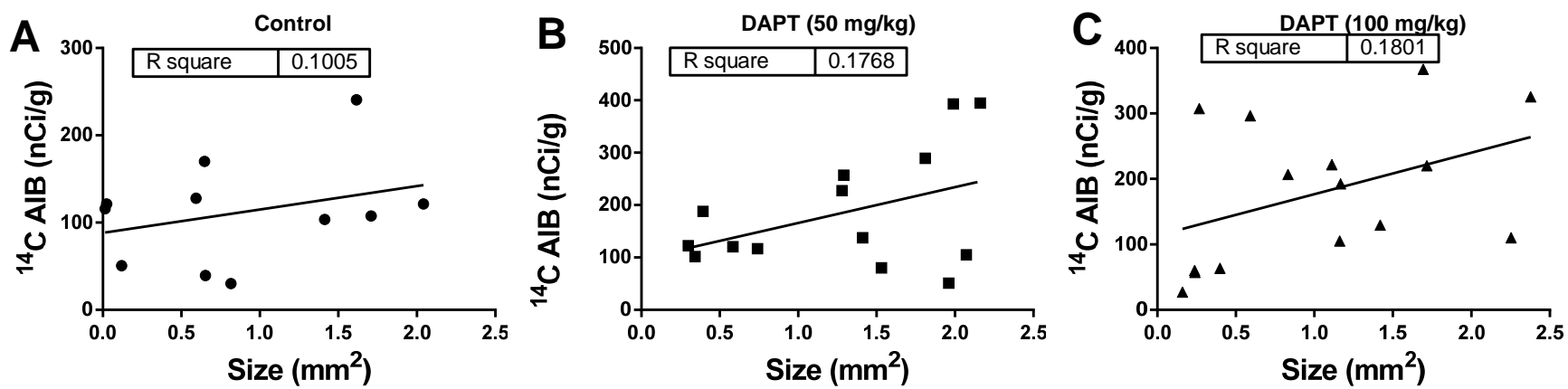
Figure 5.5 Correlation between Blood-tumor barrier permeability and size of the tumor

Cell sense software) was used to measure the area of the metastases. Tumor size and metastases were plotted on XY plots and the XY plots were analyzed by linear regression (Graph pad prism). We found that there is no correlation between size of the tumor and the permeability of 14C-AIB. (A) Represents the linear regression analysis of tumors from control animals (B) Represents linear regression analysis of tumors from DAPT (50mg/kg) group and (C) Represents linear regression analysis of tumors from DAPT (100mg/kg) group.
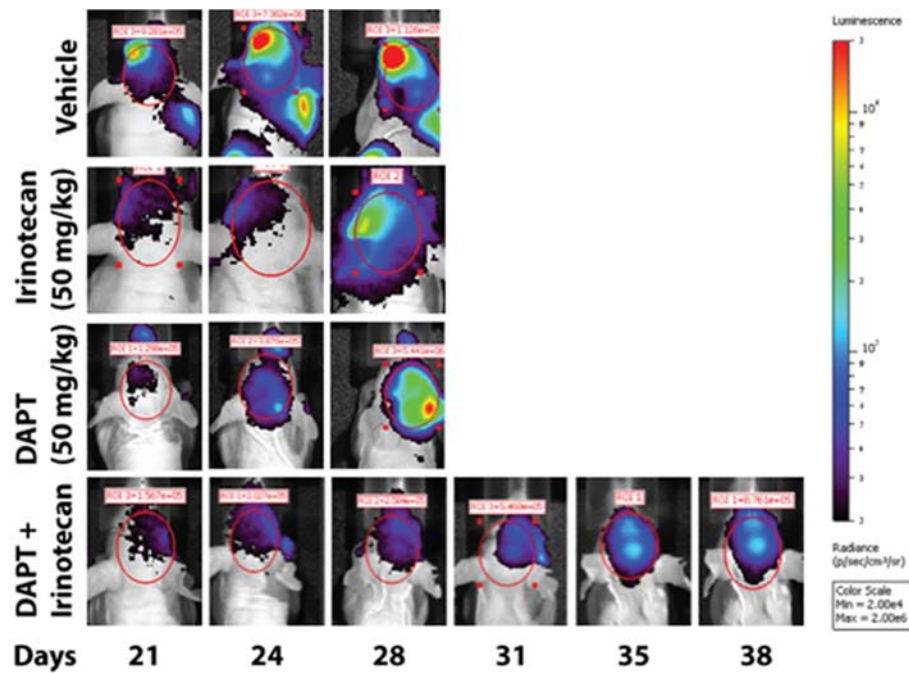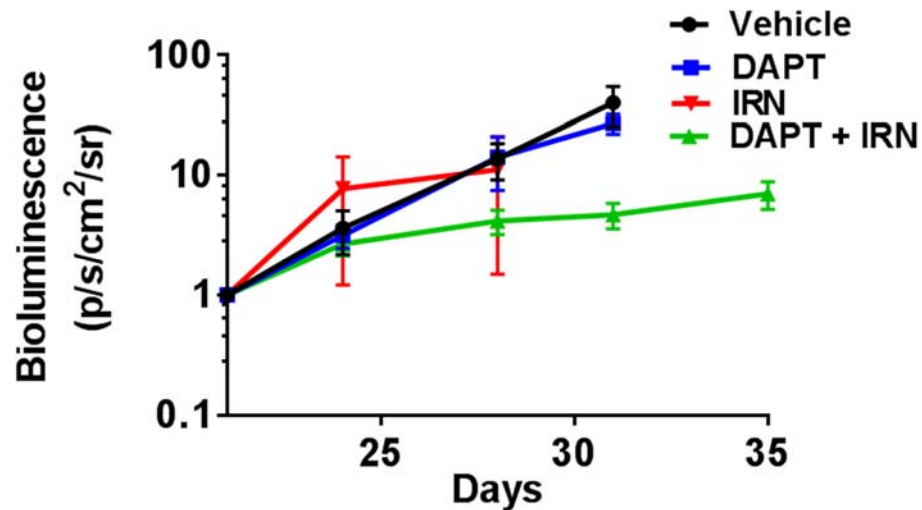
Figure 5.6 Notch-4 inhibition followed by chemotherapy administration decreases the progression of tumor burden

(A) *In vivo* optical imagining (IVIS Lumina) was used to confirm and monitor the metastatic tumor growth after intracardiac injection. (B) Mean BLI signal versus time in mice exhibiting brain metastases. Treatment was initiated on day 21. Each data point represents mean ± SEM.

F
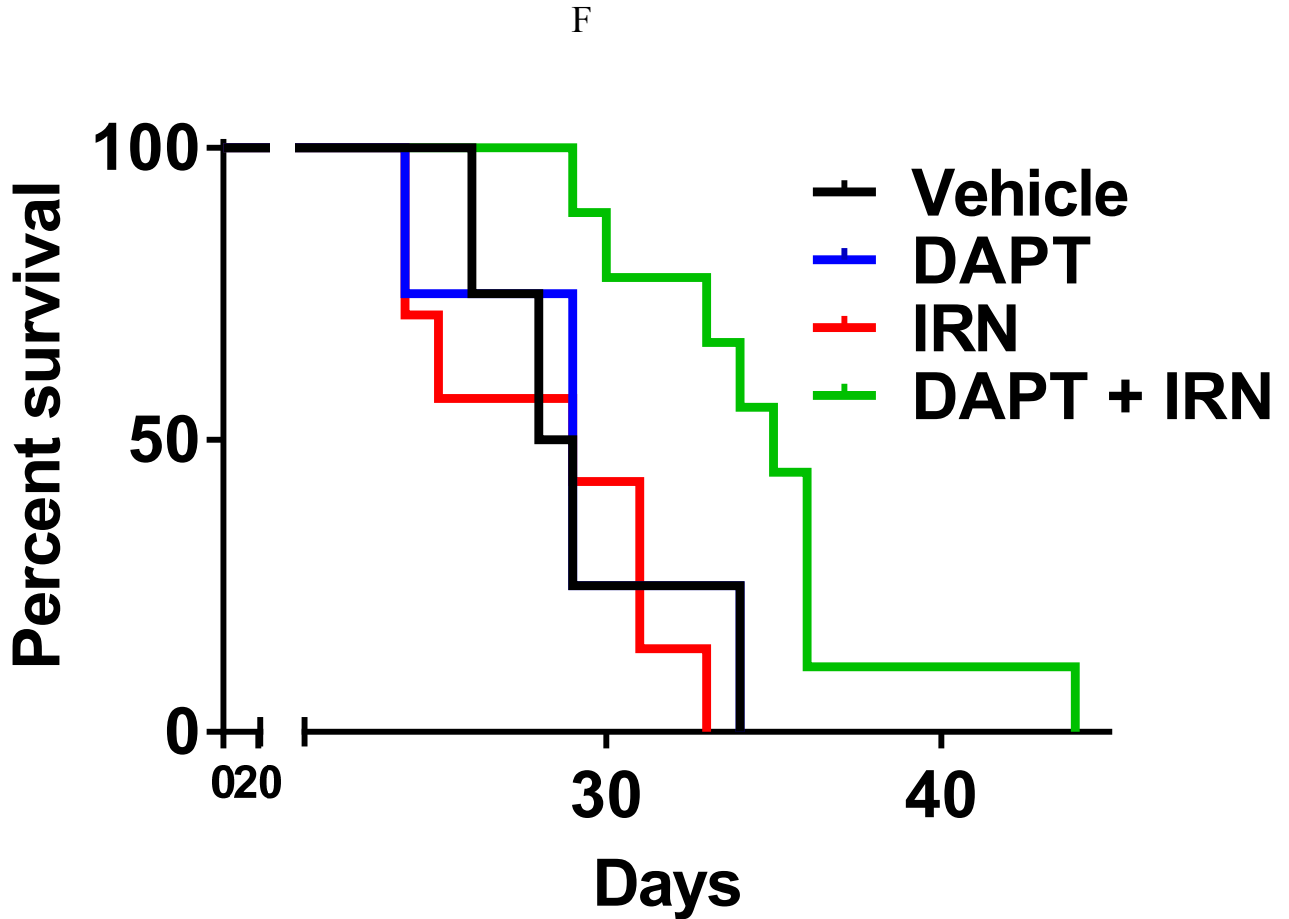
Figure 5.7 Notch-4 inhibition followed by chemotherapy administration increases the median survival

Kaplan-Meier Survival Plot of mice bearing metastatic brain tumors. The median survival time was 28.5 days for vehicle, 29 days for irinotecan (IRN), 29 and 35 days for DAPT and DAPT+ IRN respectively. DAPT+IRN treatment significantly increased ($P<0.05$) survival when compared to all other groups. The groups were compared to vehicle by Log-rank statistical analysis.

CHAPTER 6

PERMEABILITY CHANGES AND EFFECT OF CHEMOTHERAPY IN BRAIN ADJACENT TO TUMOR IN AN EXPERIMENTAL MODEL OF METASTATIC BRAIN TUMOR FROM BREAST CANCER

6.1 Introduction

The incidence of metastatic brain tumors in United States is approximately 170,000 patients annually (Platta et al. 2010). The most common primary sites for brain metastases are lung, breast and skin, with more than 70% of the patients account for cancers from lung and breast (Rivkin and Kanoff 2013). The incidence of breast cancer metastases to brain is increasing, as there is significant improvement in 5-year survival from primary breast cancer (Frisk et al. 2012, Leone and Leone 2015). Once diagnosed with metastatic brain tumors from breast cancer, 4 out of 5 patients will die within one year (Adkins et al. 2015).

Conventional chemotherapy fails in metastatic brain tumors due to the presence of blood-brain barrier (BBB)/ blood-tumor barrier (BTB), which prevents a sufficient concentration of chemotherapeutics from reaching lesions (Adkins et al. 2015). However, we have previously found that there is an increase in drug permeation in metastatic lesions when compared to normal brain (Lockman, Mittapalli et al. 2010, Adkins et al. 2016). Many newer strategies to treat metastatic brain tumors include methods to improve chemotherapeutic penetration by overcoming the BBB/BTB, including nanoparticles, osmotic BBB disruption, BBB disruption using ultrasound, etc. (Guillaume et al. 2010, Konofagou et al. 2012, El-Habashy et al. 2014, Adkins et al. 2015). All of these strategies have shown increased penetration through BBB, but

the effect of chemotherapy on tumor-adjacent healthy tissue has not been thoroughly investigated.

In this study, we hypothesize that the area around tumor is more accessible to drug penetration, or there is diffusion from the tumor into normal brain tissues, which may result in chemotherapy accumulation and effect in the brain adjacent to tumor (BAT). We tested the penetration of two different fluorescent permeability markers, texas red free dye (Mol. Wt. 625 Da.) and texas red dextran 3kDa. (Mol. wt. 3000 Da.). We then determined the distribution of ^{14}C-paclitaxel in normal brain, tumors, and BAT regions. Finally, we studied the effect of chemotherapy on BAT by staining for a marker of neuro-inflammation.

6.2 Methods

Chemicals & Reagents

The fluorescent tracers texas red (625Da) and texas red dextran (3kDa) was purchased from Molecular Probes-Life Technologies (Carlsbad, CA). Radiolabeled (^{14}C)-Paclitaxel was purchased from Moravek, Inc (Brea, CA). Cresyl violet acetate (0.1%) was purchased from Sigma-Aldrich (St. Louis, MO). All chemicals and reagents used were of analytical grade and were used as supplied.

Cell culture

Human MDA-MB-231Br metastatic breast cancer cells were cultured in DMEM supplemented with 10% FBS. MDA-MB-231Br cell lines were transfected to stably express enhanced green fluorescent protein (eGFP). All cells used in experimental conditions came from passages 1-10 and were maintained at 37°C with 5% CO_2. For all cell preparations for intracardiac injection, cells were harvested at 70% confluency.

Experimental brain metastases model

All animal handling and procedures were approved by institutional Animal Care and Use Committee protocol (WVU #13-1207), and all work followed internationally recognized animal welfare guidelines. Female athymic nu/nu mice (24-30 g) were purchased from Charles River Laboratories (Wilmington, MA) and were used for the experimental metastases model in this study. Mice were 6 to 8 weeks of age at the initiation of the brain metastases models and were housed in a barrier facility with chow and water available *ad libitum* before and after inoculation of tumor cells. For inoculation of MDA-MB-231BR cells, mice were anesthetized under 2% isoflurane and injected with 175,000 cells in the left cardiac ventricle using a sterile 27-gauge tuberculin syringe with the aid of a stereotaxic device (Stoelting, Wood Dale, IL). Injection accuracy was evaluated by a pulsatory flash of bright-red blood into the syringe upon little retraction of the plunger prior to injection. After intra-cardiac injection, mice were placed in a warmed (37°C) sterile cage and vitals monitored until fully recovered. Metastases were allowed to develop until neurologic symptoms appeared (~28 days for MDA-MB-231Br), and animals were then anesthetized with ketamine/xylazine (100mg/kg and 8mg/kg, respectively) prior to texas red (6mg/kg) and ^{14}C-Paclitaxel (10 µCi/animal) injection via IV bolus dose (femoral vein). The Texas Red dye and dextrans were allowed to circulate for 10 minutes prior to euthanasia, and ^{14}C-Paclitaxel was allowed to circulate for 8 hours before sacrifice. Brains were rapidly removed (less than 60 seconds), flash-frozen in isopentane (-65°C), and stored at negative 20°C.

Tissue processing and analysis

Brain slices (20μm) were acquired with a cryotome (Leica CM3050S; Leica Microsystems, Wetzlar, Germany) and transferred to charged microscope slides. Fluorescent images of brain slices were acquired using a stereomicroscope (Olympus MVX10; Olympus, Center Valley, PA) equipped with a 0.5 NA 2X objective and a monochromatic cooled CCD scientific camera (Retiga 4000R, QIMaging, Surrey, BC, Canada). texas red fluorescence was imaged using a DsRed sputter filter (excitation/band λ 545/25nm, emission/band λ 605/70nm and dichromatic mirror at λ 565nm) (Chroma Technologies, Bellows Falls, VT) and enhanced green fluorescent protein (expressed in MDA-MB-231Br) using an ET-GFP sputter filter (excitation/band λ 470/40nm, emission/band λ 525/50nm and dichromatic mirror at λ 495nm) (Chroma Technologies, Bellows Falls, VT). Fluorescent image capture and analysis software (SlideBook 5.0; Intelligent Imaging Innovations Inc., Denver, CO) was used to capture and quantitate images. Binary mask methodology was used to analyze brain slices based upon the eGFP fluorescence from MDA-MB-231Br cells. Binary mask methodology is simply voxel-defined regions of interest where tumor was defined by the presence of eGFP fluorescence from MDA-MB-231Br on a voxel-by-voxel basis. By this methodology, the eGFP fluorescence roughly >3-fold above background was considered as brain tumor. Once the images were acquired, circumferential fluorescent analysis was performed using software analysis (SlideBook 5.0; Intelligent Imaging Innovations Inc., Denver, CO), where 8 micron thick region of interest (ROI) were drawn 300 micron beyond and within the tumor**(Fig 6.1A and 6.1B)**. texas red permeability fold-changes were determined by texas red sum intensity (SI) per unit area of metastases relative to that of contralateral normal brain regions. The transfer coefficient (K_{in}) of texas red tracers were determined in tumor, BAT and normal brain by multiple uptake time

approach after analyzing the blood and tumor concentrations of texas red tracers as previously described by Mittapalli et al.(Mittapalli, Adkins et al. 2017)

The unidirectional blood to brain, blood to tumor and blood to BAT transfer constant K_{in} was determined for fluorescent tracers using multiple-time uptake approach (Patlak et al. 1983, Blasberg et al. 1984, Asotra et al. 2003). A single-time uptake method was used to calculate K_{in} because of heterogeneity of the metastatic tumors. K_{in} was calculated using the flowing equation(Blasberg et al. 1984)

$$K_{in=} \frac{C_{br}(T)}{\int_0^t C_{bl}(T)dt}$$

Where, C_{br} is the amount of compound in brain/metastatic tumor/ BAT per unit mass of the tissue at time T and C_{bl} is the blood concentration of the tracer. For ^{14}C-Paclitaxel permeation studies, 20μm thick brain slices were exposed for 20 days to phosphor screens along with tissue-calibrated standards for quantitative autoradiographic analysis. The phosphor screens were developed using GE Typhoon FLA 7000 and images were processed using MCID software (Imaging Research) and Adobe Photoshop to acquire color-coded drug concentrations (ng/g or μg/g) in regions of interest.

Effect of Drug on BAT

Female athymic nu/nu mice were inoculated with human MDA-MB-231-Br-Luc cells and allowed to develop metastases. On day 21, the presence of metastases is confirmed using an IVIS bioluminescent imaging system and then treated with chemotherapeutic agents including Docetaxel (10mg/kg I.V, once a week), Eribulin (1.5 mg/kg I.P, twice every week) and

Paclitaxel (10mg/kg I.V, once a week). The treatment regimen was continued until mice showed neurological symptoms, and the then mice were sacrificed and the brains collected. The brains were sectioned and stained for the presence of activated astrocytes.

6.3 Results

BAT Permeability

Regional barrier integrity was evaluated using permeability tracers' texas red 625Da and texas red dextran (3kDa), which fall within the upper-limit molecular weight of most conventional and non-biological chemotherapeutic drugs. The margins of metastases were demarcated based on eGFP fluorescence around cancer cell clusters that were confined within 100μm of each other, as previously described. Once the tumor margin was defined for each metastasis, a series of consecutive circumferential masks (8μm wide) extending 300μm beyond the original metastasis margin were generated automatically using custom written SlideBook 5.0 software scripts (**Fig. 6.1A and 6.1B**). The additional 200 μm region was drawn to also allow for analysis of brain distant to tumor. Additional circumferential masks (8μm wide) that extend 300μm internally from the metastasis margin were created using the software scripts (**Fig. 6.1C and 6.1D**).

Texas red 625Da and texas red Dextran 3kDa permeation were plotted relative to the distance from the tumor edge for three different metastases exhibiting different magnitudes of mean permeability increases (**Fig. 6.2A**). Analysis of texas red 3kDa permeation within the BAT region 100μm beyond the tumor edge for each metastasis demonstrated mean permeability increase ranging from 1.0 to 2.5-fold compared to normal brain (**Fig. 6.2B**). The mean permeability of texas red 625Da within BAT region increased 1.0 to 3.8-fold when compared to normal brain.

We then calculated K_{in} for tumor, normal brain, and BAT, and we found that there was a significant increase in K_{in} in BAT for both texas red free dye and texas red Dextran 3 kDa when compared with normal brain (**Fig. 6.3A and 6.3B**). The K_{in} values for texas red 625 Da in normal brain was found to be $1.2 \pm 0.16 \times 10^5$ mL/s/g. For tumor, it was $11.3 \pm 1.9 \times 10^5$ mL/s/g, and for BAT the K_{in} was $4.32 \pm 0.2 \times 10^5$ mL/s/g. The K_{in} values for texas red 3kDa was found to be $0.4 \pm 0.14 \times 10^5$ mL/s/g, $2 \pm 0.3 \times 10^5$ mL/s/g and $1.6 \pm 1.4 \times 10^5$ mL/s/g for normal brain, tumor and BAT respectively.

Distribution of paclitaxel in normal brain, BAT and tumor

After analyzing texas red tracer permeability and transfer coefficients in the BAT, we determined the distribution of ^{14}C-Paclitaxel using autoradiography. The tumor was identified by cresyl violet stain **(Fig. 6.4A)** and the corresponding overlaid autoradiogram **(Fig. 6.4B)** was used to analyze the concentrations of paclitaxel in 100×100 μm squares (50×50 μm squares in BAT) as shown in **Fig 6.4A** and **6.4B**. We found that there is increase in concentration of ^{14}C-Paclitaxel in BAT regions and the increase in concentration was heterogeneous as seen in the metastases. We found that the concentration of ^{14}C-paclitaxel in BAT (0-50 μm) to be 86.7 ± 31 ng/g and BAT (50-100 μm) 35.4 ± 11 ng/g (**Fig. 6.4C**), whereas the concentrations of ^{14}C-Paclitaxel beyond 100μm of tumor and normal brain was consistently found to be 1 ng/g. The concertation of ^{14}C-Paclitaxel in the tumor was 529 ± 223 ng/g consistent with our previous studies (Lockman et al. 2010).

Chemotherapeutic drugs induce astrocyte activation in BAT

After studying the permeability of tracers and ^{14}C-paclitaxel in BAT, we sought to study the effect of chemotherapeutic drugs on BAT. For this study, we treated mice with various chemotherapeutic drugs after the confirmation of metastases as mentioned above. To visualize activated astrocytes, we stained for glial fibrillary acidic protein (GFAP), which is over-expressed when astrocytes are activated (Eng et al. 2000). We observed GFAP over-expression in BAT in all the groups treated with chemotherapeutic drugs and found that there is increase in expression of GFAP in BAT (**Fig. 6.5B-F**). However, GFAP expression in BAT in vehicle group was not noticeable (**Fig. 6.5A**).

6.4 Discussion

Many studies have shown the permeability and effect of chemotherapy in the brain metastases (Lockman et al. 2010), but surprisingly, there are not many studies investigating those same effects in BAT. With increase in strategies to overcome BBB and BTB to treat metastases (Guillaume et al. 2010, Platta et al. 2010, and Konofagou et al. 2012), it is important to study the permeability in BAT and effect of chemotherapy in metastatic tumors. In this study, we found that the permeability of tracers and ^{14}C-palcitaxel increased in BAT when compared to normal brain regions distant to the tumor. We also found that administration of chemotherapeutic drugs induced activation of astrocytes in these adjacent regions.

In this work, we studied permeability for two tracers, Texas red 625Da and Texas red dextran 3kDa using quantitative fluorescence microscopy. The methodology was developed based on previous study by Mittapalli et al.,(Mittapalli et al. 2017), where all fluorescent images were captured using the same settings in the microscope to maintain uniformity in fluorescence emission (Song et al. 1996). Permeation of Texas red tracers in brain metastases were previously

characterized by Adkins et al. (Adkins et al. 2016), and we found similar fold-increase in tumor core. Unidirectional BBB/BTB transfer constants K_{in} for both dyes were calculated using an established multiple-time uptake approach (Patlak et al. 1983). The K_{in} values obtained in these studies for normal brain and tumor were consistent with our previous published data (Mittapalli et al. 2017). The increased K_{in} values in BAT when compared to normal brain clearly suggest the permeability in BAT region was increased.

Once we had confirmed the increase in permeability of the tracers, we studied the distribution of a chemotherapeutic agent, ^{14}C-paclitaxel in BAT. We used quantitative autoradiography (QAR) to determine the distribution of ^{14}C-paclitaxel in BAT, normal brain, and within the tumor (Knight, Nagaraja et al. 2005, Knight, Karki et al. 2009). We found that there is increase in accumulation of ^{14}C-paclitaxel in the BAT region and this increase is heterogeneous similar to what we have found in brain lesions previously (Lockman et al. 2010, Mittapalli et al. 2017). The increase in permeation of BTB can be accounted for angiogenesis in the tumor (Carmeliet and Jain 2000, Fukumura and Jain 2007, van Tellingen et al. 2015) and the reasons for this heterogeneous permeability within the lesion is due to dynamics of angiogenic process as reported in the previous studies (Eilken and Adams 2010).

The most common transport mechanism for drugs across BBB is through passive diffusion (Pardridge 2012). For passive diffusion of drugs across the BBB, the drugs which are lipid soluble, low molecular weight (< 400 Da) and which form ≤ 7 hydrogen bonds are better candidates(Lipinski 2000). Diffusion through lipid membrane like BBB is dependent on molecular volume of the solute, which in turn depends on its molecular weight (Levin 1980, van de Waterbeemd et al. 1998). BBB permeability decreases 100 fold with the increase is solute's molecular weight from 300 Da to 450 Da (Fischer, Gottschlich et al. 1998). In addition to solute

136

related limitations, the active efflux transporters like p-glycoprotein (P-gp) and other members of ABC (ATP-binding cassette) family of transporters present at the BBB play a significant role in efflux of chemotherapeutic agents from the brain to blood (Sharom 2008, Uchida et al. 2011). However, in metastatic lesions the BBB is disrupted (BTB) which results in an increase in penetration of chemotherapeutic agents (Hiesiger et al. 1986). The higher tumor concentration of chemotherapeutic agents in the tumor creates a concentration gradient with the surrounding normal brain allowing the chemotherapeutic agent to diffuse into normal brain (Walker and Weiss 1975). Accordingly we hypothesize that the increased accumulation of paclitaxel in the BAT region is due to higher concentration in the brain metastasis. Other studies observed increased blood flow in brain metastases and lowered in the BAT when compared to normal brain. Regarding permeability, the blood-to-tissue transfer constant (K_i) for ^{14}C-α-aminoisobutyric acid (AIB) was increased in both tumor and BAT when compared to normal brain, suggesting irregular neovascularization with increased permeability in the brain metastases (Blasberg et al. 1980, Fidler et al. 2002, Langley and Fidler 2013).

Finally, once we confirmed the increased permeation of tracers and increased distribution of ^{14}C-paclitaxel in BAT, we studied the effect of chemotherapy on BAT. After treating with various chemotherapeutic agents, we stained for GFAP to determine whether there was any inflammatory effect of chemotherapeutic drugs in CNS. GFAP is expressed in astrocytes in the brain (Baba et al. 1997), and when there is injury, inflammation or neurodegeneration in the central nervous system (CNS), the common reaction of astrocytes is hypertrophy, referred to as reactive astrocytosis or activated astrocytes (Khurgel and Ivy 1996, Niranjan et al. 2014, Yang and Wang 2015). This hypertrophy increases the expression of GFAP in astrocytes as well as the binding affinity to GFAP antibody (Hozumi et al. 1990). Expression of GFAP is altered by

many factors like brain injury and disease (Eng et al. 2000). Expression of GFAP has been shown to be increased in various diseases such as Alzheimer's, Amyotrophic lateral sclerosis (ALS), Parkinson's, Pick's, Huntington's and Autism (Murayama et al. 1991, Troost et al. 1992, Banati et al. 1998, Tsuji et al. 1999, Laurence and Fatemi 2005). In Autism, increase in autoantibodies of GFAP has also been found in plasma (Rosengren et al. 1992, Singh et al. 1997). In the case of acute CNS injuries like brain infarction and traumatic brain injury, there was increase in levels of GFAP in CSF (Aurell et al. 1991, Hausmann et al. 2000). On the other hand, decrease in GFAP expression was associated with depression and growth of gliomas (Johnston-Wilson et al. 2000, Chumbalkar et al. 2005).We found that treating with chemotherapy increased expression of GFAP protein in BAT (**Fig. 6.5**), confirming the presence of activated astrocytes after pharmacological chemotherapy regimens.

Recent studies indicate, chemotherapy may induce numerous deleterious effects within CNS such as altered cognitive function, memory and attention (Kovalchuk and Kolb 2017). Fading of cognitive function after chronic chemotherapy administration in patients with cancer has been termed "chemo-fog" or "chemo-brain" (Raffa 2010). With improvements in survival for women with breast cancer over the past decade, there is also increased number of survivors expressing concerns with memory and concentration post treatment (Schagen et al. 1999, Ahles et al. 2002, Castellon et al. 2004). Recent studies suggest that the mechanism for chemo-fog is secondary to the toxic effects imposed by sub-lethal concentrations of chemotherapy on the normal cellular population of CNS (Kaiser et al. 2014). Many studies suggests that chemotherapeutic agents not only induce oxidative stress and apoptosis in CNS but they also inhibit proliferation and differentiation of cellular population of CNS leading to abnormal

expression of neurotrophic proteins in the brains (Seigers et al. 2010, Seigers et al. 2010, Seigers and Fardell 2011, Seigers et al. 2015).

In summary, we observed permeation of fluorescent tracers were increased in the BAT compared to normal brain, which was accompanied by increased distribution of ^{14}C-paclitaxel. The increase in permeation resulted in increased uptake of chemotherapeutic agents and increased the expression of GFAP in regions adjacent to tumor, indicating reactive astrocytosis. As many new clinical strategies to treat brain metastases tend to increase drug permeation, it is also important to study potential damage in normal brain.

6.5 References

Adkins, C. E., A. S. Mohammad, T. B. Terrell-Hall, E. L. Dolan, N. Shah, E. Sechrest, J. Griffith and P. R. Lockman (2016). "Characterization of passive permeability at the blood-tumor barrier in five preclinical models of brain metastases of breast cancer." Clin Exp Metastasis **33**(4): 373-383.

Adkins, C. E., A. S. Mohammad, T. B. Terrell-Hall, E. L. Dolan, N. Shah, E. Sechrest, J. Griffith and P. R. Lockman (2016). "Characterization of passive permeability at the blood–tumor barrier in five preclinical models of brain metastases of breast cancer." Clinical & Experimental Metastasis **33**(4): 373-383.

Adkins, C. E., M. I. Nounou, T. Hye, A. S. Mohammad, T. Terrell-Hall, N. K. Mohan, M. A. Eldon, U. Hoch and P. R. Lockman (2015). "NKTR-102 Efficacy versus irinotecan in a mouse model of brain metastases of breast cancer." BMC Cancer **15**: 685.

Adkins, C. E., M. I. Nounou, R. K. Mittapalli, T. B. Terrell-Hall, A. S. Mohammad, R. Jagannathan and P. R. Lockman (2015). "A novel preclinical method to quantitatively evaluate early-stage metastatic events at the murine blood-brain barrier." Cancer Prev Res (Phila) **8**(1): 68-76.

Adkins, C. E., M. I. Nounou, R. K. Mittapalli, T. B. Terrell-Hall, A. S. Mohammad, R. Jagannathan and P. R. Lockman (2015). "A Novel Preclinical Method to Quantitatively Evaluate Early-Stage Metastatic Events at the Murine Blood–Brain Barrier." Cancer Prevention Research **8**(1): 68-76.

Ahles, T. A., A. J. Saykin, C. T. Furstenberg, B. Cole, L. A. Mott, K. Skalla, M. B. Whedon, S. Bivens, T. Mitchell, E. R. Greenberg and P. M. Silberfarb (2002). "Neuropsychologic impact of

standard-dose systemic chemotherapy in long-term survivors of breast cancer and lymphoma." <u>J Clin Oncol</u> **20**(2): 485-493.

Asotra, K., N. Ningaraj and K. L. Black (2003). "Measurement of blood-brain and blood-tumor barrier permeabilities with [14C]-labeled tracers." <u>Methods Mol Med</u> **89**: 177-190.

Aurell, A., L. E. Rosengren, B. Karlsson, J. E. Olsson, V. Zbornikova and K. G. Haglid (1991). "Determination of S-100 and glial fibrillary acidic protein concentrations in cerebrospinal fluid after brain infarction." <u>Stroke</u> **22**(10): 1254-1258.

Baba, H., K. Nakahira, N. Morita, F. Tanaka, H. Akita and K. Ikenaka (1997). "GFAP gene expression during development of astrocyte." <u>Dev Neurosci</u> **19**(1): 49-57.

Banati, R. B., S. E. Daniel and S. B. Blunt (1998). "Glial pathology but absence of apoptotic nigral neurons in long-standing Parkinson's disease." <u>Mov Disord</u> **13**(2): 221-227.

Blasberg, R. G., J. Gazendam, C. S. Patlak, W. S. Shapiro and J. D. Fenstermacher (1980). "Changes in blood-brain transfer parameters induced by hyperosmolar intracarotid infusion and by metastatic tumor growth." <u>Adv Exp Med Biol</u> **131**: 307-319.

Blasberg, R. G., W. R. Shapiro, P. Molnar, C. S. Patlak and J. D. Fenstermacher (1984). "Local blood-to-tissue transport in Walker 256 metastatic brain tumors." <u>J Neurooncol</u> **2**(3): 205-218.

Carmeliet, P. and R. K. Jain (2000). "Angiogenesis in cancer and other diseases." <u>Nature</u> **407**(6801): 249-257.

Castellon, S. A., P. A. Ganz, J. E. Bower, L. Petersen, L. Abraham and G. A. Greendale (2004). "Neurocognitive performance in breast cancer survivors exposed to adjuvant chemotherapy and tamoxifen." <u>J Clin Exp Neuropsychol</u> **26**(7): 955-969.

141

Chumbalkar, V. C., C. Subhashini, V. M. Dhople, C. S. Sundaram, M. V. Jagannadham, K. N. Kumar, P. N. Srinivas, R. Mythili, M. K. Rao, M. J. Kulkarni, S. Hegde, A. S. Hegde, C. Samual, V. Santosh, L. Singh and R. Sirdeshmukh (2005). "Differential protein expression in human gliomas and molecular insights." Proteomics **5**(4): 1167-1177.

Eilken, H. M. and R. H. Adams (2010). "Dynamics of endothelial cell behavior in sprouting angiogenesis." Curr Opin Cell Biol **22**(5): 617-625.

El-Habashy, S. E., A. M. Nazief, C. E. Adkins, M. M. Wen, A. H. El-Kamel, A. M. Hamdan, A. S. Hanafy, T. O. Terrell, A. S. Mohammad, P. R. Lockman and M. I. Nounou (2014). "Novel treatment strategies for brain tumors and metastases." Pharm Pat Anal **3**(3): 279-296.

Eng, L. F., R. S. Ghirnikar and Y. L. Lee (2000). "Glial fibrillary acidic protein: GFAP-thirty-one years (1969-2000)." Neurochem Res **25**(9-10): 1439-1451.

Eng, L. F., R. S. Ghirnikar and Y. L. Lee (2000). "Glial Fibrillary Acidic Protein: GFAP-Thirty-One Years (1969–2000)." Neurochemical Research **25**(9): 1439-1451.

Fidler, I. J., S. Yano, R. D. Zhang, T. Fujimaki and C. D. Bucana (2002). "The seed and soil hypothesis: vascularisation and brain metastases." Lancet Oncol **3**(1): 53-57.

Fischer, H., R. Gottschlich and A. Seelig (1998). "Blood-brain barrier permeation: molecular parameters governing passive diffusion." J Membr Biol **165**(3): 201-211.

Frisk, G., T. Svensson, L. M. Bäcklund, E. Lidbrink, P. Blomqvist and K. E. Smedby (2012). "Incidence and time trends of brain metastases admissions among breast cancer patients in Sweden." British Journal of Cancer **106**(11): 1850-1853.

Fukumura, D. and R. K. Jain (2007). "Tumor microvasculature and microenvironment: targets for anti-angiogenesis and normalization." Microvasc Res **74**(2-3): 72-84.

Guillaume, D. J., N. D. Doolittle, S. Gahramanov, N. A. Hedrick, J. B. Delashaw and E. A. Neuwelt (2010). "Intra-Arterial Chemotherapy with Osmotic Blood-Brain Barrier Disruption for Aggressive Oligodendroglial tumors: Results of a Phase I Study." Neurosurgery **66**(1): 48-58.

Hausmann, R., R. Riess, A. Fieguth and P. Betz (2000). "Immunohistochemical investigations on the course of astroglial GFAP expression following human brain injury." Int J Legal Med **113**(2): 70-75.

Hiesiger, E. M., R. M. Voorhies, G. A. Basler, L. E. Lipschutz, J. B. Posner and W. R. Shapiro (1986). "Opening the blood-brain and blood-tumor barriers in experimental rat brain tumors: the effect of intracarotid hyperosmolar mannitol on capillary permeability and blood flow." Ann Neurol **19**(1): 50-59.

Hozumi, I., F. C. Chiu and W. T. Norton (1990). "Biochemical and immunocytochemical changes in glial fibrillary acidic protein after stab wounds." Brain Res **524**(1): 64-71.

Johnston-Wilson, N. L., C. D. Sims, J. P. Hofmann, L. Anderson, A. D. Shore, E. F. Torrey and R. H. Yolken (2000). "Disease-specific alterations in frontal cortex brain proteins in schizophrenia, bipolar disorder, and major depressive disorder. The Stanley Neuropathology Consortium." Mol Psychiatry **5**(2): 142-149.

Kaiser, J., C. Bledowski and J. Dietrich (2014). "Neural correlates of chemotherapy-related cognitive impairment." Cortex **54**: 33-50.

Khurgel, M. and G. O. Ivy (1996). "Astrocytes in kindling: relevance to epileptogenesis." Epilepsy Res **26**(1): 163-175.

Knight, R. A., K. Karki, J. R. Ewing, G. W. Divine, J. D. Fenstermacher, C. S. Patlak and T. N. Nagaraja (2009). "Estimating blood and brain concentrations and blood-to-brain influx by magnetic resonance imaging with step-down infusion of Gd-DTPA in focal transient cerebral ischemia and confirmation by quantitative autoradiography with Gd-[(14)C]DTPA." J Cereb Blood Flow Metab **29**(5): 1048-1058.

Knight, R. A., T. N. Nagaraja, J. R. Ewing, V. Nagesh, P. A. Whitton, E. Bershad, S. C. Fagan and J. D. Fenstermacher (2005). "Quantitation and localization of blood-to-brain influx by magnetic resonance imaging and quantitative autoradiography in a model of transient focal ischemia." Magn Reson Med **54**(4): 813-821.

Konofagou, E. E., Y.-S. Tung, J. Choi, T. Deffieux, B. Baseri and F. Vlachos (2012). "Ultrasound-Induced Blood-Brain Barrier Opening." Current pharmaceutical biotechnology **13**(7): 1332-1345.

Kovalchuk, A. and B. Kolb (2017). "Chemo brain: From discerning mechanisms to lifting the brain fog-An aging connection." Cell Cycle: 1-5.

Langley, R. R. and I. J. Fidler (2013). "The biology of brain metastasis." Clin Chem **59**(1): 180-189.

Laurence, J. A. and S. H. Fatemi (2005). "Glial fibrillary acidic protein is elevated in superior frontal, parietal and cerebellar cortices of autistic subjects." Cerebellum **4**(3): 206-210.

Leone, J. P. and B. A. Leone (2015). "Breast cancer brain metastases: the last frontier." Experimental Hematology & Oncology **4**(1): 33.

Levin, V. A. (1980). "Relationship of octanol/water partition coefficient and molecular weight to rat brain capillary permeability." J Med Chem **23**(6): 682-684.

Lipinski, C. A. (2000). "Drug-like properties and the causes of poor solubility and poor permeability." J Pharmacol Toxicol Methods **44**(1): 235-249.

Lockman, P. R., R. K. Mittapalli, K. S. Taskar, V. Rudraraju, B. Gril, K. A. Bohn, C. E. Adkins, A. Roberts, H. R. Thorsheim, J. A. Gaasch, S. Huang, D. Palmieri, P. S. Steeg and Q. R. Smith (2010). "Heterogeneous blood-tumor barrier permeability determines drug efficacy in experimental brain metastases of breast cancer." Clin Cancer Res **16**(23): 5664-5678.

Mittapalli, R. K., C. E. Adkins, K. A. Bohn, A. S. Mohammad, J. A. Lockman and P. R. Lockman (2017). "Quantitative Fluorescence Microscopy Measures Vascular Pore Size in Primary and Metastatic Brain Tumors." Cancer Res **77**(2): 238-246.

Mittapalli, R. K., C. E. Adkins, K. A. Bohn, A. S. Mohammad, J. A. Lockman and P. R. Lockman (2017). "Quantitative Fluorescence Microscopy Measures Vascular Pore Size in Primary and Metastatic Brain Tumors." Cancer Research **77**(2): 238-246.

Murayama, S., K. Inoue, H. Kawakami, T. W. Bouldin and K. Suzuki (1991). "A unique pattern of astrocytosis in the primary motor area in amyotrophic lateral sclerosis." Acta Neuropathol **82**(6): 456-461.

Niranjan, R., R. Nagarajan, K. Hanif, C. Nath and R. Shukla (2014). "LPS induces mediators of neuroinflammation, cell proliferation, and GFAP expression in human astrocytoma cells

U373MG: the anti-inflammatory and anti-proliferative effect of guggulipid." <u>Neurol Sci</u> **35**(3): 409-414.

Pardridge, W. M. (2012). "Drug Transport across the Blood–Brain Barrier." <u>Journal of Cerebral Blood Flow & Metabolism</u> **32**(11): 1959-1972.

Patlak, C. S., R. G. Blasberg and J. D. Fenstermacher (1983). "Graphical evaluation of blood-to-brain transfer constants from multiple-time uptake data." <u>J Cereb Blood Flow Metab</u> **3**(1): 1-7.

Patlak, C. S., R. G. Blasberg and J. D. Fenstermacher (1983). "Graphical Evaluation of Blood-to-Brain Transfer Constants from Multiple-Time Uptake Data." <u>Journal of Cerebral Blood Flow & Metabolism</u> **3**(1): 1-7.

Platta, C. S., D. Khuntia, M. P. Mehta and J. H. Suh (2010). "Current treatment strategies for brain metastasis and complications from therapeutic techniques: a review of current literature." <u>Am J Clin Oncol</u> **33**(4): 398-407.

Raffa, R. B. (2010). "Is a picture worth a thousand (forgotten) words?: neuroimaging evidence for the cognitive deficits in 'chemo-fog'/'chemo-brain'." <u>J Clin Pharm Ther</u> **35**(1): 1-9.

Rivkin, M. and R. B. Kanoff (2013). "Metastatic brain tumors: current therapeutic options and historical perspective." <u>J Am Osteopath Assoc</u> **113**(5): 418-423.

Rosengren, L. E., G. Ahlsen, M. Belfrage, C. Gillberg, K. G. Haglid and A. Hamberger (1992). "A sensitive ELISA for glial fibrillary acidic protein: application in CSF of children." <u>J Neurosci Methods</u> **44**(2-3): 113-119.

Schagen, S. B., F. S. van Dam, M. J. Muller, W. Boogerd, J. Lindeboom and P. F. Bruning (1999). "Cognitive deficits after postoperative adjuvant chemotherapy for breast carcinoma." Cancer **85**(3): 640-650.

Seigers, R. and J. E. Fardell (2011). "Neurobiological basis of chemotherapy-induced cognitive impairment: a review of rodent research." Neurosci Biobehav Rev **35**(3): 729-741.

Seigers, R., M. Loos, O. Van Tellingen, W. Boogerd, A. B. Smit and S. B. Schagen (2015). "Cognitive impact of cytotoxic agents in mice." Psychopharmacology (Berl) **232**(1): 17-37.

Seigers, R., L. Pourtau, S. B. Schagen, F. S. van Dam, J. M. Koolhaas, J. P. Konsman and B. Buwalda (2010). "Inhibition of hippocampal cell proliferation by methotrexate in rats is not potentiated by the presence of a tumor." Brain Res Bull **81**(4-5): 472-476.

Seigers, R., J. Timmermans, H. J. van der Horn, E. F. de Vries, R. A. Dierckx, L. Visser, S. B. Schagen, F. S. van Dam, J. M. Koolhaas and B. Buwalda (2010). "Methotrexate reduces hippocampal blood vessel density and activates microglia in rats but does not elevate central cytokine release." Behav Brain Res **207**(2): 265-272.

Sharom, F. J. (2008). "ABC multidrug transporters: structure, function and role in chemoresistance." Pharmacogenomics **9**(1): 105-127.

Singh, V. K., R. Warren, R. Averett and M. Ghaziuddin (1997). "Circulating autoantibodies to neuronal and glial filament proteins in autism." Pediatr Neurol **17**(1): 88-90.

Song, L., C. A. Varma, J. W. Verhoeven and H. J. Tanke (1996). "Influence of the triplet excited state on the photobleaching kinetics of fluorescein in microscopy." Biophys J **70**(6): 2959-2968.

Troost, D., P. A. Sillevis Smitt, J. M. de Jong and D. F. Swaab (1992). "Neurofilament and glial alterations in the cerebral cortex in amyotrophic lateral sclerosis." Acta Neuropathol **84**(6): 664-673.

Tsuji, T., S. Shimohama, S. Kamiya, T. Sazuka and O. Ohara (1999). "Analysis of brain proteins in Alzheimer's disease using high-resolution two-dimensional gel electrophoresis." J Neurol Sci **166**(2): 100-106.

Uchida, Y., S. Ohtsuki, Y. Katsukura, C. Ikeda, T. Suzuki, J. Kamiie and T. Terasaki (2011). "Quantitative targeted absolute proteomics of human blood-brain barrier transporters and receptors." J Neurochem **117**(2): 333-345.

van de Waterbeemd, H., G. Camenisch, G. Folkers, J. R. Chretien and O. A. Raevsky (1998). "Estimation of blood-brain barrier crossing of drugs using molecular size and shape, and H-bonding descriptors." J Drug Target **6**(2): 151-165.

van Tellingen, O., B. Yetkin-Arik, M. C. de Gooijer, P. Wesseling, T. Wurdinger and H. E. de Vries (2015). "Overcoming the blood-brain tumor barrier for effective glioblastoma treatment." Drug Resist Updat **19**: 1-12.

Walker, M. D. and H. D. Weiss (1975). "Chemotherapy in the treatment of malignant brain tumors." Adv Neurol **13**: 149-191.

Yang, Z. and K. K. Wang (2015). "Glial fibrillary acidic protein: from intermediate filament assembly and gliosis to neurobiomarker." Trends Neurosci **38**(6): 364-374.
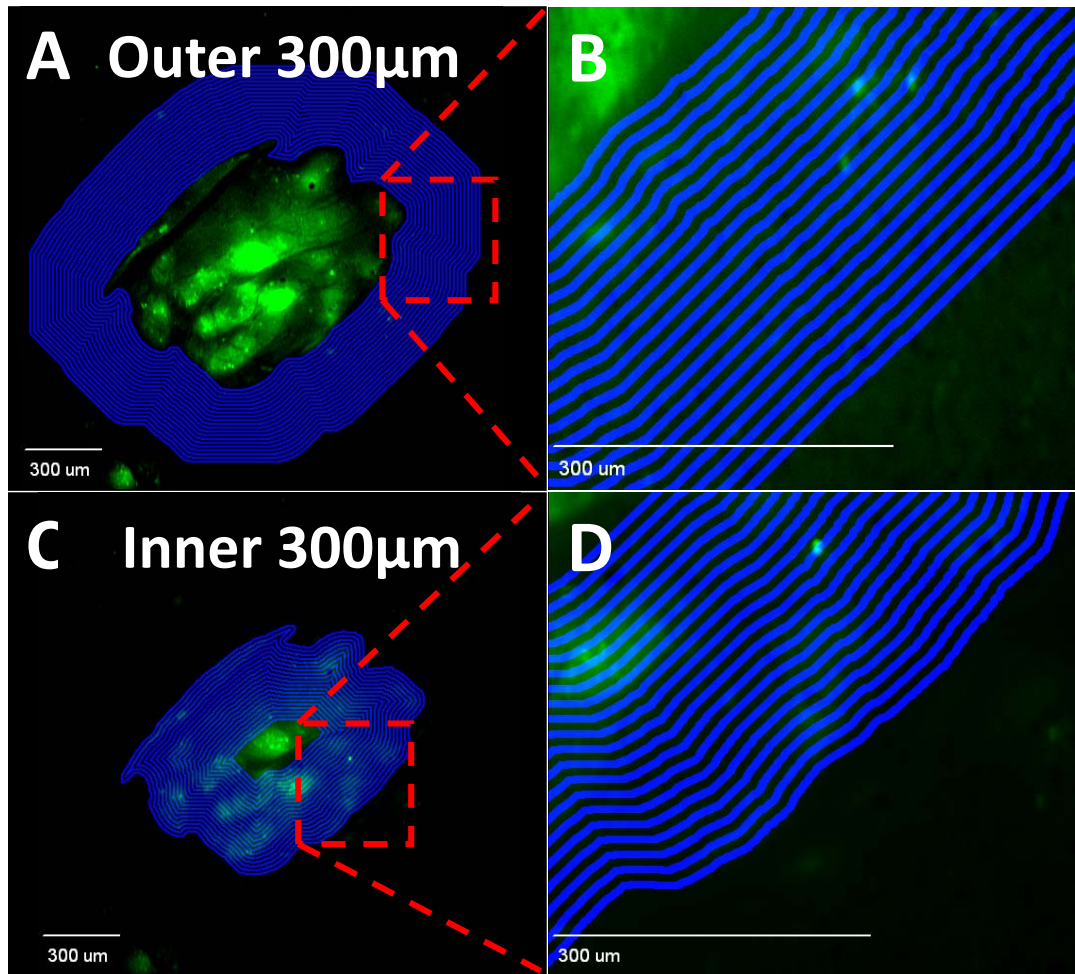
Figure 6.1: Image representing Circumferential Fluorescent Analysis by Quantitative Fluorescence Microscopy.

Fluorescent image of eGFP transfected MDA-MB-231Br metastasis in brain with circumferential 8 micron thick regions of interest (ROI) drawn to 300 microns beyond the metastasis margin (A and B). To distinguish between BAT and tumor regions, the inner 300 microns from the metastasis margin were used to create 8 micron thick circumferential ROIs (C and D).
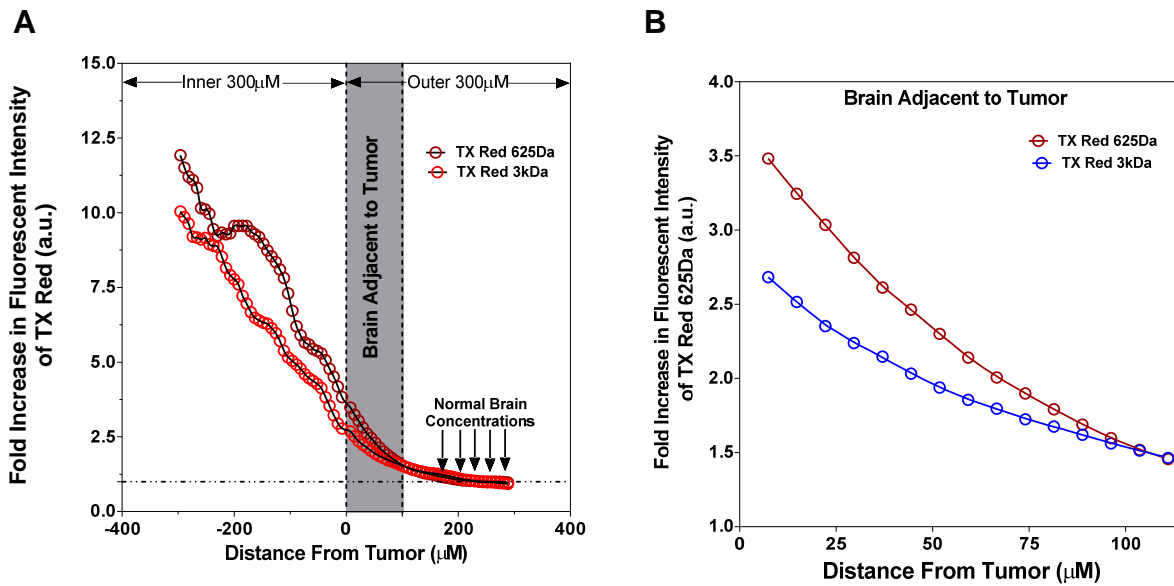
Figure 6.2: Circumferential Fluorescent Analysis by Quantitative Fluorescence Microscopy for Texas Red 625Da and Texas Red Dextran (3 kDa).

(A) Image showing fluorescence intensity fold increase over normal brain in Texas Red 625Da and Texas Red Dextran (3 kDa) after circumferential fluorescent analysis of in tumor and BAT regions in metastases

(B) Image showing fluorescence intensity fold increase over normal brain in Texas Red 625Da and Texas Red Dextran (3 kDa) after circumferential fluorescent analysis within 100µm beyond the tumor edge.

Fold increase in TR 625da permeability: 1.8-3.8. Fold increase in TRD 3KD permeability: 1-2.5

Figure 6.3: Transfer coefficient (K_{in}) of texas red tracers in tumor, BAT and normal brain by multiple uptake time approach

(A). Uptake of Texas Red (625 Da) in normal brain (Control), BAT and Tumor regions. The transfer coefficient (K_{in}) for Texas Red (625 Da) in BAT was significantly higher than normal brain (Control)

(B)Uptake of Texas Red Dextran (3 kDa) in normal brain (Control), BAT and Tumor regions. The transfer coefficient (K_{in}) for Texas Red Dextran (3 kDa) in BAT was significantly higher than normal brain (Control)
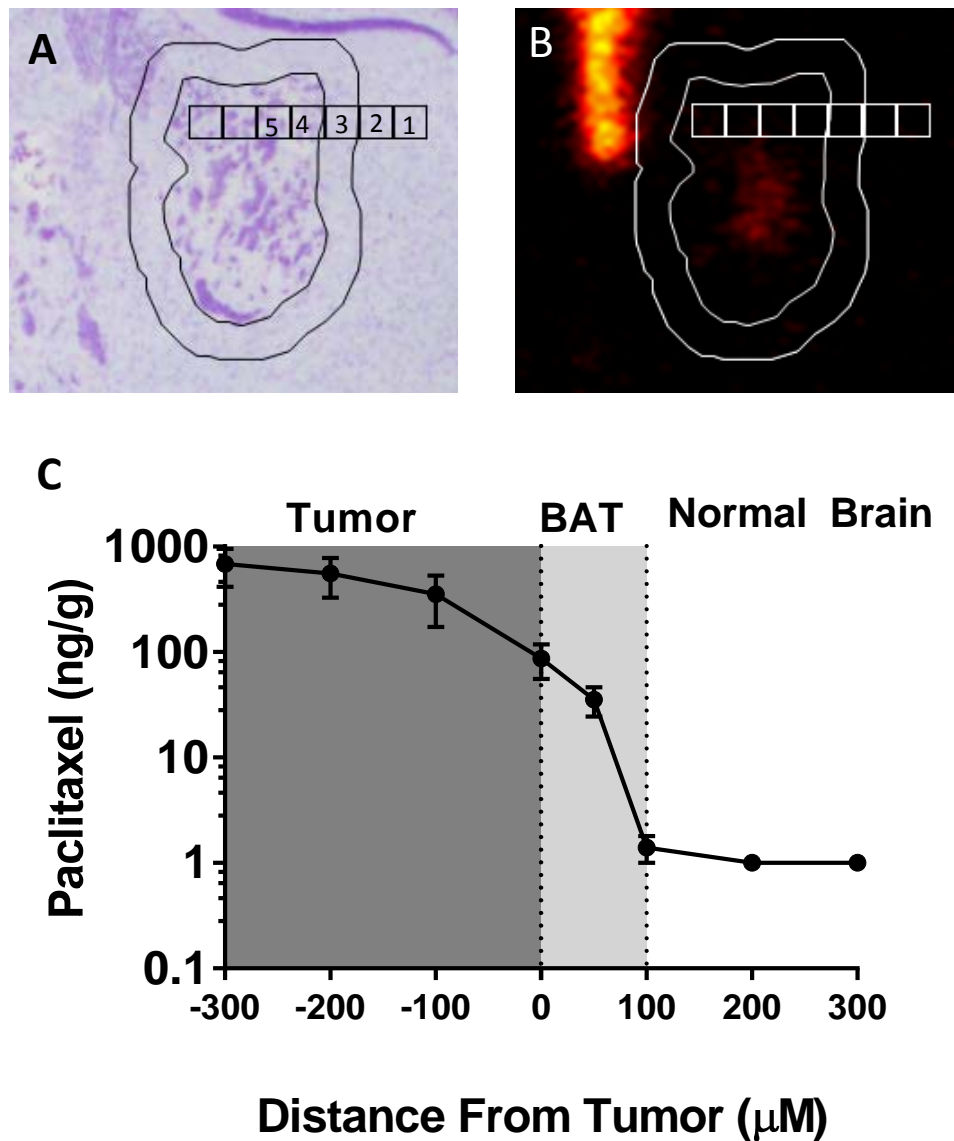
Figure 6.4: Analysis of ^{14}C-Paclitaxel concentration in tumor, normal brain and BAT regions.

Representative image of 231Br brain metastases (**A**) and corresponding ^{14}C-Paclitaxel accumulation (**B**) in metastases 8 h after intravenous administration of radiolabeled paclitaxel. Paclitaxel concentrations from 100 μm squares as shown in image A and B were determined (**1**=1 ng/g, **2**=1 ng/g, **3**=10.5 ng/g, **4**= 293 ng/g, **5**= 261 ng/g). (**C**) Analysis of ^{14}C-Paclitaxel concentration in tumor regions (-300 μm to 0) and normal brain regions (0 to 300 μm)
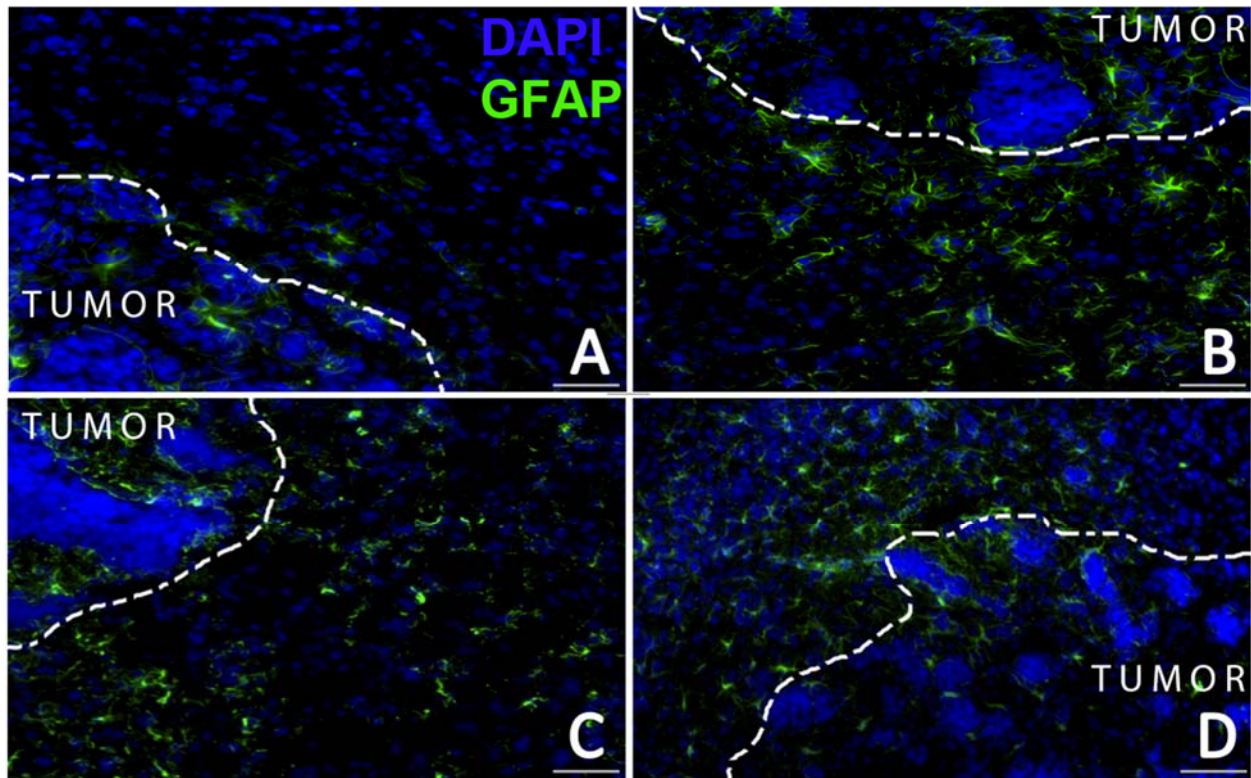
Figure 6.5: Image showing activated astrocytes (GFAP) after treatment with chemotherapy

Fluorescent images representing presence of nuclei (DAPI) in blue and activated astrocytes (GFAP) in green after treating with A.Saline (Vehicle), B. Eribulin (1.5mg/kg I.P), C. Docetaxel: (10mg/kg I.V), D. Paclitaxel: (10mg/kg I.V). The GFAP expression in BAT regions in chemotherapeutic treated group appears are higher than that of vehicle group

CHAPTER 7

FUTURE DIRECTIONS

In conclusion, this dissertation investigated novel approaches to treat metastatic brain tumors from breast cancer. The presence of blood-brain barrier (BBB) and blood-tumor barrier (BTB) makes the permeability of chemotherapeutic agents into the tumor challenging. The permeability of any solute or anti-cancer agent across the BBB/BTB is dependent of physico-chemical properties of drugs/solutes. Most of the anti-cancer drugs do not qualify to penetrate BTB in concentrations enough to elicit cytotoxic activity. To overcome this we first, we encapsulated a chemotherapeutic agent irinotecan into a liposome. Then we studied the pharmacokinetics of liposomal irinotecan in our mouse model of brain metastases from breast cancer. We found that liposomal irinotecan has better pharmacokinetic profile than non-liposomal conventional irinotecan. The plasma half-lives and mean residence times (MRT) of liposomal irinotecan significantly improved while compared to non-liposomal irinotecan. In addition to that clearance and volume of distribution of liposomal irinotecan decreased when compared to non-liposomal irinotecan. The plasma drug exposure for liposomal irinotecan was significantly improve when compared non-liposomal irinotecan. This improved plasma pharmacokinetics also reflected in brain tumor pharmacokinetics. We found that the drug exposure of liposomal irinotecan in brain tumors were significantly higher than that of non-liposomal irinotecan.

After studying the pharmacokinetics, we evaluated the accumulation of liposomes and its effect on tumor burden and survival in a mouse model of metastatic breast cancer. We found that with liposomal irinotecan the tumor burden was decreased and the median survival in our mouse model was significantly improved. We previously reported that brain tumors have leakier BTB compared to BBB (Lockman et al. 2010) and we believe that this leakier BTB is responsible for

the liposomes to penetrate into the brain tumors by enhanced permeation and retention (EPR) effect and by bypassing efflux transporters present at the BBB. We found that liposomal irinotecan improved median survival by 40% when compared to non-liposomal irinotecan.

Using another strategy, we want modulate the BTB and increase the permeability of chemotherapeutic agents. Notch-4 signaling pathway play an important role in angiogenesis by downregulating vascular endothelial growth receptor-2 (VEGFR-2)(Taylor et al. 2002). We want to increase permeation specifically in tumors by increasing angiogenesis as angiogenic vessels are leakier when compared to normal brain blood vessels. Notch-4 inhibition will lead to increased expression of VEGFR-2, which then leads to increase in angiogenic vessels, ultimately leading to increased permeation of chemotherapy. We observed in our study that inhibition of Notch-4 by DAPT significantly increased the permeability of ^{14}C-AIB in our mouse model. We then studied chemotherapy administration with concurrent Notch-4 inhibition and found that the survival was significantly improved in a mouse model of metastatic brain tumors form breast cancer. We also found that the progression of tumor burden was delayed.

Lastly, we want to investigate the effect of chemotherapy in normal brain around the brain metastases. Brain tumor vasculature can be significantly compromised and leakier than that of normal brain blood vessels but only a little is known if there are vascular permeability alterations in the brain adjacent to tumor (BAT). Changes in BAT permeability may also suggest increased drug permeation in the BAT which may exert toxicity on cells of the central nervous system. Herein, we studied permeation changes in BAT using quantitative fluorescent microscopy and autoradiography, while effect of chemotherapy within the BAT region was determined by staining for activated astrocytes and DNA damage. The mean permeability of fluorescent dyes within BAT region significantly increased when compared to normal brain. The

K_{in} values in the BAT for both Texas Red (625 Da) and Texas Red dextran (3kDa) were found to be significantly higher than normal brain. We also found that there is significant increase in accumulation of ^{14}C-Paclitaxel in BAT compared to normal brain. We also observed animals treated with chemotherapy (paclitaxel (10mg/kg), erubilin (1.5mg/kg and docetaxel (10mg/kg)) showed activated astrocytes in BAT. As many new strategies to treat brain tumors tend to overcome BBB/BTB, the adverse effect of normal brain should also be considered.

Future studies, based on the results within the dissertation, include:

1. We have found that liposomal irinotecan crosses the BTB and accumulates in brain metastases of breast cancer and acts as a depot for the sustained release of irinotecan in our mouse model. This accumulation and sustained release of drug ultimately resulted in prolonged survival of animals in our mouse model. A phase I study with liposomal irinotecan (MM-398) is recruiting patients to determine tumor drug levels and to predict patient response to treatment for metastatic brain tumors from triple negative breast cancer (NCT01770353).

2. We observed that inhibition of Notch-4 increased the permeation of the BTB in our studies and we also found that the liposomes accumulated in brain metastases. We want to combine both strategies and administer liposomal irinotecan with concurrent Notch-4 inhibition. With liposomal irinotecan the median survival improved by 40 % and with Notch-4 inhibition it was 20%. We hypothesize, combining both strategies will result in a better outcome.

3. Finally, we want to design and develop liposomes where, both DAPT (Notch-4 inhibitor) and a chemotherapy drug (Irinotecan) will be encapsulated in it. We believe encapsulation of DAPT will improve the pharmacokinetics of DAPT and also will

decrease the dose DAPT administered as the formulation will be administered intravenously. DAPT is lipophilic in nature and will be encapsulated in lipid part of liposome, whereas hydrophilic irinotecan HCl will be encapsulated in the hydrophilic core of liposome.

Clinically, treatment strategies for metastatic brain tumors involve surgery, radiation therapy and chemotherapy. Often more than one modality is employed for the treatment and the treatment for cancer has become individualized. In addition to improving the uptake of chemotherapy, other modalities like radiation therapy should be improved. The use of radio-sensitizers and radio-protective agents improved the radiation therapy. Radio-sensitizers further sensitize the cancer cells for the radiation while radio-protective agents protect normal tissue. We believe effective treatment modality for treatment of metastatic brain tumors is the combination of improved multimodal approach. Nanoparticles showed improved the drug distribution into the brain metastases and our studies showed that distribution is localized into the brain tumors. Future studies should focus in exploiting nanoparticles like liposomes for delivery chemotherapy, radio-sensitizers and other agents like P-gp inhibitors in a single delivery system along with radiation therapy. We believe brain metastases will be managed effectively by employing multiple improved treatment modalities.

7.1 References

Lockman, P. R., R. K. Mittapalli, K. S. Taskar, V. Rudraraju, B. Gril, K. A. Bohn, C. E. Adkins, A. Roberts, H. R. Thorsheim, J. A. Gaasch, S. Huang, D. Palmieri, P. S. Steeg and Q. R. Smith (2010). "Heterogeneous Blood-Tumor Barrier Permeability Determines Drug Efficacy in Experimental Brain Metastases of Breast Cancer." Clinical cancer research : an official journal of the American Association for Cancer Research **16**(23): 5664-5678.

Taylor, K. L., A. M. Henderson and C. C. W. Hughes (2002). "Notch Activation during Endothelial Cell Network Formation in Vitro Targets the Basic HLH Transcription Factor HESR-1 and Downregulates VEGFR-2/KDR Expression." Microvascular Research **64**(3): 372-383.